GOVERNMENT OF
NEWFOUNDLAND AND LABRADOR
Department of Mines and Energy
Geological Survey

TILL GEOCHEMISTRY OF THE WHITE BAY AREA

S. McCuaig

Open File NFLD 2823

St. John's, Newfoundland
June 25, 2003

NOTE

The purchaser agrees not to provide a digital reproduction or copy of this product to a third party. Derivative products should acknowledge the source of the data.

DISCLAIMER

The Geological Survey, a division of the Department of Mines and Energy (the "authors and publishers"), retains the sole right to the original data and information found in any product produced. The authors and publishers assume no legal liability or responsibility for any alterations, changes or misrepresentations made by third parties with respect to these products or the original data. Furthermore, the Geological Survey assumes no liability with respect to digital reproductions or copies of original products or for derivative products made by third parties. Please consult with the Geological Survey in order to ensure originality and correctness of data and/or products.

Cover photo:
Boulder-strewn landscape, Micmac Pond area.

GOVERNMENT OF
NEWFOUNDLAND AND LABRADOR
Department of Mines and Energy
Geological Survey

TILL GEOCHEMISTRY OF THE WHITE BAY AREA

S. McCuaig

Open File NFLD 2823

St. John's, Newfoundland
June 25, 2003

Recommended citation:
S. McCuaig
2003: Till geochemistry of the White Bay area. Newfoundland Department of Mines and Energy, Geological Survey, Open File NFLD 2823, 51 pages plus appendices and figures.

TABLE OF CONTENTS

LIST OF FIGURES

LIST OF TABLES

INTRODUCTION

Gold exploration has been an ongoing activity in the White Bay area of northeastern Newfoundland from 1889 (Betz, 1948) to the present. However, other mineralization types are also present in the region. These include copper, fluorite, molybdenum and lead on the west side of White Bay, and titanium, copper and lead on the east side of the bay (Davenport et al., 1999). Lake sediment geochemistry shows several areas around the bay with anomalous values of Zn, Pb, Mo, Mn, Cr, Cu, Ni, Au, Ag and U (Davenport *et al.*, 1999).

A surficial mapping project (McCuaig, 2003) was undertaken in NTS map areas 12H/10 and 12H/15. Ice flow indicators were recorded, and much of the area was sampled for till geochemistry. This report will focus on the geochemistry, the aim of which is to identify areas of possible mineralization in more detail than that shown by regional lake sediment geochemistry.

Physiography and Access

White Bay separates the Great Northern and Baie Verte peninsulas. It is a north-northeast trending bay that narrows to a point in the south (Figure 1). The coastal margin generally consists of steeply sloping bedrock cliffs.

The Long Range Mountains in the northwestern part of the study area form a hilly plateau and reach a maximum elevation of 509 m asl (metres above sea level). Rolling linear hills and valleys on both sides of the bay take their shape from bedrock structure, which also trends north-northeast. An exception to this is Purbeck's Fiord (near Purbeck's Cove), a curving fiord that cuts through the bedrock structure. Drainage patterns are directly related to bedrock geology, except in the southeastern part of the study area, near Micmac Pond. Glacial sediments are thicker in this area, covering much of the bedrock and creating a locally subdued hummocky topography. Narrow beaches are located in sheltered coves and at river mouths, but they are uncommon.

The area has three main roads, and an extensive network of woods roads, which together provided a reasonable amount of vehicle access (4x4 truck and ATV). The remainder of the area was reached by helicopter.

Bedrock Geology

The bedrock geology of the study area is complex (Figure 2). Rocks of the Humber Zone dominate the region, although Dunnage Zone rocks outcrop in the southeastern corner of the study area. The Humber Zone was once the margin of the Early Paleozoic continent Laurentia (Williams, 1979). The Dunnage Zone contains mostly volcanic oceanic rocks that were thrust over Humber Zone rocks when the Iapetus Ocean closed (Hibbard, 1983).

Humber Zone rocks

The oldest rocks, which have been subjected to high grade metamorphism, belong to the Long Range Inlier of the Great Northern Peninsula (Owen, 1991). These rocks form the Middle Proterozoic Long Range Gneiss Complex, composed of granitic to granodioritic gneiss and minor migmatite (Owen, 1991). They were intruded first by the Late Proterozoic Lake Michel Intrusive Suite (Aspy and Main River granites) and much later by the Devonian Devils Room granite (Owen, 1991).

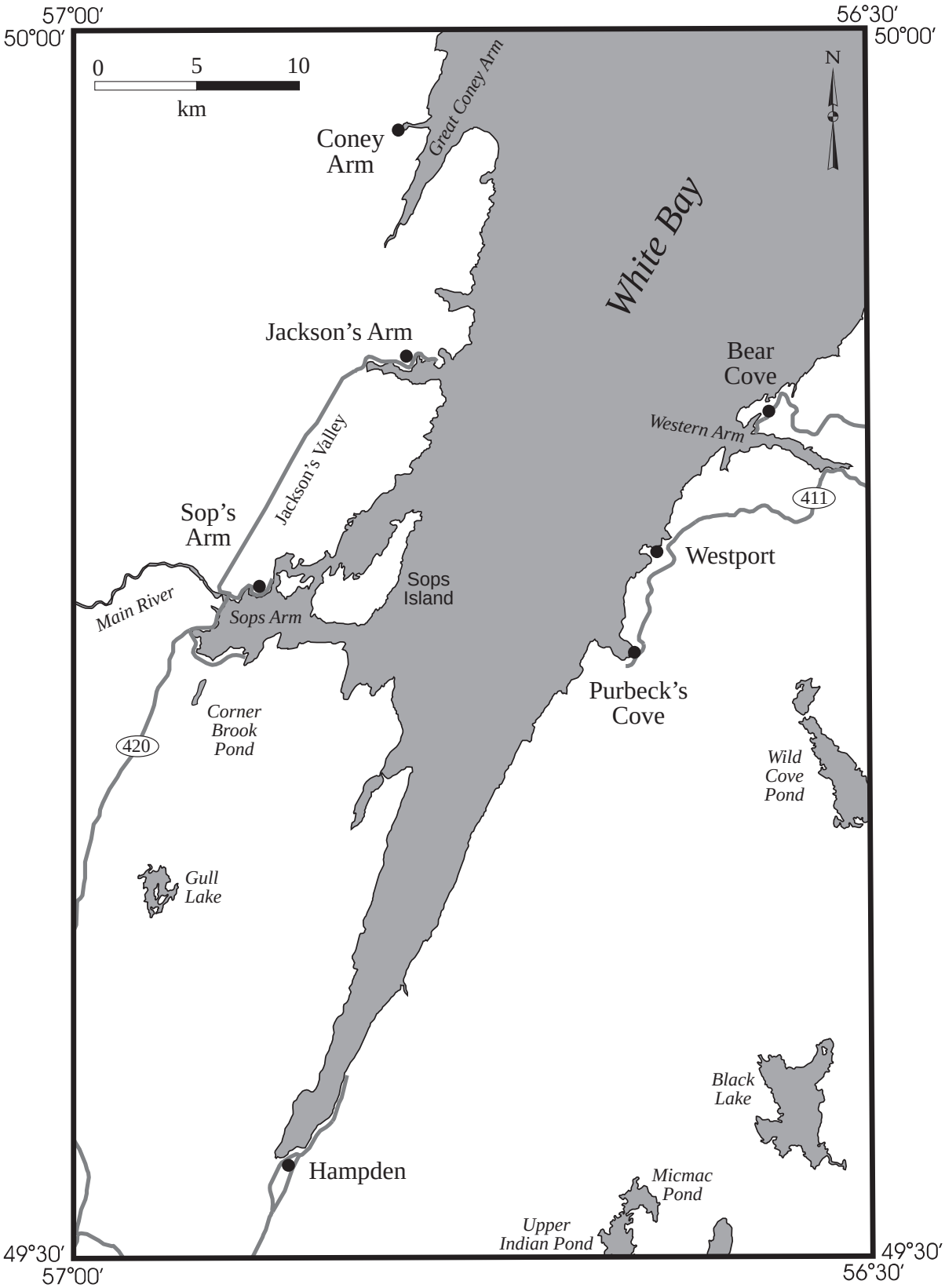

Figure 1. Location map of the White Bay area. Jackson's Valley is an informal name introduced to help clarify localities in the western zone of the study area.

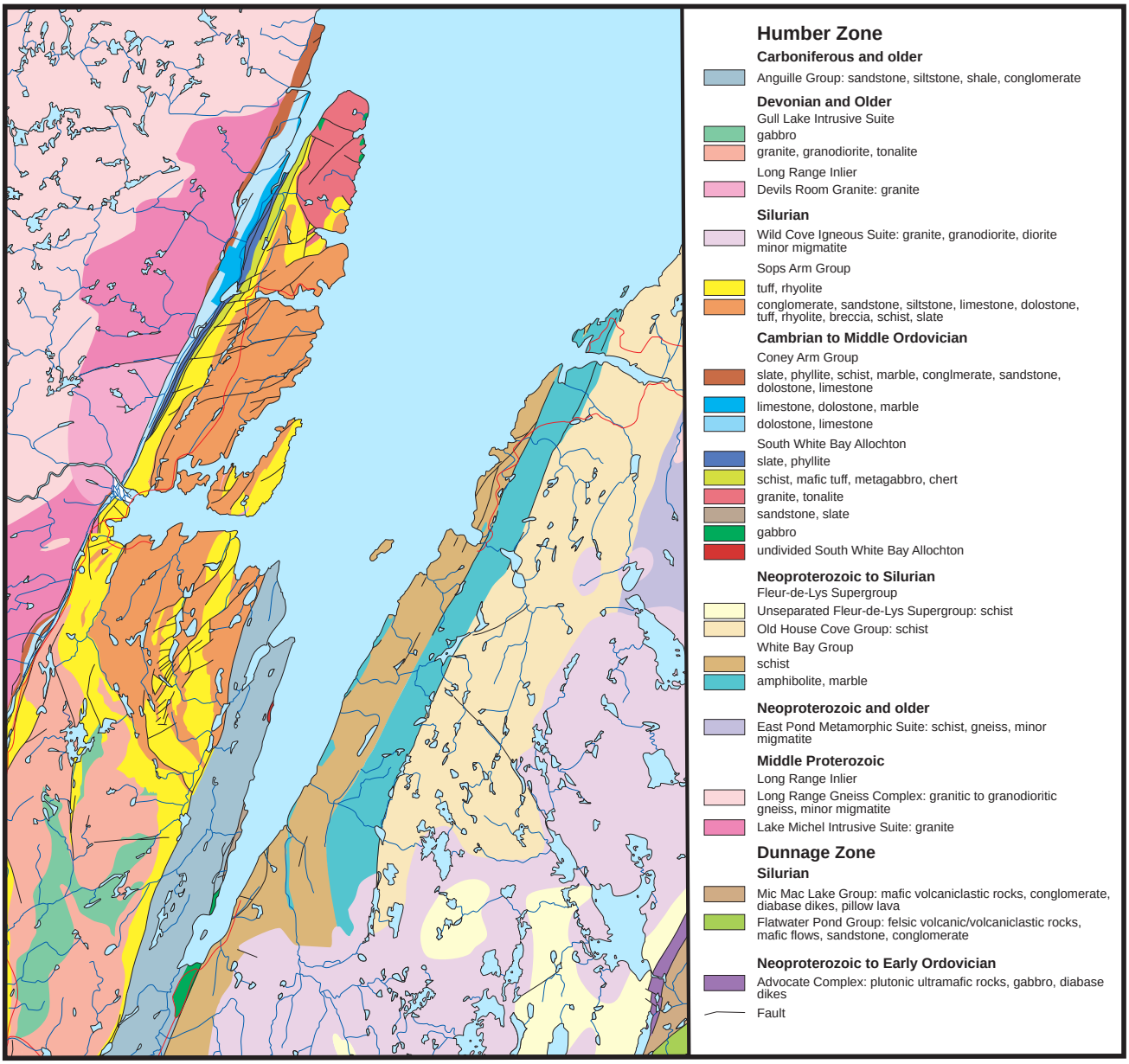

Figure 2. Bedrock geology of the White Bay area.

The Proterozoic rocks are unconformably overlain by much younger sandstone, conglomerate, dolostone, limestone, slate, schist, phyllite and marble of the Cambrian to Middle Ordovician Coney Arm Group; ophiolitic volcanic/volcaniclastic rocks, sandstone, slate, phyllite, granite, tonalite and gabbro of the Cambrian to Middle Ordovician Southern White Bay Allochthon; and conglomerate, felsic tuff, rhyolite, breccia, sandstone, siltstone, dolostone, limestone, schist and slate of the Silurian Sops Arm Group (Smyth and Schillereff, 1982). The Devonian and older Gull Lake Intrusive Suite lies to the south of these rocks. It consists of gabbro, granodiorite, tonalite and granite (Smyth and Schillereff, 1982). The Carboniferous Anguille Group borders southern White Bay, east of the Sops Arm Group and the Gull Lake Intrusive Suite. It is mainly sandstone and shale (Smyth and Schillereff, 1982).

The Doucers Valley fault complex separates the Grenvillian rocks in the west and the younger Sops Arm and Coney Arm Groups to the east, and extends from Doucers Valley to Great Coney Arm (Tuach, 1987). The northern extension of the fault complex falls in a valley, which is informally named ‘Jackson’s Valley’ here. The Birchy Ridge strike-slip fault and the Cabot-Hampden fault separate the Anguille and Sops Arm groups (Smyth and Schillereff, 1982; Tuach, 1987).

Rocks outcropping on the Baie Verte Peninsula include the Neoproterozoic to Silurian Fleur-de-Lys Supergroup, the highly deformed, Neoproterozoic or older East Pond Metamorphic Suite and the Silurian Wild Cove Pond Igneous Suite (Cawood et al., 1994; Hibbard, 1983). Schistose rocks dominate the Fleur-de-Lys Supergroup, which is mainly continental and is less deformed than the East Pond Suite. The Fleur-de-Lys Supergroup is subdivided into the White Bay Group, which contains schist, amphibolite and marble, and the Old House Cove Group, which consists of schist (Hibbard, 1983). The East Pond Metamorphic Suite includes banded and granitic gneiss, schist and minor migmatite (Hibbard, 1983). These rocks are intruded by the Wild Cove Pond Igneous Suite, which is composed of diorite, granodiorite, granite, and minor migmatite (Hibbard, 1983)

Dunnage Zone rocks

The oceanic rocks in the southeastern-most portion of the study area include Neoproterozoic to Early Ordovician plutonic ultramafic rocks, gabbro and diabase dikes of the Advocate Complex (Hibbard, 1983). A younger Silurian sequence consists of mafic volcaniclastic rocks, conglomerate, diabase dikes and pillow lava of the Mic Mac Lake Group and felsic volcanic/volcaniclastic rocks, sandstone, conglomerate and mafic flows of the Flatwater Pond Group (Hibbard, 1983).

Economic geology

Gold mineralization is found in shear zones in the Aspy Granite, in the Sop’s Arm Group, and along the Doucers Valley fault complex (Owen, 1991; Tuach, 1987). Browning’s Mine, near Sops Arm, was one of Newfoundland’s first gold mines, and operated from 1903 to 1904 (Betz, 1948).

Localized fluorite and molybdenite are found in the Devils Room granite (Smyth and Schillereff, 1982) and in the Gull Lake Intrusive Suite (Tuach, 1987). Fluorite-bearing breccia is exposed along the Main River’s north bank. Lead is found in limestone and rhyolite in the fault zone at the western edge of the Gull Lake Intrusive Suite, as well as minor copper and uranium (Tuach, 1987).

The Doucers Valley fault complex consists of steeply dipping faults that transect carbonate and clastic rocks, which suggests that the area has potential for Carlin-type gold mineralization. If such mineralization is present, then As, Hg, Sb and Tl (Bonham Jr., 1985; Rytuba, 1985) will be pathfinders for gold in this area. Arsenic and antimony have already been found to be pathfinders for gold in lake sediments in the Doucers/Jackson's valley areas (Davenport and Nolan, 1989; McConnell and Honarvar, 1989).

QUATERNARY GEOLOGY

The surficial geology is described in McCuaig (2003) and is summarized here. There is a single stratigraphic unit of till, which is thin and discontinuous. Bedrock outcrop is profuse, especially at higher elevations and along the coastline. Till thickness increases in the southeastern part of the study area, where large hummocks are common. Tills are normally massive, matrix-supported, and very poorly sorted. Clast content is 40-70%. The matrix ranges from silt to very coarse sand, and is calcareous in Doucers and Jackson's valleys. Clasts are granule to boulder size and generally subangular. Very large clasts are quite common and can be up to 12 m in diameter. Boulders 2 to 4 m in diameter are not uncommon, especially in the southeastern portion of the study area, where till is thickest. The largest boulders are found in the upper part of the till and on the ground surface. These boulders probably represent the englacial load of the ice sheet and were thus the last debris to be released from the melting ice.

Glaciofluvial sediments are uncommon. Two eskers were identified in the southern part of the map area, but most other glaciofluvial sediments are subaerially deposited outwash plains. These are found in valleys and generally terminate near the sea at deltas that are elevated above current sea level. A few ice-contact deltas are also present. Glaciofluvial sediments consist of moderately to well-sorted beds of sand to boulder gravel. Pleistocene and early Holocene fossils are found only in deltaic sediments.

There are two types of marine deposits in the White Bay area: glaciomarine diamicton and raised beaches. The diamicton deposits have a finer matrix than the till typical of the region (clay to fine sand) and clast content is low (about 30%). They are also massive or crudely stratified, poorly sorted, and contain granule to boulder sized dropstones. The raised beach deposits are much coarser and are better sorted than the diamicton (moderately to well sorted). The deposits form low (about 3 m high) terraces up to 10 m asl. Sediments are crudely stratified or have well defined horizontal bedding. Common clast sizes are pebbles and cobbles, but granules and boulders are also present; the matrix is medium to very coarse sand.

GLACIAL HISTORY

Evidence of the last (Late Wisconsinan) glaciation was found in the White Bay area (McCuaig, 2003). Ice flowed across the entire study area at the glacial maximum, changing flow directions as it retreated during deglaciation. Till was deposited beneath the ice, and was reworked by meltwater in some areas when ice retreated. Marine sediments, deposited when sea levels were higher, record a series of sea level stands.

Ice Flow

Ice flow was determined from various ice-flow indicators, including striations and the provenance of clasts within till. The ice flow history of the area is complex (Figure 3). The earliest flow (Flow 1) was eastward or southeastward out of the Long Range Mountains, as suggested by Liverman (1992) and Vanderveer and Taylor (1987). This flow did not extend across White Bay - it likely represents the ice build-up phase of the last glaciation. Ice probably accumulated in a similar manner over the Baie Verte Peninsula but evidence for early westward ice flow was not found in that area.

The next flow event was northward and north-northeastward along White Bay (Flow 2, Figure 3). Flow was from a major ice centre south of the study area, which probably occurred when ice reached its maximum extent.

The last flow phase is shown by Flow 3 (Figure 3). A gradual drawdown of ice into White Bay (indicated by younger striations that are more strongly oriented toward the bay than older ones), along with overall ice retreat after the glacial maximum, changed the locations of major ice caps. Ice centres shifted from south of the study area to new locations on the Baie Verte Peninsula and over the Long Range Mountains. This caused ice flow to be northwestward or southeastward into the bay from the surrounding uplands. The change in ice cap locations was gradual, and ice flow directions slowly changed as a consequence.

A study of clast lithologies within till shows that Flow 3 was the most important mover of debris and that transport distances were variable (approximately 1 to 20 km) (McCuaig, 2003).

Sea Level

Several geomorphic features bordering White Bay record a series of former higher sea level stands (deltas, glaciomarine terraces and raised beaches). The highest stand (the regional marine limit) is 70 m above present sea level. There were also sea level stands of 60 and 40 m asl; the latter occurred at 11 200 ± 100 ^{14}C years BP (based on marine shells in an ice-proximal delta at Jackson's Arm (Blake, 1988)). A 30 m stand is dated at 10 200 ± 100 years BP (based on marine shells from a delta southwest of Corner Brook Pond (Blake, 1988)). The final sea level stand represented on land was at 10 m asl, shown by several raised beach deposits in the Coney Arm and Western Arm/Purbeck's Cove areas.

METHODS

Sampling

A total of 355 1-kg till samples were taken for geochemical analysis. The region was sampled at a spacing of about 1 sample per 4 km^2, with the exception of the Long Range Mountains, which were sampled only near the roads, as till was scarce in that area (Figure 4). The sample target was the C soil horizon (unaltered till). The majority of samples were taken from test pits at 40-60 cm depths and from road cuts. Road cut sample depths averaged 100 cm below the surface. Mudboils were sampled at shallower depths (average 25 cm), and in areas of thin till samples were taken near the bedrock-till interface. A number of B- and BC-horizon samples were taken in areas where the soil was too thin for a C-horizon to be present or where till was too bouldery to penetrate to greater depths. However, 81% of all samples are either from the BC- or C-horizon (45% are from the C-horizon).

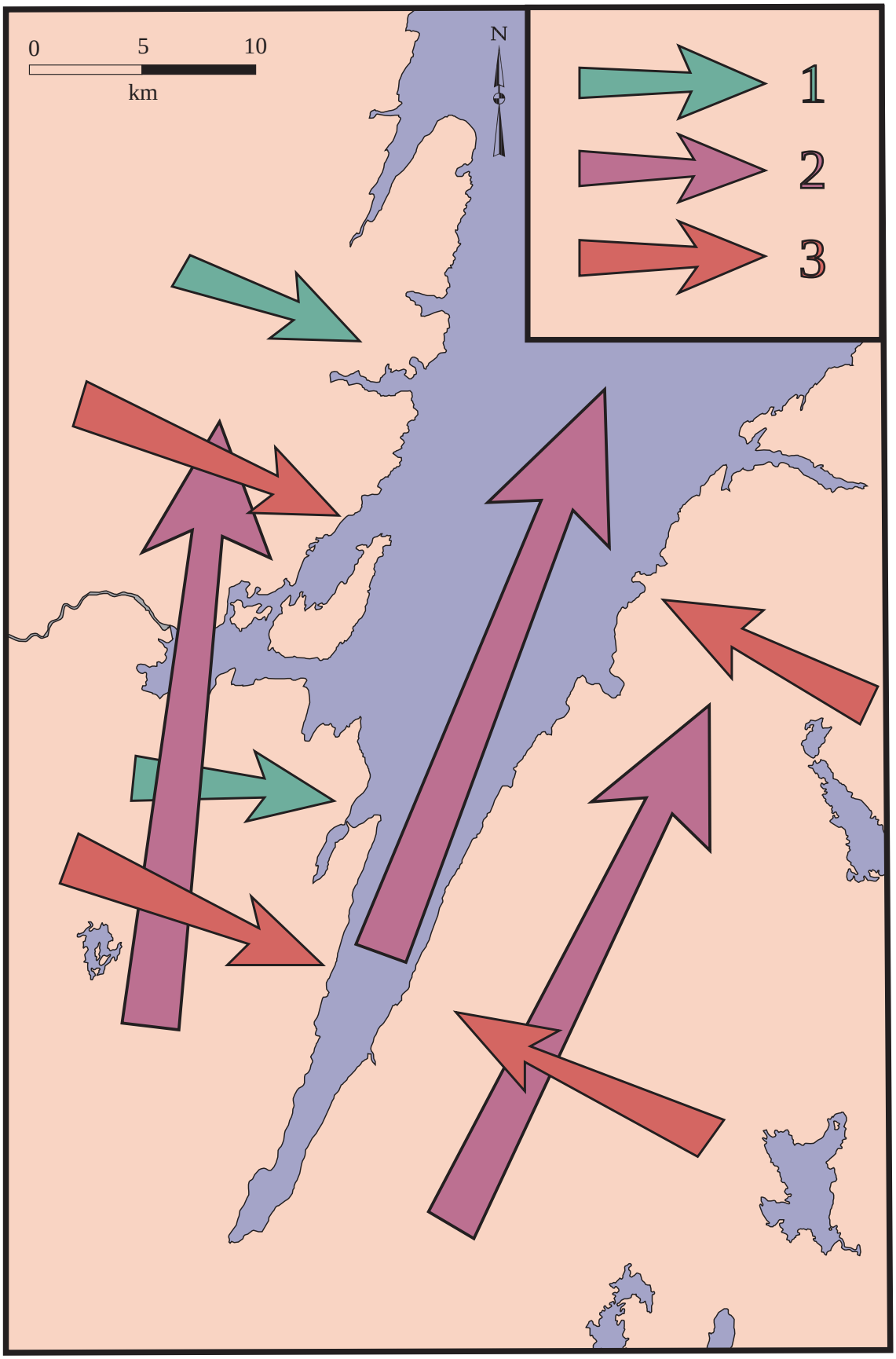

Figure 3. Former ice flow directions. 1 is the oldest; 3 the most recent.

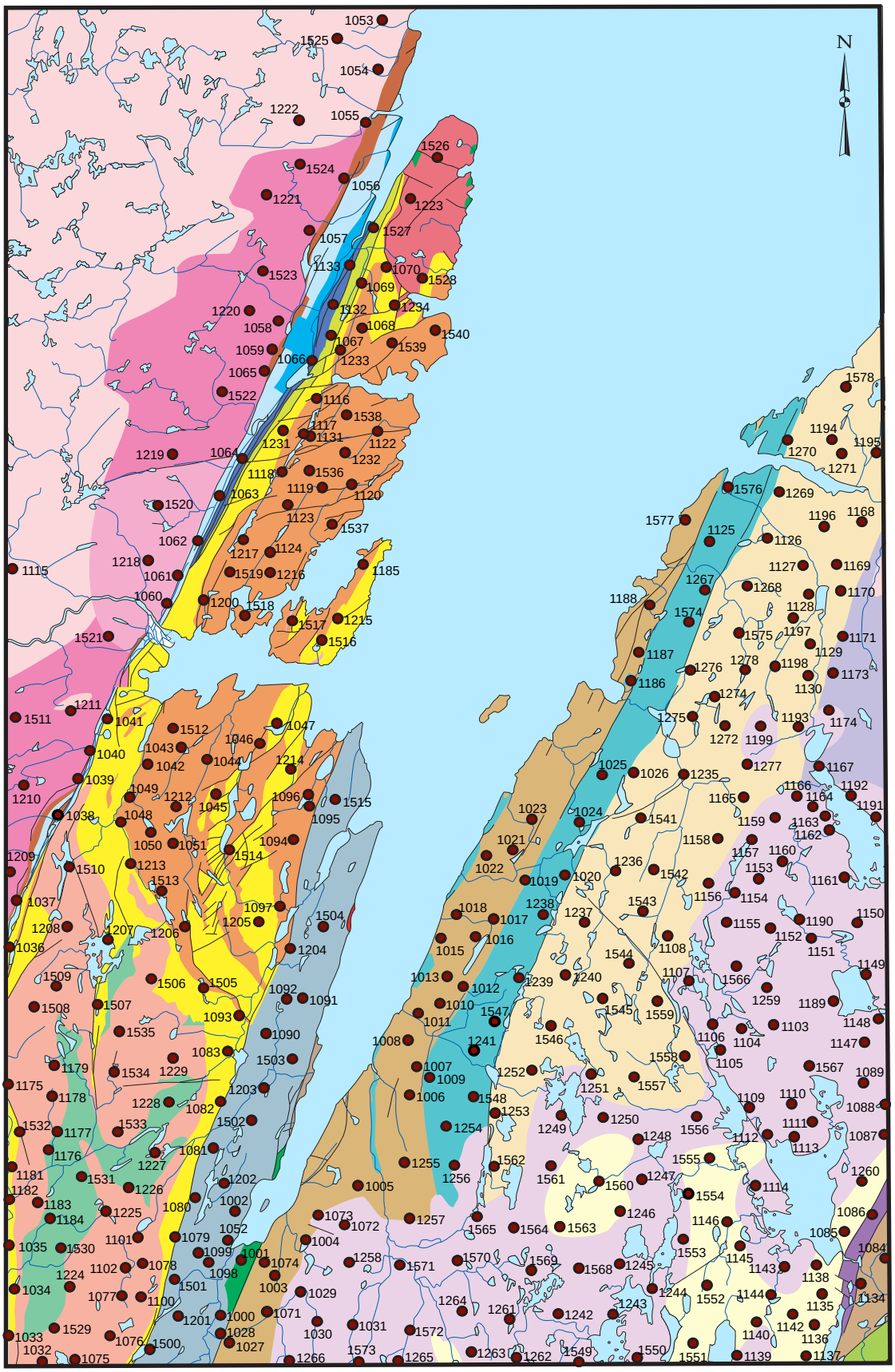

Figure 4. Sample locations overlain on the bedrock map of Figure 2.

Geochemical Analysis

The silt-clay fraction of the till samples was analyzed for trace elements. At the Geological Survey laboratory, the samples were oven-dried at 40°C and were sieved through 63 µm stainless steel sieves. The < 63 µm fraction was analyzed.

Analytical Methods

A suite of 355 samples was analyzed for trace element geochemistry. At the Geological Survey laboratory, Ag and Rb were analyzed using atomic absorption spectroscopy (AAS), while Al, As, Ba, Be, Ca, Cd, Ce, Co, Cr, Cu, Dy, Fe, K, La, Li, Mg, Mn, Mo, Na, Nb, Ni, P, Pb, Sc, Sr, Ti, V, Y, Zn and Zr were analyzed with inductively coupled plasma emission spectroscopy (ICP-ES). Activation Laboratories (Ancaster, Ontario) did instrumental neutron activation analysis (INAA) for the following elements: As, Au, Ba, Br, Ca, Ce, Co, Cr, Cs, Eu, Fe, Hf, Hg, Ir, La, Lu, Mo, Na, Nd, Ni, Rb, Sb, Sc, Se, Sm, Sn, Sr, Ta, Tb, Th, U, W, Yb, Zn, Zr. Field duplicates and control reference materials are included incognito in all internal and external analyses. The trace elements are labeled with their elemental abbreviation, a numeric code to distinguish the analysis type and the applicable unit of measurement (Table 1).

Gravimetric analysis (LOI)

Organic carbon content was estimated from weight loss on ignition (LOI) during a controlled combustion, in which 1 g aliquots of sample were gradually heated to 500°C in air, over a 3-hour period.

Atomic absorption spectroscopy (AAS)

Silver (Ag) and Rubidium (Rb) were determined on 0.5 g aliquots of sample following digestion in 2 ml of concentrated nitric acid overnight at room temperature, and then in a water bath at 90°C for 2 hours (Wagenbauer *et al.*, 1983).

Inductively coupled plasma emission spectroscopy (ICP-ES)

For these analyses, the residue of the 1g aliquot of sample remaining from the LOI determination was digested in a mixture of 15 ml of concentrated hydrofluoric acid, 5 ml of concentrated hydrochloric acid, and 5 ml of 50 volume percent $HClO_4$ in a 100 ml teflon beaker, and was allowed to stand overnight before being heated to dryness on a hot plate. The residue was taken up in 10 volume percent hydrochloric acid by gentle heating on a hot plate, was allowed to cool and was made up to 50 ml with 10 percent volume hydrochloric acid (Wagenbauer *et al.,* 1983). For most elements dissolution is total with the exception of Cr from chromite, Ba from barite and Zr from zircon.

Instrumental neutron activation analysis (INAA)

An approximately 30 g aliquot is encapsulated and weighed in a polyethylene vial and irradiated with flux wires and an internal standard (1 for 11 samples) at a thermal neutron flux of 7×10^{11} n/cm^{2}s. After seven days (to allow Na^{24} to decay), the samples are counted on a high purity Ge detector with a resolution of better than 1.7 KeV. Using the flux wires, the decay-corrected activities are compared to a calibration developed from multiple certified international reference materials. The standard present is only a check on accuracy of the analysis and is not used for calibration purposes. 10-30% of the samples are checked by re-measurement.

Table 1. Variable list and description of data.

VARIABLE	DESCRIPTION
As1 ppm	Arsenic, ppm, INAA
Au1 ppb	Gold, ppb, INAA
Ag1 ppm	Silver, ppm, INAA
Ba1 ppm	Barium, ppm, INAA
Br1 ppm	Bromine, ppm, INAA
Ca1 %	Calcium, %, INAA
Ce1 ppm	Cerium, ppm, INAA
Co1 ppm	Cobalt, ppm, INAA
Cr1 ppm	Chromium, ppm, INAA
Cs1 ppm	Cesium, ppm, INAA
Eu1 ppm	Europium, ppm, INAA
Fe1 %	Iron, %, INAA
Hf1 ppm	Hafnium, ppm, INAA
Hg1 ppm	Mercury, ppm, INAA
Ir1 ppm	Iridium, ppm, INAA
La1 ppm	Lanthanum, ppm, INAA
Mo1 ppm	Molybdenum, ppm, INAA
Na1 %	Sodium, %, INAA
Nd1 ppm	Neodymium, ppm, INAA
Ni1 ppm	Nickel, ppm, INAA
Rb1 ppm	Rubidium, ppm, INAA
Sb1 ppm	Antimony, ppm, INAA
Sc1 ppm	Scandium, ppm, INAA
Se1 ppm	Selenium, ppm, INAA
Sm1 ppm	Samarium, ppm, INAA
Sr1 ppm	Strontium, ppm, INAA
Ta1 ppm	Tantalum, ppm, INAA
Tb1 ppm	Terbium, ppm, INAA
Th1 ppm	Thorium, ppm, INAA
U1 ppm	Uranium, ppm, INAA
W1 ppm	Tungsten, ppm, INAA
Yb1 ppm	Ytterbium, ppm, INAA
Zn1 ppm	Zinc, ppm, INAA
Zr1 ppm	Zirconium, ppm, INAA
Ag6 ppm	Silver, AAS
Rb6 ppm	Rubidium, AAS

VARIABLE	DESCRIPTION
Al2 %	Aluminum, %, ICP
As2 %	Arsenic, ppm, ICP
Ba2 ppm	Barium, ppm, ICP
Be2 ppm	Beryllium, ppm, ICP
Ca2 %	Calcium, %, ICP
Cd2 ppm	Cadmium, ppm, ICP
Ce2 ppm	Cerium, ppm, ICP
Co2 ppm	Cobalt, ppm, ICP
Cr2 ppm	Chromium, ppm, ICP
Cu2 ppm	Copper, ppm, ICP
Dy2 ppm	Dysprosium, ppm, ICP
Fe2 %	Iron, %, ICP
K2 %	Potassium, %, ICP
La2 ppm	Lanthanum, ppm, ICP
Li2 ppm	Lithium, ppm, ICP
Mg2 %	Magnesium, %, ICP
Mo2 ppm	Molybdenum, ppm, ICP
Mn2 ppm	Manganese, ppm, ICP
Na2 %	Sodium, %, ICP
Nb2 ppm	Niobium, ppm, ICP
Ni2 ppm	Nickel, ppm, ICP
P2 ppm	Phosphorus, ppm, ICP
Pb2 ppm	Lead, ppm, ICP
Sc2 ppm	Scandium, ppm, ICP
Sr2 ppm	Strontium, ppm, ICP
Ti2 ppm	Titanium, ppm, ICP
V2 ppm	Vanadium, ppm, ICP
Y2 ppm	Yttrium, ppm, ICP
Zn2 ppm	Zinc, ppm, ICP
Sample	Sample number
NTS	NTS sheet (1:50 000)
Easting	UTM map coordinate
Northing	UTM map coordinate
LOI %	Loss-on-ignition, %, gravimetric
Zone	UTM zone
Med	Soil horizon sampled
Depth	Sample depth (cm)

Quality Control

Duplicate samples taken at the same site in the field, as well as lab duplicates (duplicate analyses of random samples) of all elements are graphed in Appendices A-D. The extent of correlation of these graphs, which give a measure of analytical precision, is used to estimate data quality. If the duplicate samples provide identical results, a graph of sample results against duplicate results will be a straight line with slope of 1, and the correlation coefficient between the variables will be equal to 1. For elements that were analyzed using more than one method, the results were compared and the best method was chosen for mapping purposes. Duplicate data is not included in this report, but is available from the author upon request.

Accuracy estimates are given in Tables 2 and 3, which show the values from this study compared to the recommended values of standard reference materials.

The elements Ag, Hg, Ir, Lu and Sn were below detection limit in the INAA analysis and thus are not included in this report.

For some elements, the analysis of duplicates yields poor results, suggesting that the samples contain levels that are close to the element's detection limit. For this reason, it is hard to evaluate the data quality for Au, Cd, Cs, Mo, Sb, Se, Ta, Tb, U and W. Gold analyses are susceptible to the "nugget" effect, where the presence or absence of a native gold grain can cause differing results in duplicate samples.

Data presentation

Dot plots of selected elements (As, Au, Be, Cr, Cu, Fe, Mg, Mn, Ni, Pb, Sb, Ti, U, Zn) and loss on ignition (LOI) are shown on page sized colour bedrock map bases. The dots represent values within a particular size range, chosen by picking natural breaks using the Jenks statistical method. Dot plots of the remaining elements are available on the accompanying CD-ROM as .pdf files.

The appended data listings (Appendix E) provide the analytical data for all of the elements analyzed. The accompanying CD-ROM provides the same data as Excel 2001 files and as comma delimited text files (.csv). The numeric code distinguishes the type of analysis and the laboratory at which the analysis was done (Table 1).

The summary statistics for the data set are given in Table 4.

Table 2. Accuracy of till geochemical data by INAA: results of analyses of CANMET reference samples TILL-1 to 4. Observed values are compared against recommended values (from Lynch (1996)). In all cases, observed values are an average of 5 measurements.

		TILL-1		TILL-2		TILL-3		TILL-4	
		Observed	Reccom.	Observed	Reccom.	Observed	Reccom.	Observed	Reccom.
As1	ppm	17	18	26	26	89	87	110	111
Au1	ppb	15	13	2	2	5	6	3	5
Ba1	ppm	718	702	552	540	474	489	458	395
Br1	ppm	5.9	6.4	11.4	12.2	4.5	4.5	7.5	8.6
Ca1	%	1.40	1.94	0.90	0.91	1.70	1.88	0.70	0.89
Ce1	ppm	69	71	95	98	39	42	84	78
Co1	ppm	16	18	14	15	14	15	8	8
Cr1	ppm	58	65	75	74	124	123	47	53
Cs1	ppm	0.6	1.0	9.2	12.0	1.6	1.7	10.0	12.0
Eu1	ppm	1.7	1.3	1.3	1.0	0.9	<1	1.3	<1
Fe1	%	4.91	4.80	3.89	3.80	2.92	2.80	4.15	4.00
Hf1	ppm	15	13	13	11	8	8	12	10
La1	ppm	29	28	47	44	21	21	46	41
Mo1	ppm	3	<5	15	14	1.2	<5	12	16
Na1	%	2.11	2.01	1.77	1.62	2.12	1.96	1.98	1.82
Nd1	ppm	24	26	36	36	17	16	35	30
Ni1	ppm	39	24	1	32	1	39	1	17
Rb1	ppm	20	44	132	143	47	55	152	161
Sb1	ppm	6.7	7.8	0.9	0.8	1.2	0.9	1.3	1.0
Sc1	ppm	13	13	12	12	10	10	11	10
Se1	ppm	0.9	?	0.7	?	0.5	?	0.8	?
Sm1	ppm	6.0	5.9	7.5	7.4	3.3	3.3	6.6	6.1
Sr1	ppm	0.03	291	0.03	144	0.03	300	0.03	109
Ta1	ppm	0.1	0.7	1.7	1.9	0.9	<0.5	0.8	1.6
Tb1	ppm	0.8	1.1	0.9	1.2	0.4	<0.5	1.1	1.1
Th1	ppm	5.5	5.6	17.6	18.4	4.5	4.6	16.8	17.4
U1	ppm	1.9	2.2	4.8	5.7	2.3	2.1	4.3	5.0
W1	ppm	0.5	<1	4	5	0.5	<1	170	204
Yb1	ppm	4.2	3.9	4.3	3.7	1.6	1.5	3.7	3.4
Zn1	ppm	107	98	126	130	25	56	79	70
Zr1	%	0.038	502	0.030	390	0.010	390	0.032	385

Table 3. Accuracy of till geochemical data by ICP, AAS and gravimetry: results of analyses of CANMET reference samples TILL-1 to 4. Observed values are compared against recommended values (from Lynch (1996)). In all cases, observed values are an average of 5 measurements.

		TILL-1		TILL-2		TILL-3		TILL-4	
		Observed	Reccom.	Observed	Reccom.	Observed	Reccom.	Observed	Reccom.
Al2	%	6.5	7.3	7.8	8.5	6.0	6.5	7.0	7.6
As2	ppm	18	18	28	26	87	87	110	111
Ba2	ppm	706	702	546	540	491	489	391	396
Be2	ppm	1.4	2.4	3.3	4.0	1.2	2.0	2.9	3.7
Ca2	%	1.73	1.94	0.87	0.91	1.72	1.88	0.86	0.89
Cd2	ppm	0.21	?	0.23	?	0.08	?	0.10	?
Ce2	ppm	63	71	89	98	37	42	69	78
Co2	ppm	19	18	16	15	15	15	8	8
Cr2	ppm	56	65	63	74	103	123	41	53
Cu2	ppm	42	47	162	150	17	22	264	237
Dy2	ppm	4.5	?	3.8	?	2.0	?	3.3	?
Fe2	%	4.84	4.81	3.84	3.84	2.67	2.78	3.91	3.97
K2	%	1.71	1.84	2.35	2.55	1.88	2.01	2.47	2.70
La2	ppm	28	28	47	44	20	21	42	41
Li2	ppm	16	15	48	47	22	21	30	30
Mg2	%	1.22	1.30	1.05	1.10	0.99	1.03	0.72	0.76
Mn2	ppm	1514	1420	834	780	533	520	529	490
Mo2	ppm	1.7	2.0	13.8	14.0	1.4	2.0	15.2	16.0
Na2	%	2.03	2.01	1.74	1.62	2.06	1.96	1.92	1.82
Nb2	ppm	11	10	18	20	7	7	15	15
Ni2	ppm	23	24	30	32	37	39	18	17
P2	ppm	916	930	730	750	486	490	893	880
Pb2	ppm	23	22	34	31	27	26	50	50
Sc2	ppm	13.6	13.0	12.5	12.0	9.6	10.0	10.7	10.0
Sr2	ppm	297	291	152	144	309	300	118	109
Ti2	ppm	5367	5990	5214	5300	2855	2910	4864	4840
V2	ppm	98	99	78	77	58	62	61	67
Y2	ppm	28	38	20	40	13	17	17	33
Zn2	ppm	93	98	125	130	55	56	71	70
Zr2	ppm	100	502	100	390	80	390	89	385
Rb6	ppm	37	44	132	143	47	55	153	161
Ag6	ppm	0.1	0.2	0.1	0.2	1.2	1.6	0.1	<0.2
LOI	%	6.6	6.3	7.1	6.8	3.9	3.6	4.8	4.4

Table 4. Summary statistics for analyzed elements.

		Detection limit	Minimum	Maximum	Median	Mean	Standard Deviation
Ag6	ppm	0.1	0.5	0.30	0.05	0.5	0.03
Al2	%	0.01	1.35	10.68	6.75	6.83	0.99
As1	ppm	0.5	0.25	2300	3.8	13.44	122.99
As2	ppm	1	0.50	2529	4	15	135
Au1	ppb	1	0.5	2360	0.5	9.2	124.8
Ba1	ppm	50	25	1700	450	498	212
Ba2	ppm	50	52	1739	488	546	231
Be2	ppm	0.2	0.1	15.8	2.0	2.2	1.1
Br1	ppm	0.5	0.25	160	10	19	25
Ca1	%	1	0.5	8.0	1.0	1.3	1.0
Ca2	%	0.01	0.06	7.00	1.30	1.41	0.82
Cd2	ppm	0.1	0.05	2.24	0.05	0.07	0.12
Ce1	ppm	3	9	340	65	78	49
Ce2	ppm	2	11	337	67	75	42
Co1	ppm	1	0.5	49	13	14	8
Co2	ppm	2	1	57	17	17	10
Cr1	ppm	5	2.5	1300	100	188	202
Cr2	ppm	2	3	392	79	96	60
Cs1	ppm	1	0.5	17	2	2	1.7
Cu2	ppm	2	1	234	14	24	30
Dy2	ppm	0.2	0.1	35.9	3.9	4.2	2.5
Eu1	ppm	0.5	0.3	4.9	1.3	1.4	0.6
Fe1	%	0.1	0.11	13.90	3.90	4.16	1.84
Fe2	%	0.01	0.26	14.58	3.96	4.26	1.94
Hf1	ppm	1	0.5	70	12	14	8
K2	%	0.01	0.12	4.62	1.78	1.80	0.57
La1	ppm	1	3	290	30	36	25
La2	ppm	1	2	308	31	35	23
Li2	ppm	0.2	1.4	97.4	17.5	21.1	14.6
LOI	%	0.01	0.81	87.60	4.70	7.25	8.01
Mg2	%	0.01	0.03	3.87`	1.23	1.31	0.70
Mn2	ppm	2	48	5846	692	728	450
Mo1	ppm	1	0.5	11	0.5	1.4	1.9
Mo2	ppm	1	0.5	16.6	1.4	1.6	1.2
Na1	%	0.1	0.04	4.19	2.10	2.05	0.54

		Detection limit	Minimum	Maximum	Median	Mean	Standard Deviation
Na2	%	0.01	0.21	4.14	2.13	2.05	0.55
Nb2	ppm	2	1	63	15	17	8
Nd1	ppm	5	2.5	220	24	29	20
Ni1	ppm	2	1	550	29	29	65
Ni2	ppm	2	2	417	32	57	60
P2	ppm	5	47	3090	671	744	484
Pb2	ppm	2	7	95	18	21	10
Rb1	ppm	15	7.5	200	58	60	30
Rb6	ppm	5	6	266	58	63	34
Sb1	ppm	0.1	0.05	3.00	0.33	0.31	0.29
Sc1	ppm	0.1	0.5	49	12	13	6
Sc2	ppm	2	1.6	49.0	13.5	14.1	6.0
Se1	ppm	1	0.5	6.0	0.5	0.6	0.5
Sm1	ppm	0.1	0.7	43	5.3	6.2	3.8
Sr1	ppm	0.05	0.03	0.09	0.03	0.03	0.01
Sr2	ppm	2	25	937	200	146	128
Ta1	ppm	0.2	0.1	10	0.5	0.9	1.0
Tb1	ppm	0.5	0.3	6.4	0.7	0.8	0.5
Th1	ppm	0.2	0.1	52	7.1	8.3	5.3
Ti2	ppm	5	739	24830	6003	6410	2865
U1	ppm	0.5	0.25	11	2.2	2.4	1.4
V2	ppm	5	3	427	96	104	57
Y2	ppm	2	3	181	23	24	13
W1	ppm	1	0.5	170	0.5	1.1	9.0
Yb1	ppm	0.2	0.1	15.9	3.3	3.5	1.4
Zn1	ppm	5	2.5	1690	2.5	55.3	103
Zn2	ppm	2	13	1945	57	71	105
Zr1	%	0.01	0.005	0.11	0.03	0.03	0.02

GEOCHEMICAL RESULTS AND INTERPRETATION

Till in the region is generally thin (<2 m thick). It is rarer near the coast and in the upland regions of the Long Range Mountains. It is also less common below 70 m asl, the local marine limit, and could be confused with glaciomarine diamicton at these elevations. In areas where B- or BC-horizon samples were taken, the samples were noted, as they can be depleted in some elements and enhanced in others due to soil-forming processes.

Gold, Arsenic and Antimony

The analytical results for gold are highly variable (Figure 5). The duplicate graphs (Appendices B and D) show poor correlation and as a result, these values should be interpreted with caution. However, pathfinders can be useful in many cases where gold data are poor. Arsenic and antimony have been found to be pathfinders for gold in lake sediments in the region (McConnell and Honarvar, 1989) and the known gold mineralization area of the Doucers Valley fault complex (Owen, 1991; Tuach, 1987) shows high As and Sb values, which indicates that they also act as pathfinders for gold in till in this area (Figures 6 and 7). Statistical analysis of Au and As values gives a correlation coefficient of 0.986. These factors suggest that Sb, and particularly As, can be used in the White Bay area as gold pathfinders in till. When taken together with the presence of clastic and carbonate rocks in the Jackson's and Doucers valleys, the geochemistry is certainly suggestive of Carlin-type mineralization (Bonham Jr., 1985; Rytuba, 1985).

The dispersed gold values show possible areas of mineralization north of Jackson's Arm and in the Lake Michel Intrusive Suite. A few other high values (>10 ppb) are found east of White Bay, possibly reflecting northwestward dispersion from Dunnage Zone rocks. A single site with very high values (sample 1058: 2360 ppb Au; 2300 ppm As) of gold and arsenic was found at the western edge of the Doucers Valley fault complex. Such high values could reflect the nugget effect, but re-analysis of a different split of the same sample yielded similar results. A number of gold mineral occurrences around this site may be the source of the elevated gold values in the sample. The duplicate data for this sample is included for reference in the data listing (Appendix E) and on the CD-ROM.

Arsenic and antimony show stronger clustering in the Doucers and Jackson's valleys, especially north of Jackson's Arm (hereafter referred to as the Jackson's Arm gold zone). There may be some southeastward dispersal (Flow 3) in this area, but transport distances may be minimal due to the steep sides of the two valleys. Antimony, however, shows a well-developed dispersal train extending southeastward from the gold zone.

Both arsenic and antimony have high values clustered over the Anguille Group, suggesting that gold mineralization may occur there as well. This area has yet to be prospected for gold. If there is some southeastward dispersal here, then it is possible that the tuff and rhyolite of the Sops Arm Group are also prospective.

Antimony has mid to high range values that decline northwestward from Dunnage Zone rocks. This appears to be a fan-shaped dispersal train emanating from the oceanic rocks southeast and east of the study area. Sediments of the Sops Arm Group also show moderate values.

Canadian soil quality guidelines dictate that arsenic levels in soil should be below 12 ppm for health purposes. Elevated arsenic values around the communities of Hampden and Jackson's Arm may be cause for some concern. Investigation of the water supplies in these communities may be warranted.

Beryllium

Beryllium values are relatively high, reaching a maximum of 15.8 ppm (Figure 8). Higher values occur just north of Sops Arm and around Gull Lake, both possibly showing southeastward dispersal from the Long Range Mountains. Values are moderate over the schists and amphibolites of the Fleur de Lys Group.

Chromium

Chromium (Figure 9) values peak at 1300 ppm. A large fan-shaped dispersal train in the east likely reflects flow 2 and 3 transport from Dunnage Zone mafic/ultramafic rocks.

Copper, Lead and Zinc

Anomalous values of these three elements are generally found in the same areas (Figures 10-12). The Doucers Valley fault complex is the main area of interest, notably the 1945 ppm Zn value in the southwest. High values in the Hampden area could be from either the Anguille or White Bay Groups, depending on whether northeastward or southwestward dispersal was stronger. This area is one in which base metal mineralization has not previously been reported; these elements do not appear as highs in the lake sediment data (Davenport *et al.,* 1999).

Iron and Loss on Ignition

Loss on ignition results provide an indication of concentrations of organic matter present in a sample. They correlate well with the locations of B-horizon samples, which are commonly enriched in iron. A comparison of LOI with the geochemical data for iron (Figures 13 and 14) shows that some high iron values can be explained by the fact that the B-horizon was sampled. However, a few areas are not correlative and high iron values must be present in the unaltered till. These include the Jackson's Arm gold area, the Doucers Valley fault complex, the Hampden area and the area northwest of Wild Cove Pond.

Magnesium

Magnesium seems to be independent of loss on ignition (Figure 15). High values mirror those of iron except for the fact that it also shows a fan-shaped dispersal trend from the Dunnage Zone, perhaps reflecting the presence of olivine in these rocks.

Manganese

Manganese values are high in the Jackson's Arm gold zone, along the Doucers Valley Fault complex, and in the Hampden area (Figure 16). The highs also extend northward through the Anguille Group.

Nickel

Nickel values form a smooth dispersal fan originating in the Dunnage Zone rocks (Figure 17).

Titanium

Some of the titanium values are fairly high (>16 000 ppm, Figure 18), but they are neither tightly clustered nor tapering off in one direction. As a result, it is difficult to pinpoint likely source areas for this element. Vanadium (not shown) has high values in many of the same locations.

Uranium

There are several sites with uranium values over 5.4 ppm (Figure 19). The lack of clustering, however, makes the possible sources of uranium difficult to isolate. High values in the Jackson's Arm, Bear Cove and Hampden areas may be a safety concern for drinking water in those communities.

CONCLUSIONS

Not unexpectedly, the Doucers Valley fault complex appears to be highly prospective. It displays till geochemical anomalies for Au, As, Sb, Cu, Pb, Zn, Fe, Mg and Mn. In particular, the association of Au, As and Sb is suggestive of Carlin-type mineralization. The most prospective area is the Jackson's Arm gold zone, which is just north of Jackson's Arm.

A new possible prospective zone encompasses the town of Hampden and the Anguille Group to the west of it. As, Cu, Fe, Mg, Mn, Sb and Zn are all enriched in this vicinity.

Some elements (Cr, Mg, Ni and Sb) form fan-shaped dispersal trains that appear to emanate from Dunnage Zone oceanic rocks that outcrop to the southeast of the study area.

ACKNOWLEDGMENTS

General field assistance (till sampling and mapping) was provided by Amy Newport; Martin Batterson and Dave Taylor helped with the helicopter component of the till sampling. Sid Parsons and Jerry Hickey provided logistical support and Dave Leonard drafted part of Figure 1. Dave Liverman and Martin Batterson provided helpful reviews of the manuscript.

REFERENCES

Betz, F.J.
1948: Geology and mineral deposits of southern White Bay. Newfoundland Geological Survey Bulletin, Volume 24, page 28.

Blake, W.J.
1988: Geological Survey of Canada Radiocarbon Dates XXVII, 100 pages.

Bonham Jr., H.F.
1985: Characteristics of bulk-minable gold-silver deposits in Cordilleran and island-arc settings. *In* Geologic Characteristics of Sediment- and Volcanic-Hosted Disseminated Gold Deposits-Search for an Occurrence Model. U.S.G.S. Bulletin 1646. *Edited by* E.W. Tooker. United States Geological Survey, Washington, pages 71-77.

Cawood, P.A., Dunning, G.R., Lux, D., and Van Gool, J.A.M.
1994: Timing of peak metamorphism and deformation along the Appalachian margin of Laurentia in Newfoundland – Silurian, not Ordovician. Geology, Volume 22, pages 399-402.

Davenport, P.H., and Nolan, L.W.
1989: Mapping the regional distribution of gold in Newfoundland using lake sediment geochemistry. *In* Current Research. Newfoundland Department of Mines and Energy, Geological Survey Branch, Report 89-1, pages 259-266.

Davenport, P.H., Nolan, L.W., Wardle, R.W., Stapleton, G.J., and Kilfoil, G.J.
1999: Digital Geoscience Atlas of Labrador. Geological Survey of Newfoundland and Labrador.

Hibbard, J.P.
1983: Geology of the Baie Verte Peninsula, Newfoundland. Newfoundland Department of Mines and Energy, Memoir 2, 279 pages.

Liverman, D.G.E.
1992: Application of regional Quaternary mapping to mineral exploration, northeastern Newfoundland, Canada. Transactions of the Institution of Mining and Metallurgy, Volume 101, pages B89-98.

Lynch, J.
1996: Provisional Elemental Values for Four New Geochemical Soil and Till Reference Materials, Till-1, Till-2, Till-3 and Till-4. Geostandards Newsletter, Volume 20, pages 277-287.

McConnell, J.W., and Honarvar, P.
1989: A study of the distribution of Au and associated elements in soils in proximity to gold mineralization. Newfoundland and Labrador Geological Survey, Open File 1790, 135 pages.

McCuaig, S.J.
2003: Glacial history and Quaternary geology of the White Bay region. *In* Current Research. Newfoundland Department of Mines and Energy, Geological Survey, Report 03-1, pages 279-292.

Owen, J.V.
1991: Geology of the Long Range Inlier, Newfoundland. Geological Survey of Canada, Bulletin 395, 89 pages.

Rytuba, J.J.
1985: Geochemistry of hydrothermal transport and deposition of gold and sulfide minerals in Carlin-type gold deposits. *In* Geologic Characteristics of Sediment- and Volcanic-Hosted Disseminated Gold Deposits-Search for an Occurrence Model. U.S.G.S. Bulletin 1646. *Edited by* E.W. Tooker. United States Geological Survey, Washington, pages 27-34.

Smyth, W.R., and Schillereff, S.
1982: The pre-Carboniferous geology of southwest White Bay. *In* Current Research. Newfoundland Department of Mines and Energy, Mineral Development Division, Report 82-1, pages 78-98.

Tuach, J.
1987: Mineralized environments, metallogenesis, and the Doucers Valley Fault complex, western White Bay: a philosophy for gold exploration in Newfoundland. *In* Current Research. Newfoundland Department of Mines and Energy, Geological Survey Branch, Report 87-1, pages 129-144.

Vanderveer, D.G., and Taylor, D.M.
1987: Quaternary mapping – glacial-dispersal studies, Sops Arm area, Newfoundland. *In* Current Research. Newfoundland Department of Mines and Energy, Geological Survey Branch, Report 87-1, pages 31-38.

Wagenbauer, H.A., Riley, C.A., and Dawe, G.
1983: The Geochemical Laboratory. In Current Research. Newfoundland Department of Mines and Energy, Mineral Development Division, Report 83-1, pages 133-137.

Williams, H.
1979: Appalachian orogen in Canada. Canadian Journal of Earth Science, Volume 16, pages 792-807.

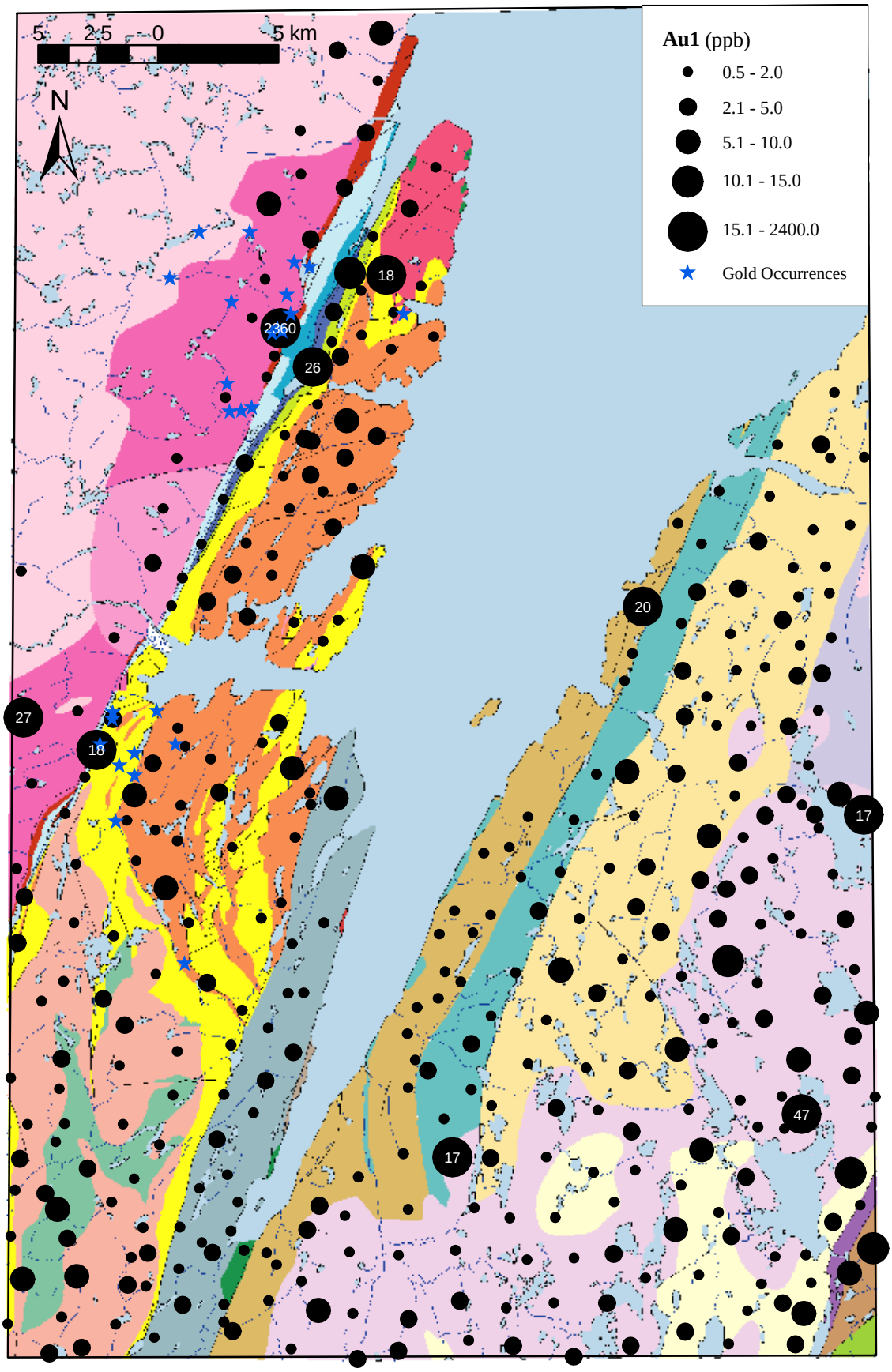

Figure 5. Gold values in till. Open File NFLD/2823.

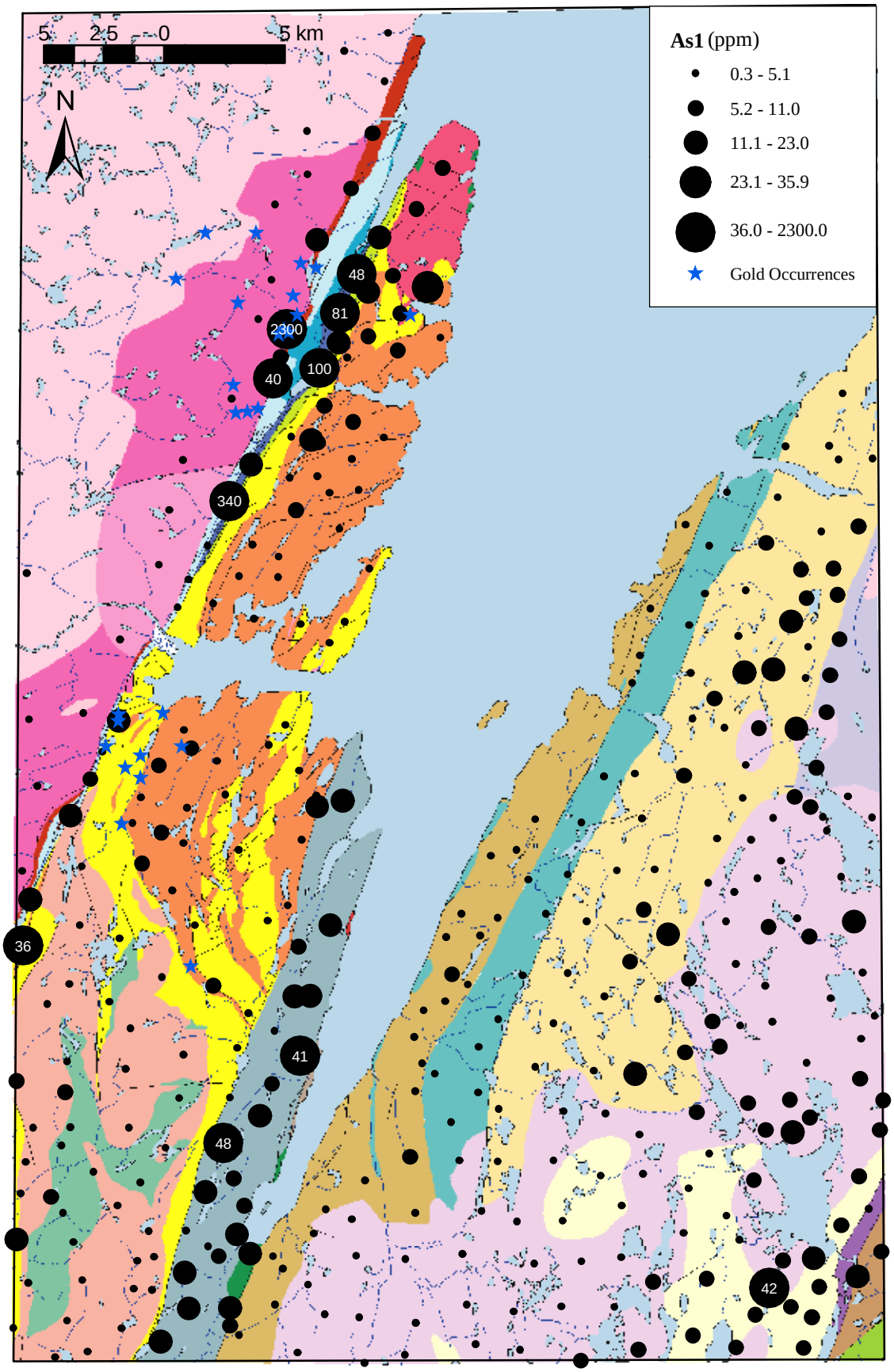

Figure 6. Arsenic values in till. Open File NFLD/2823.

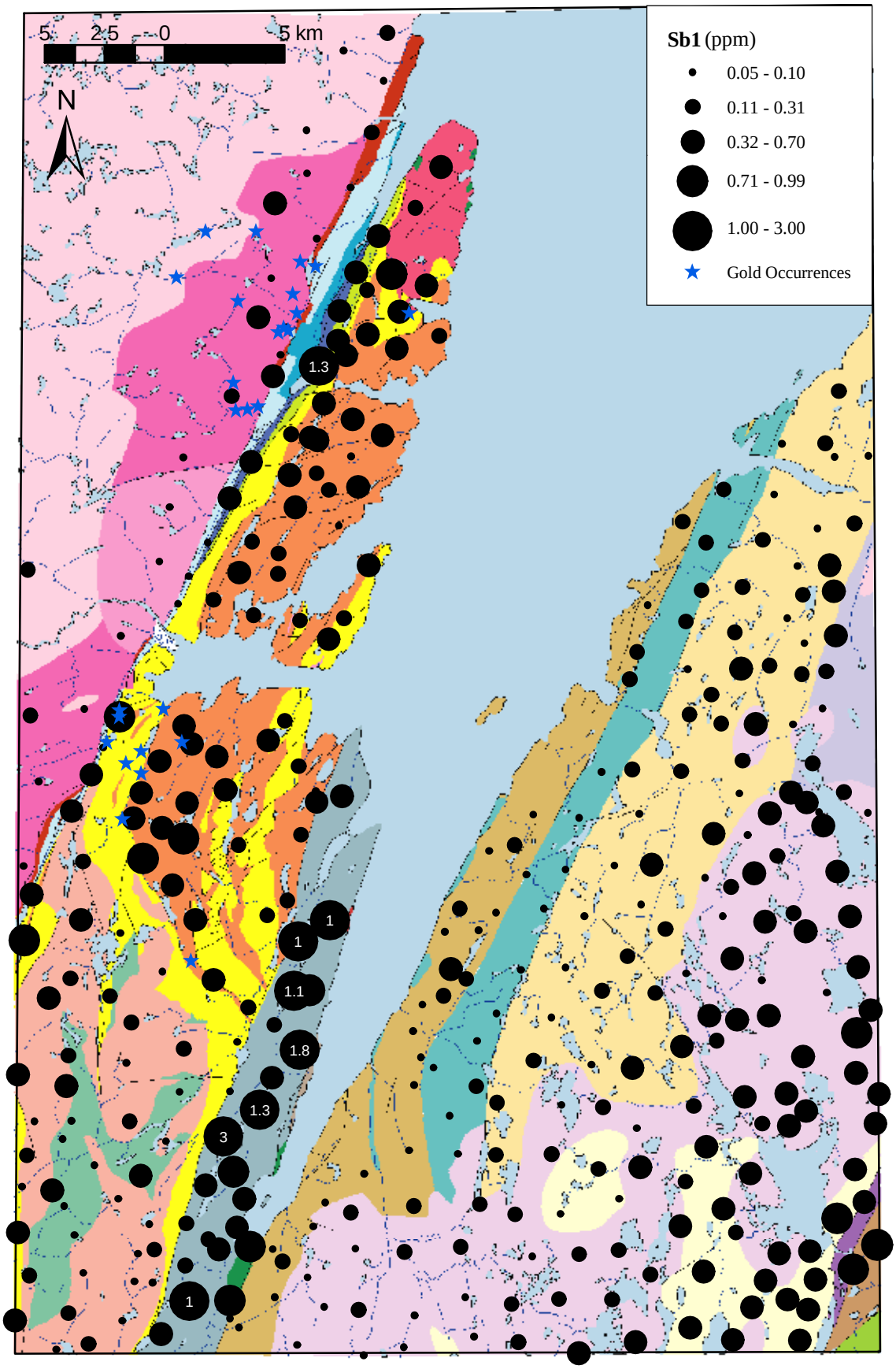

Figure 7. Antimony values in till. Open File NFLD/2823.

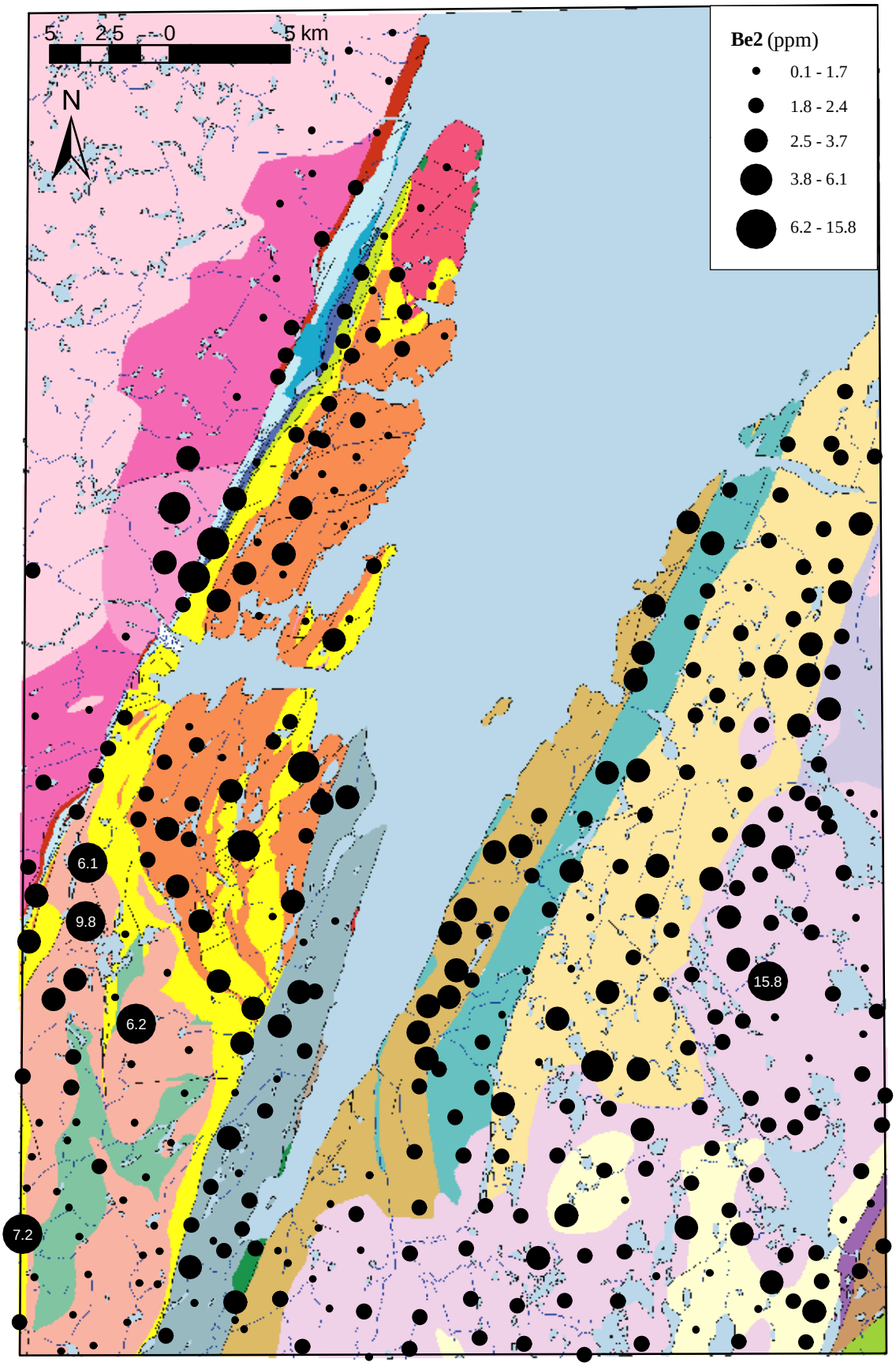

Figure 8. Beryllium values in till. Open File NFLD/2823.

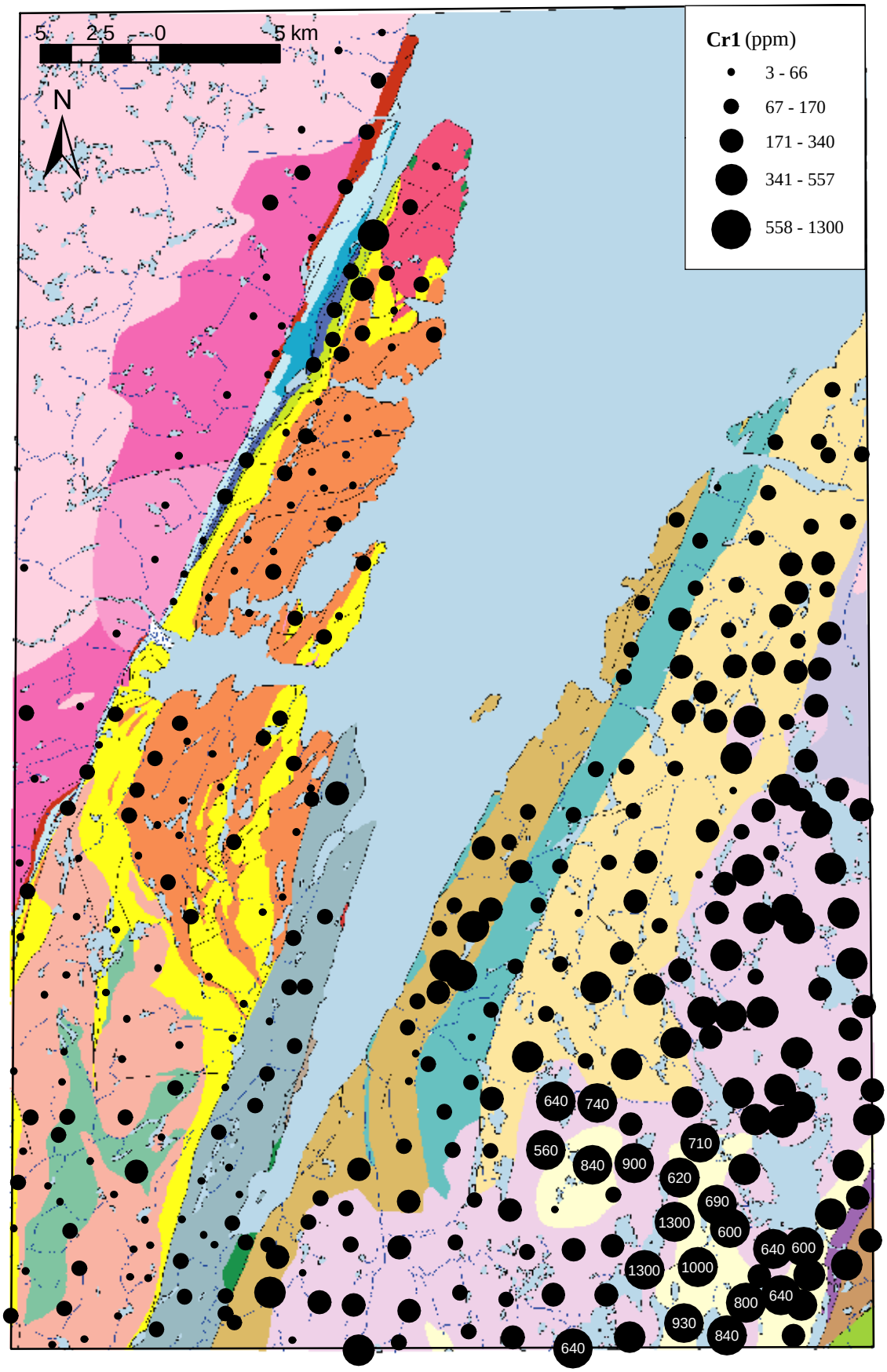

Figure 9. Chromium values in till. Open File NFLD/2823.

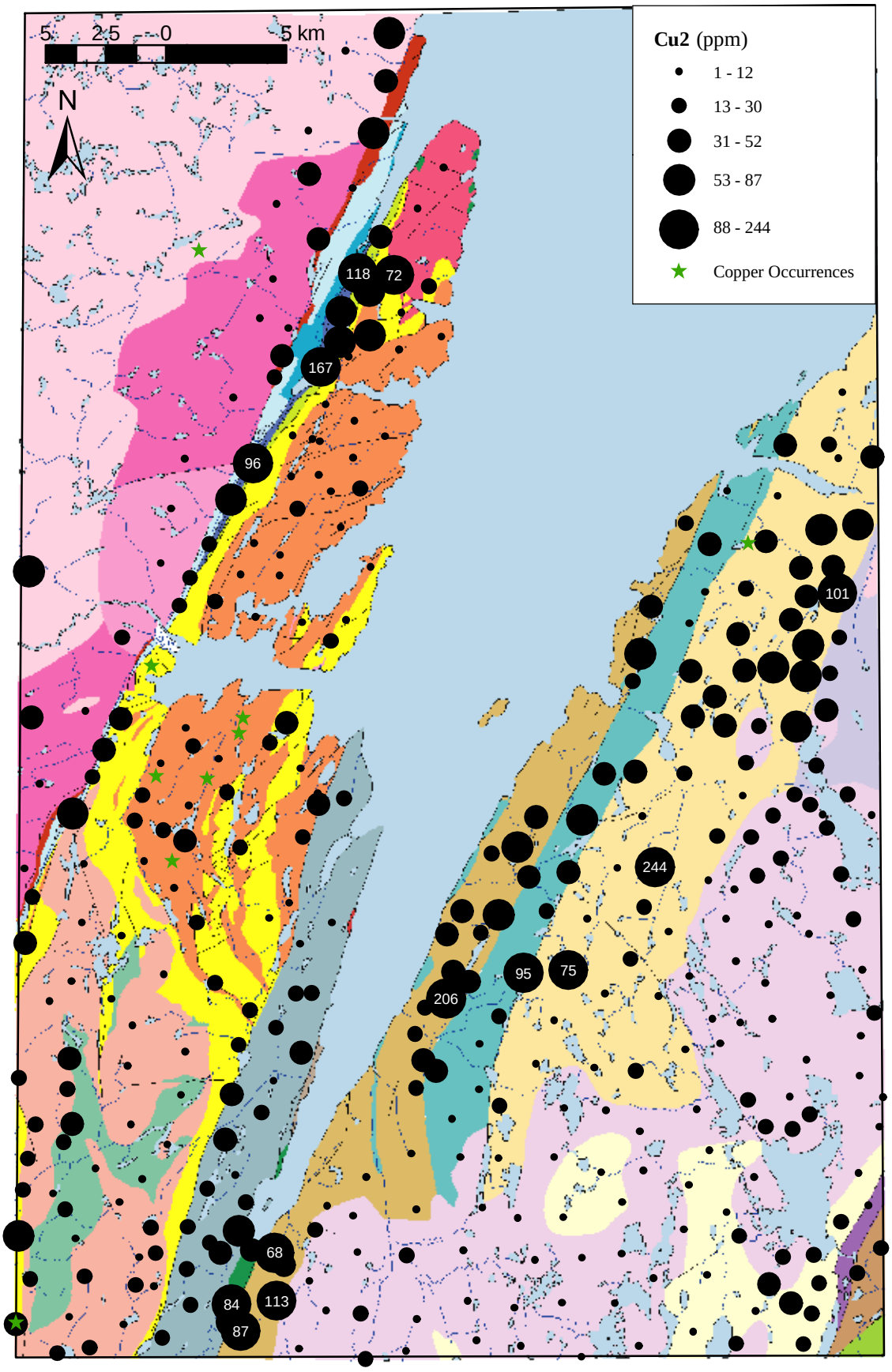

Figure 10. Copper values in till. Open File NFLD/2823.

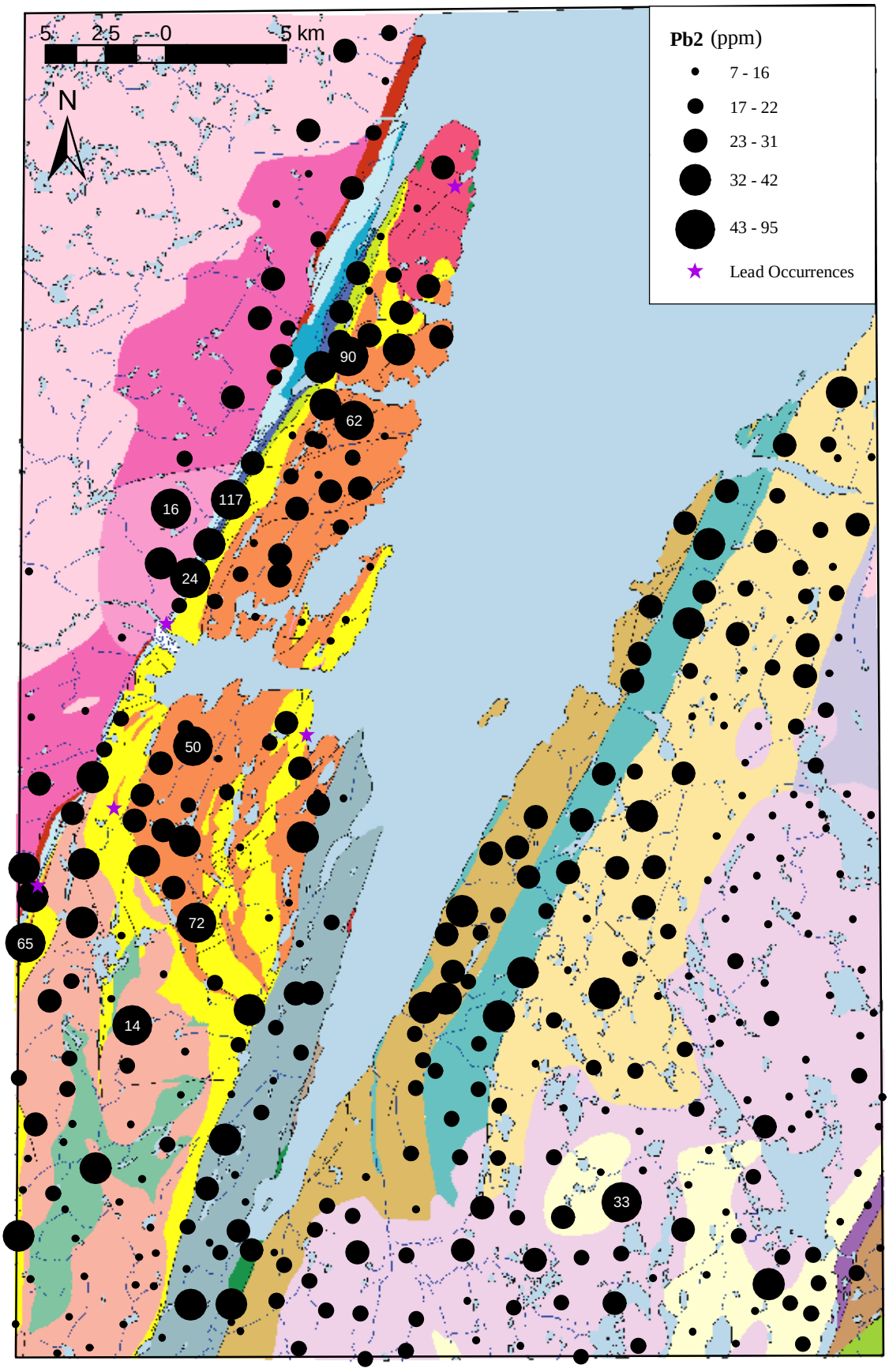

Figure 11. Lead values in till. Open File NFLD/2823.

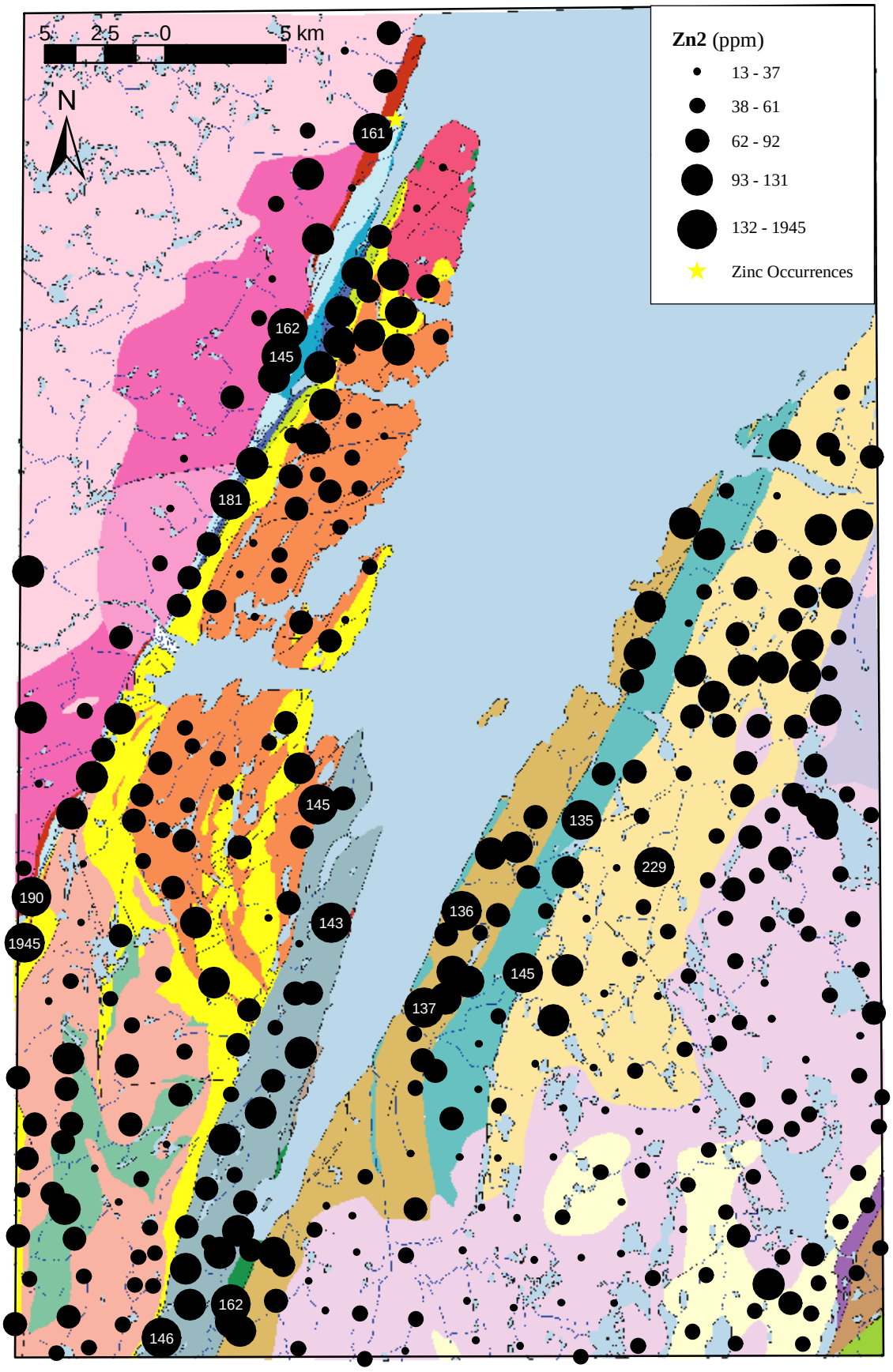

Figure 12. Zinc values in till. Open File NFLD/2823.

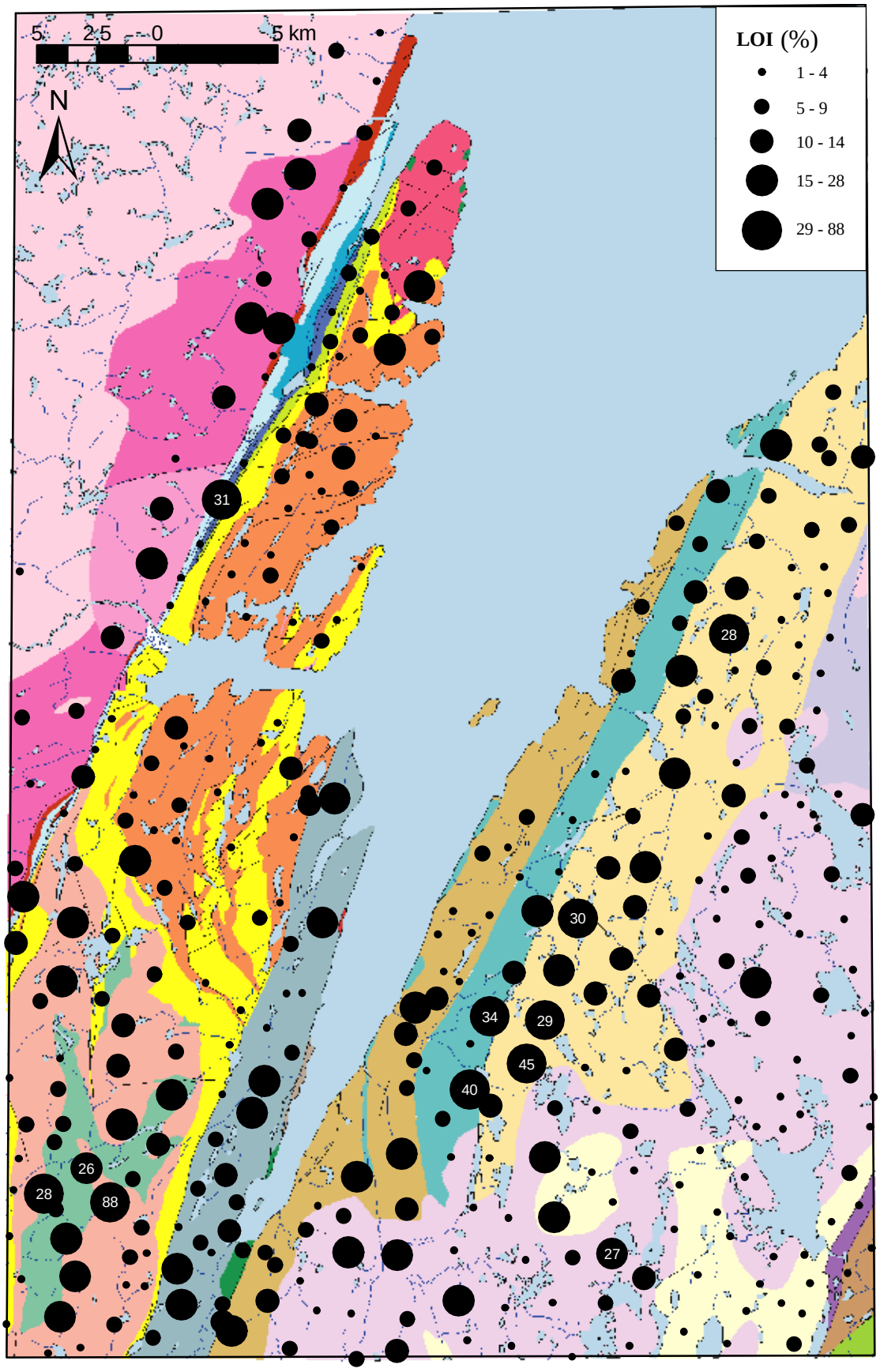

Figure 13. Loss on ignition values in till. Open File NFLD/2823.

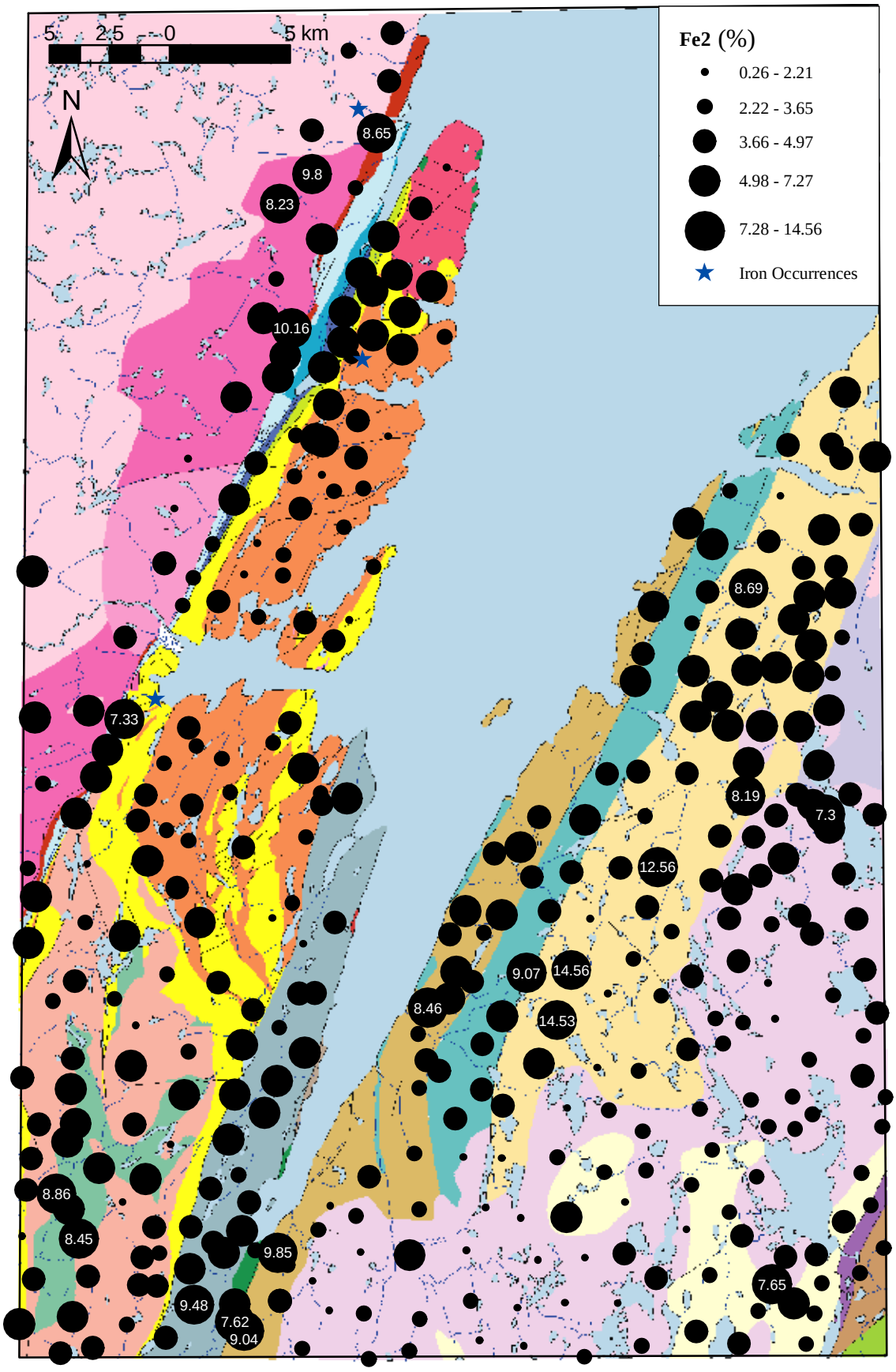

Figure 14. Iron values in till. Open File NFLD/2823.

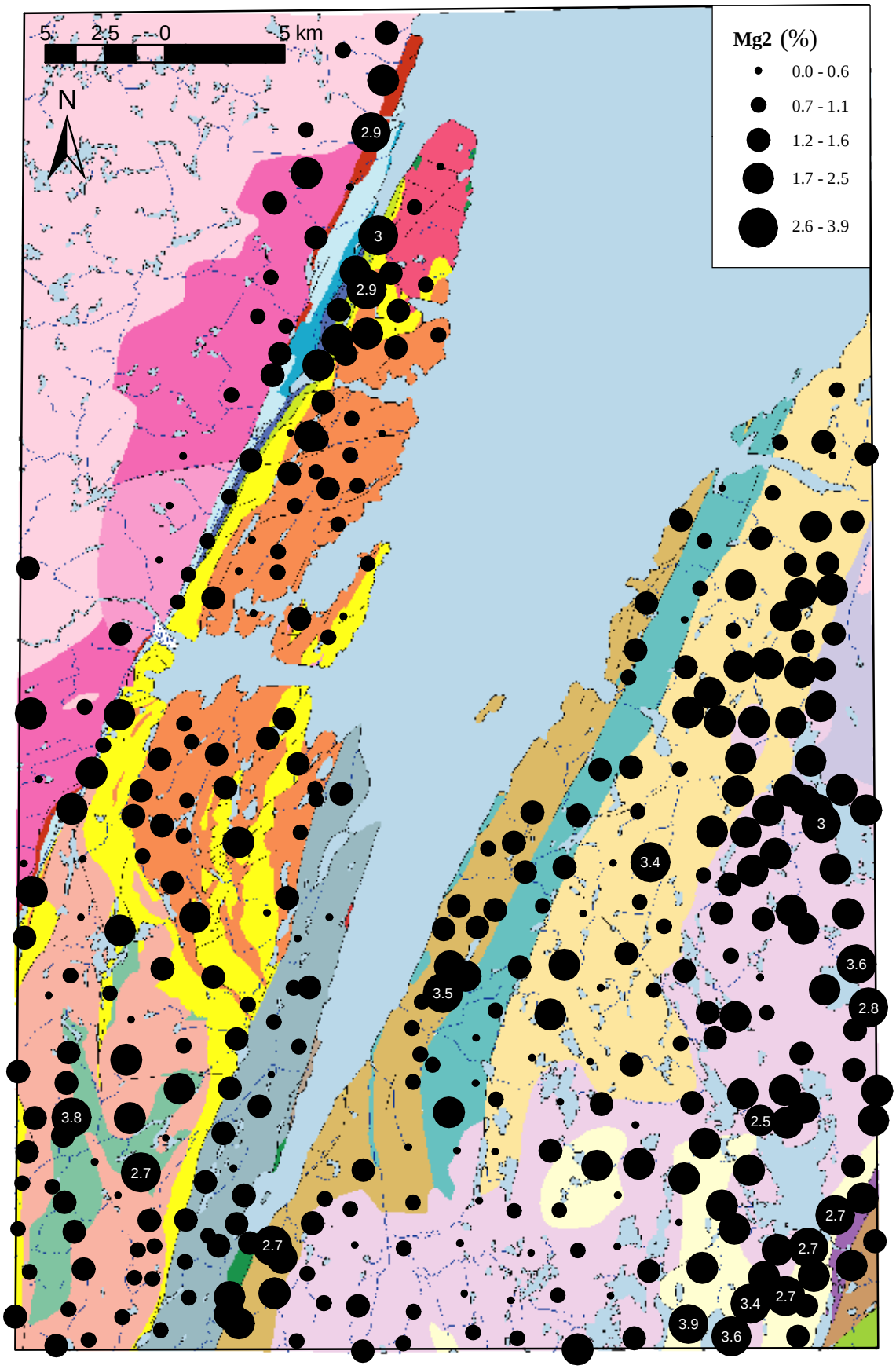

Figure 15. Magnesium values in till. Open File NFLD/2823.

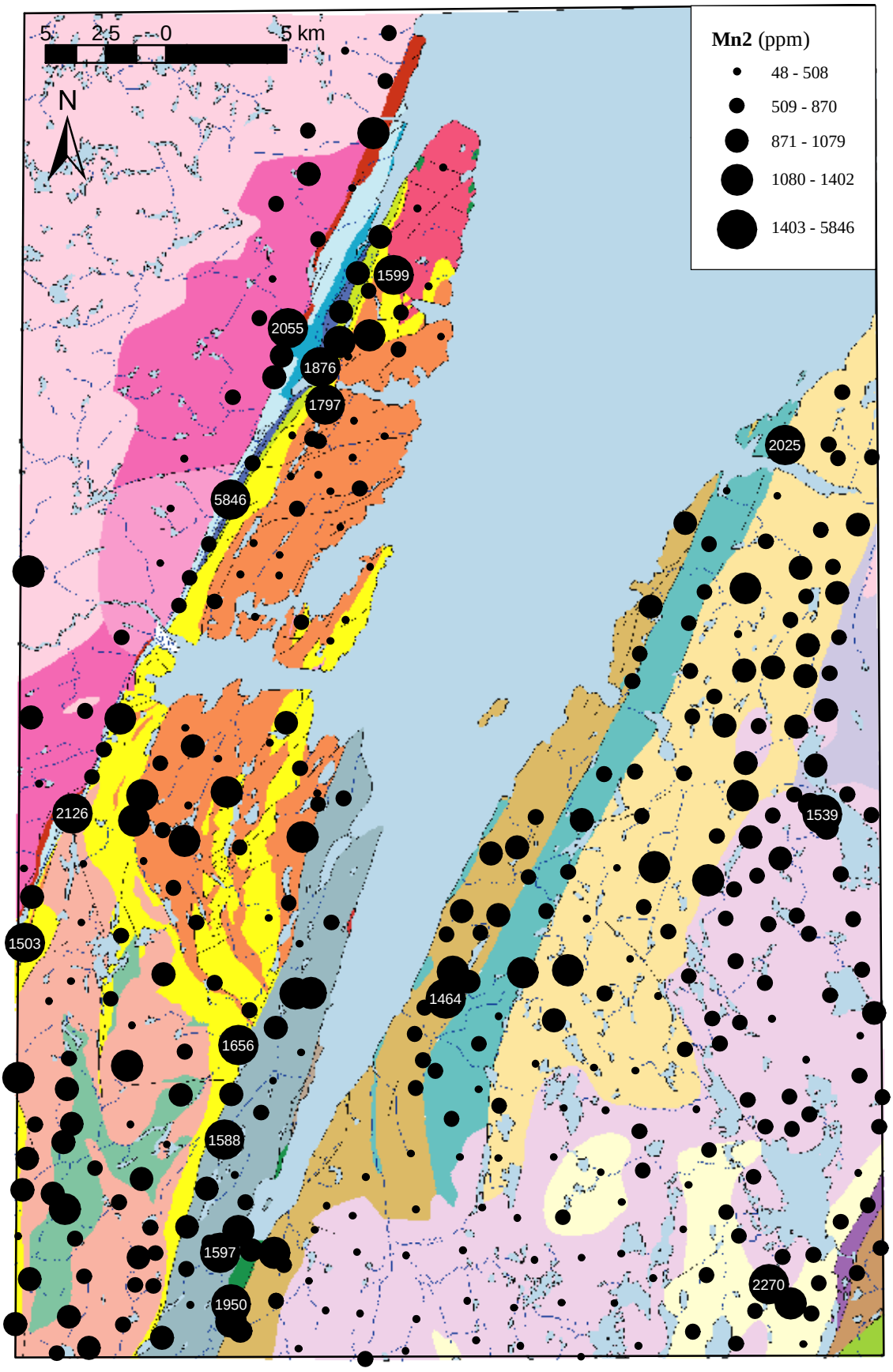

Figure 16. Manganese values in till. Open File NFLD/2823.

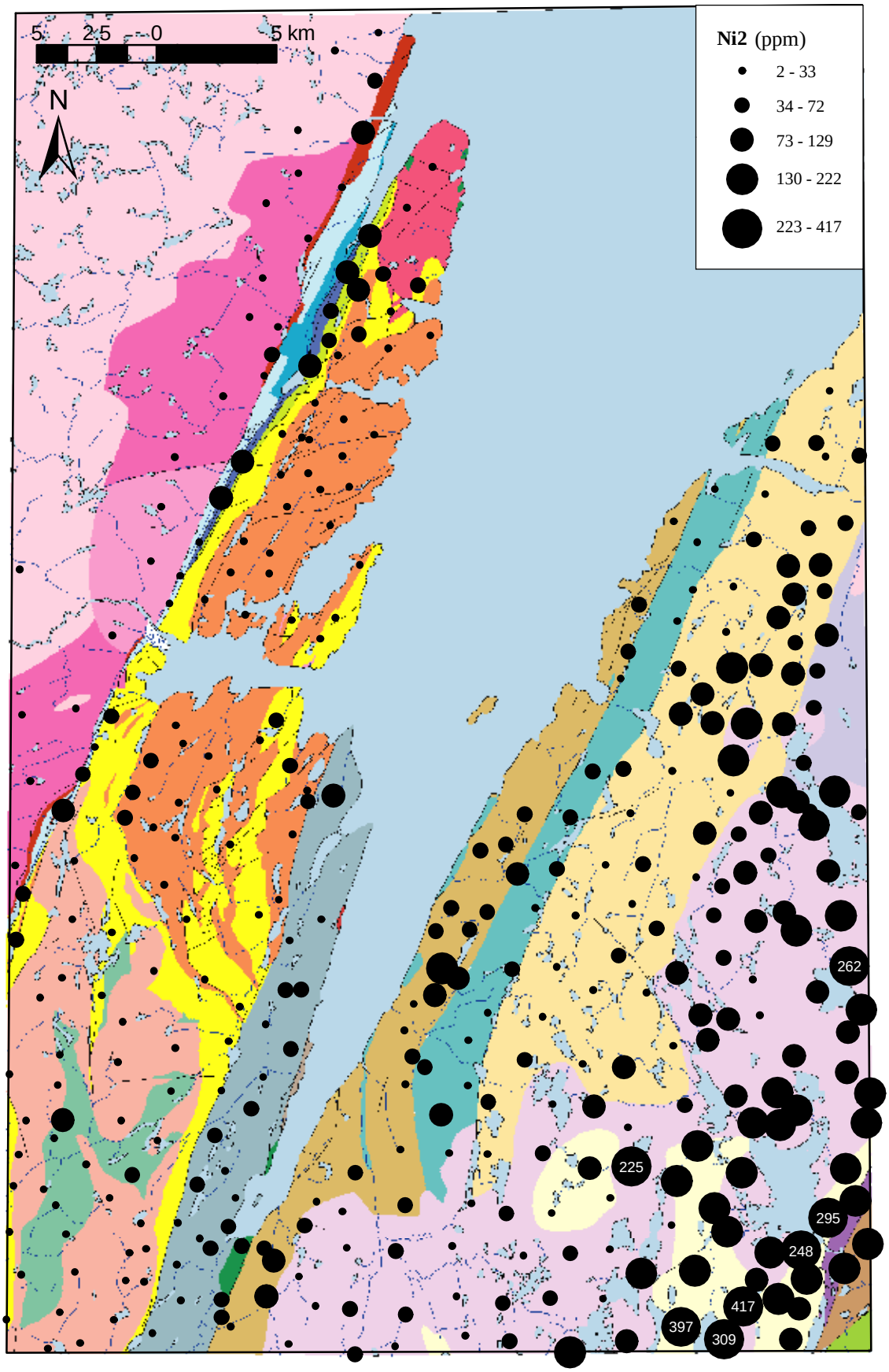

Figure 17. Nickel values in till. Open File NFLD/2823.

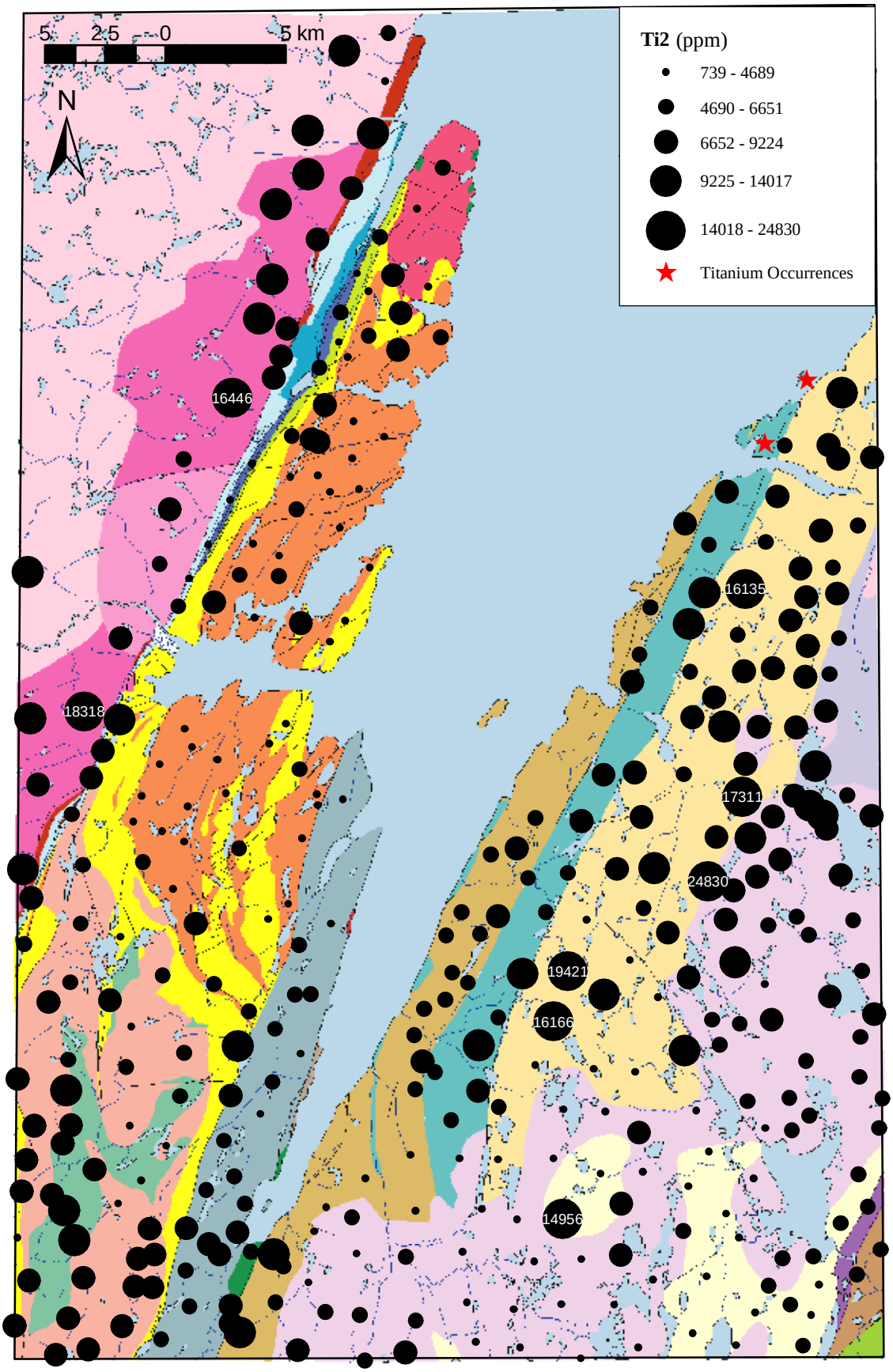

Figure 18. Titanium values in till. Open File NFLD/2823.

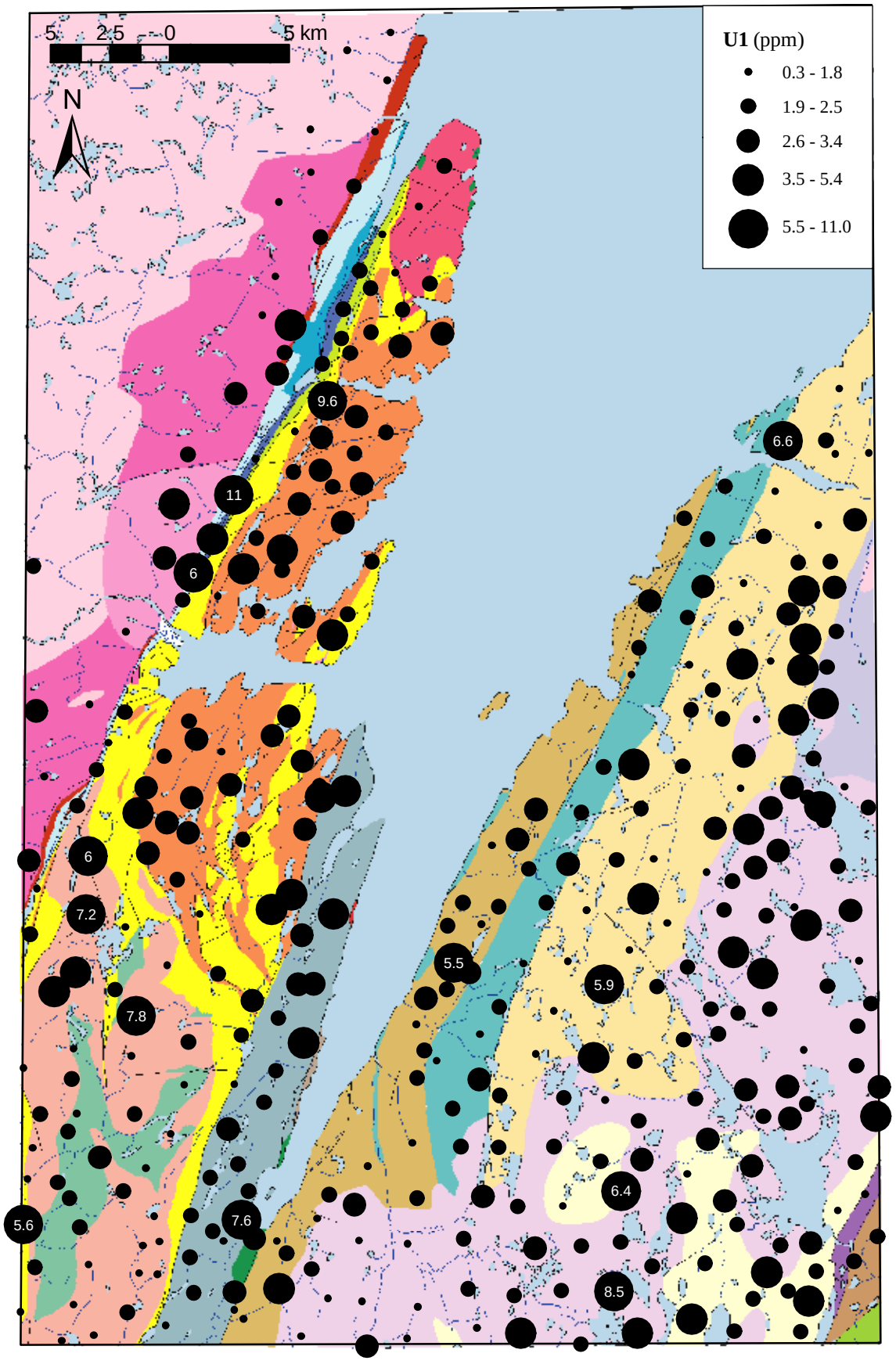

Figure 19. Uranium values in till. Open File NFLD/2823.

Appendix A: Comparison plots of laboratory duplicates for elements analysed by ICP and AAS (Ag, Rb).

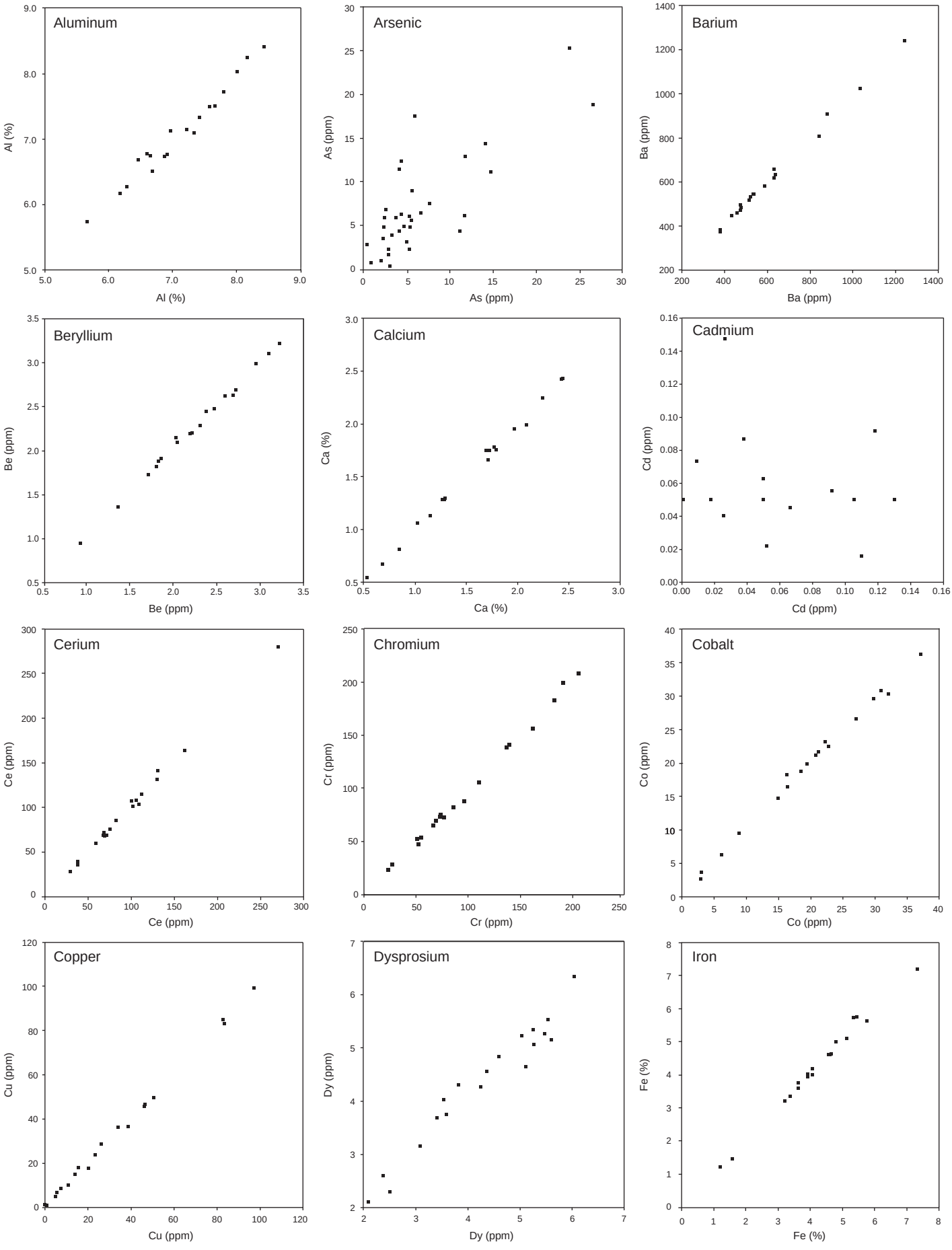

Appendix A: cont.

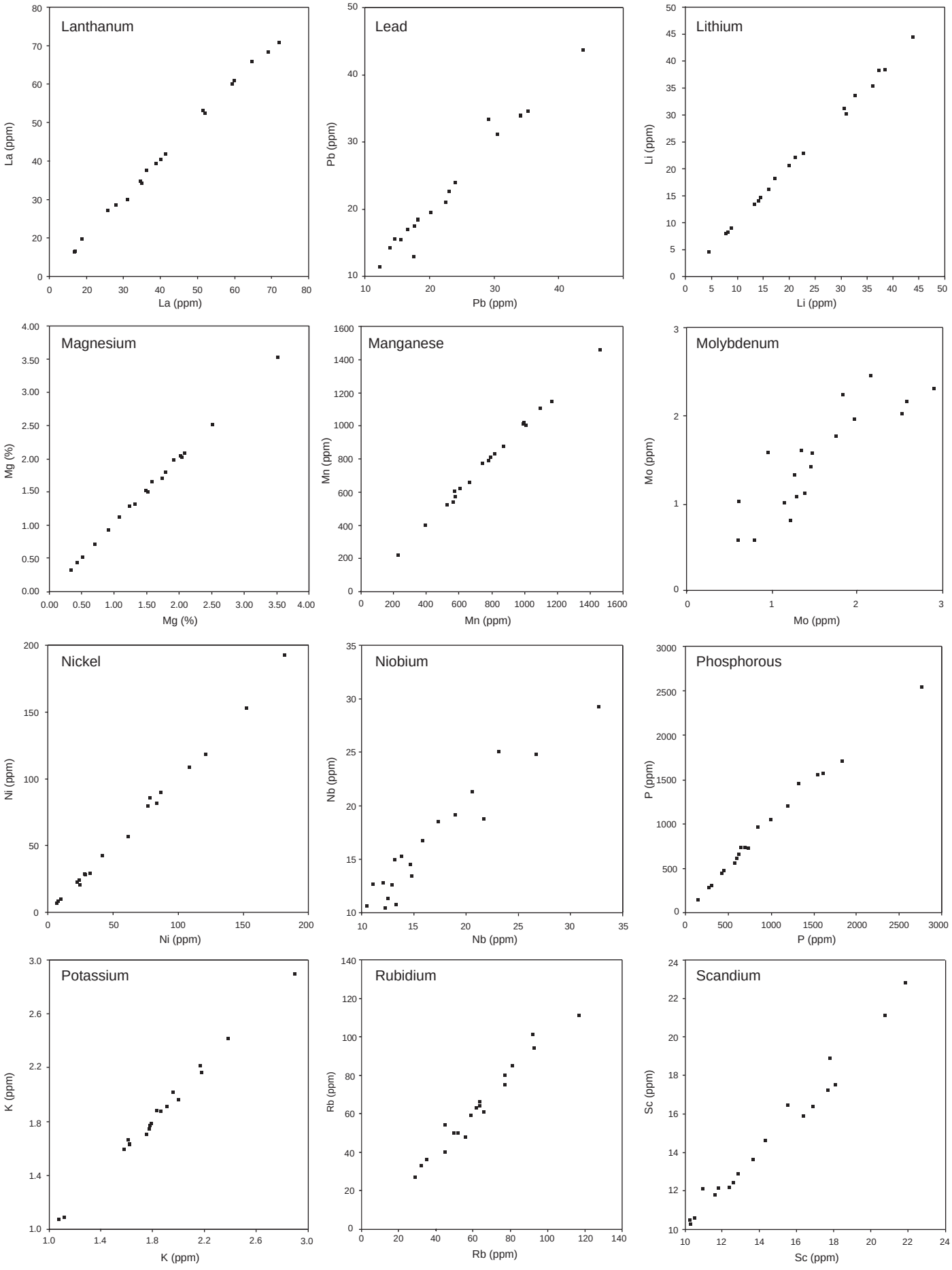

Appendix A: cont.

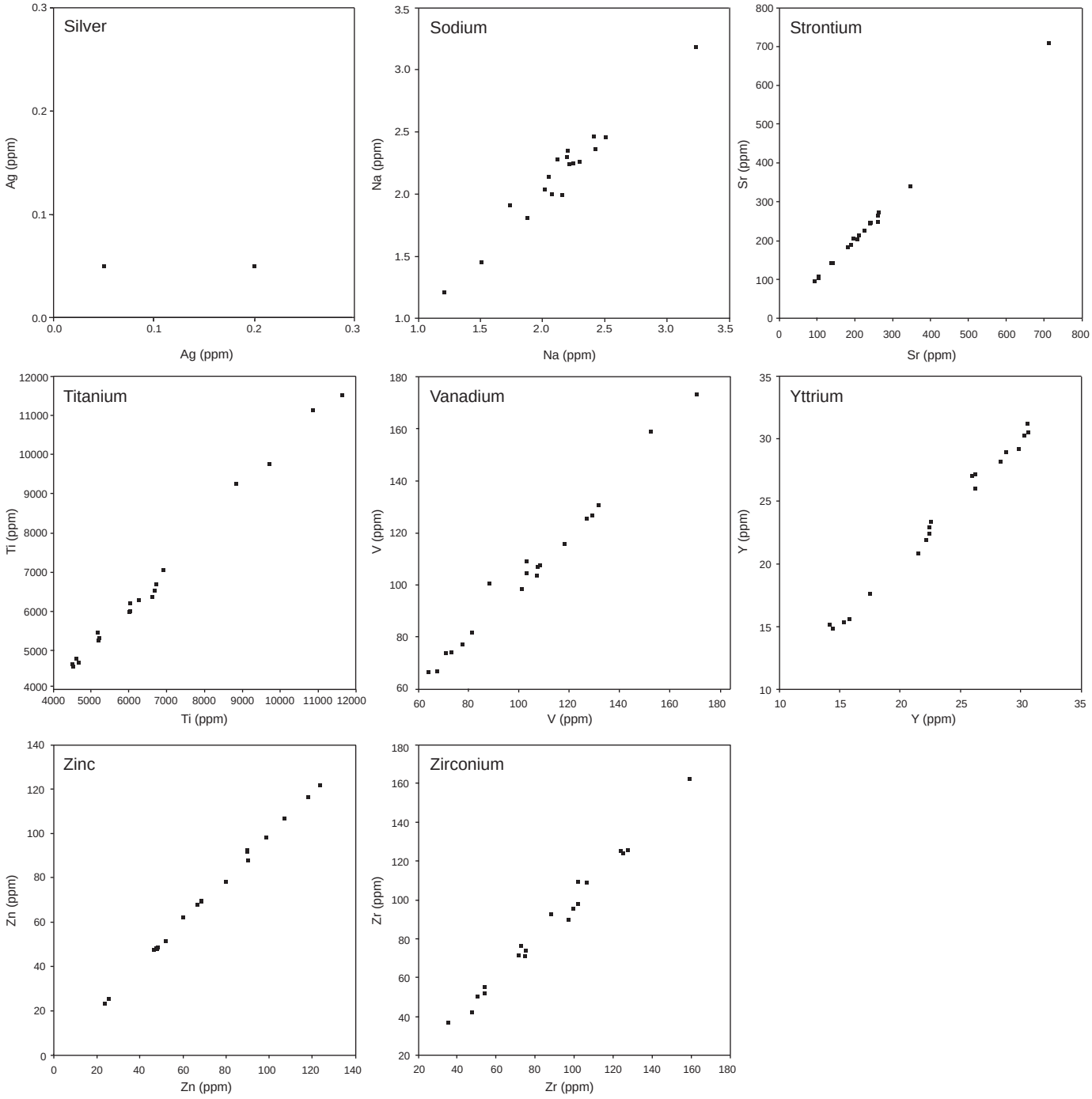

Appendix B: Comparison plots of laboratory duplicates for elements analysed by INAA.

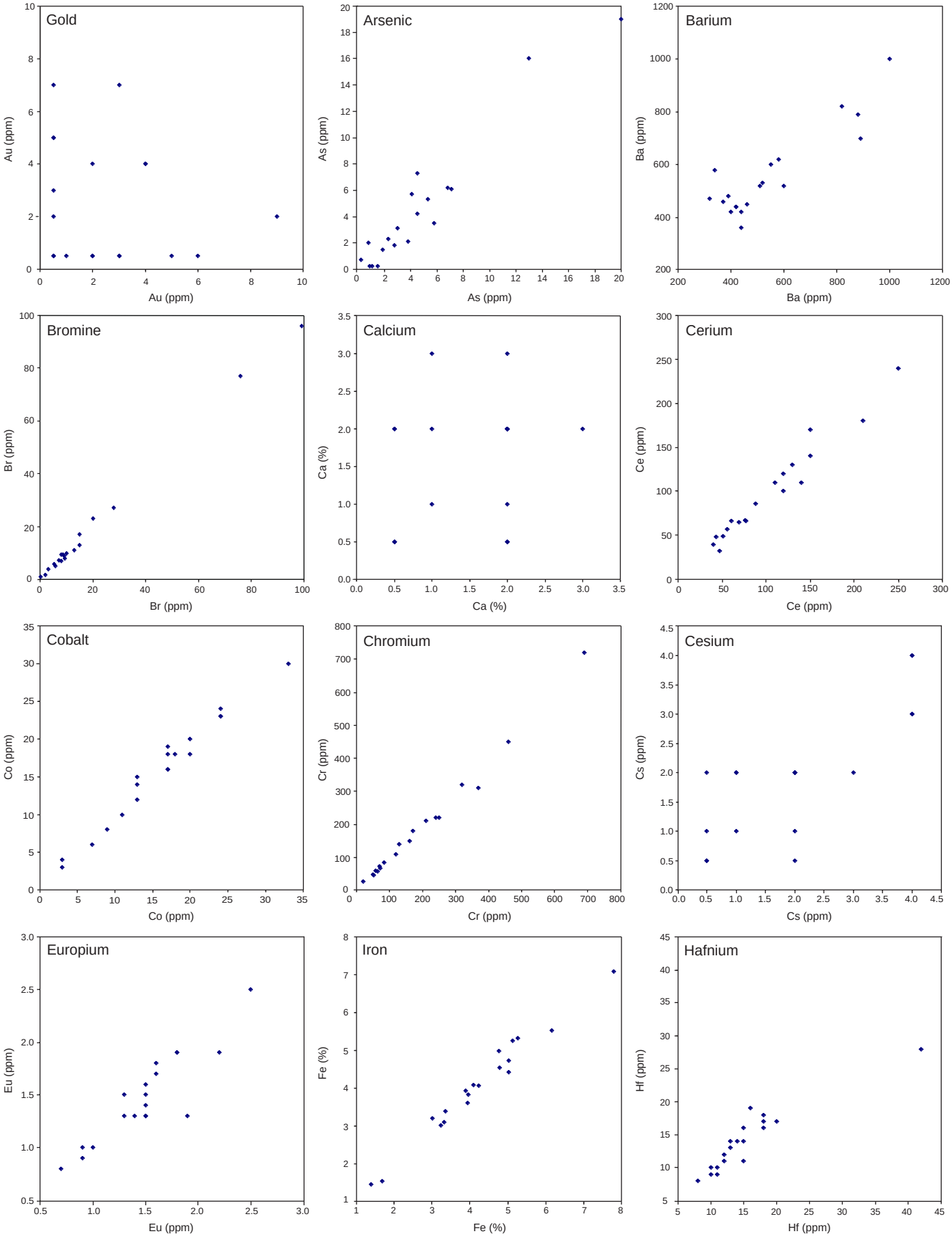

Appendix B: cont.

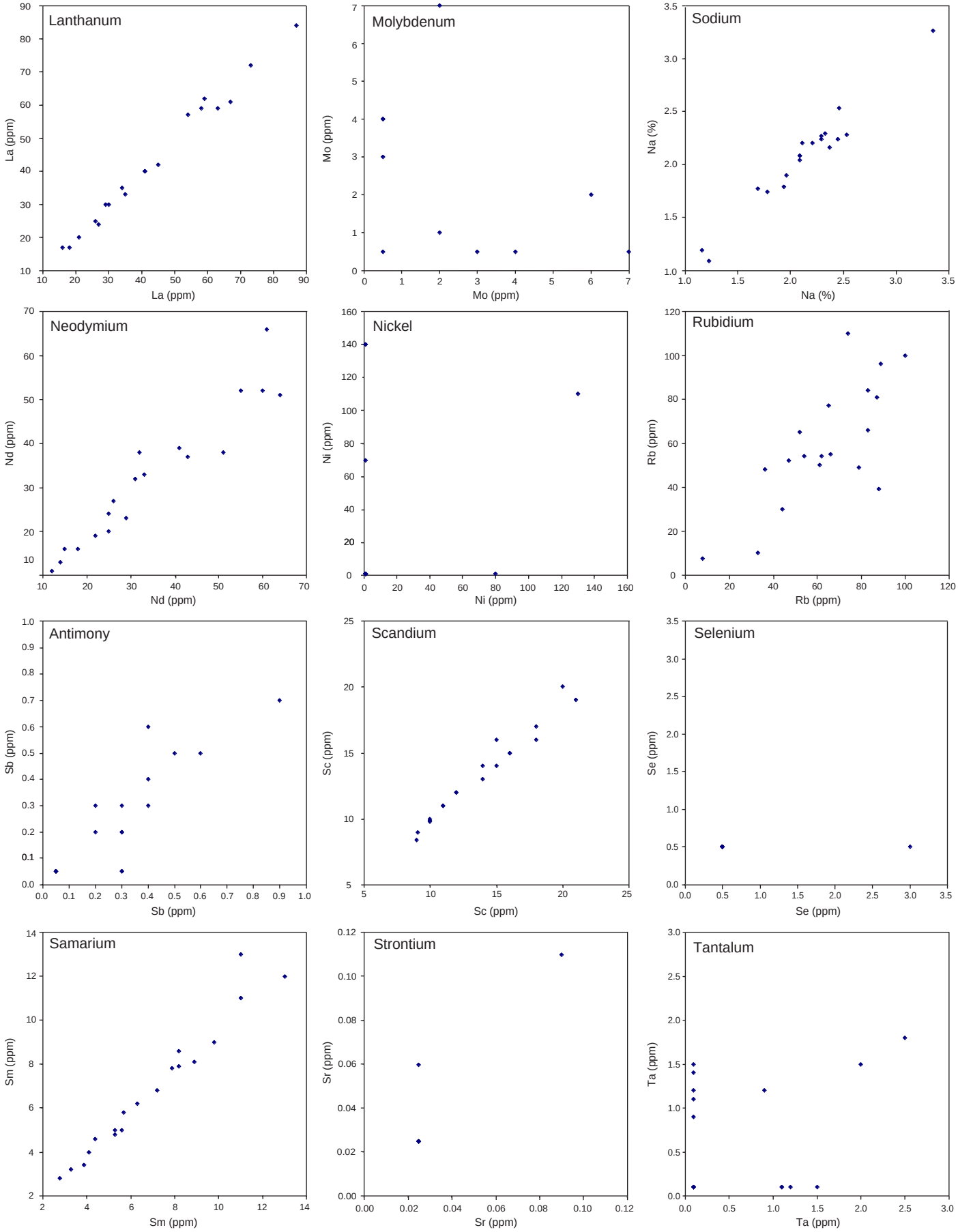

Appendix B: cont.

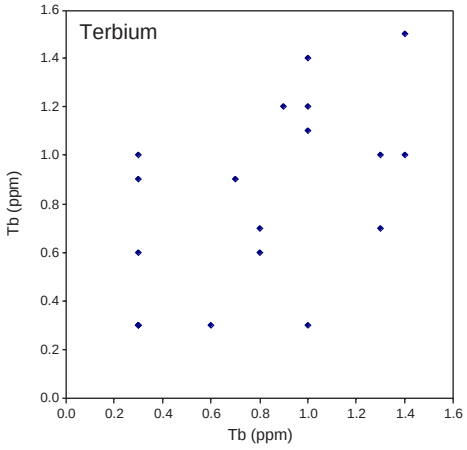

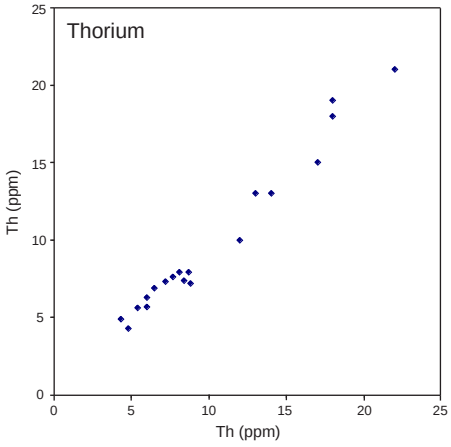

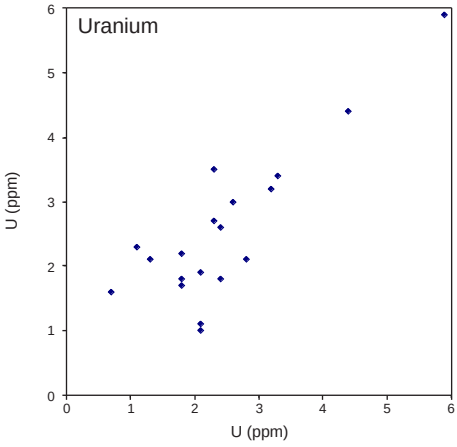

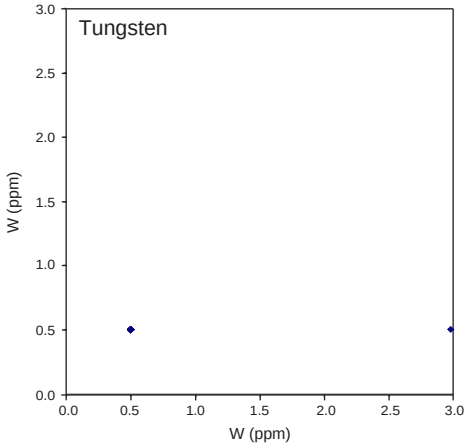

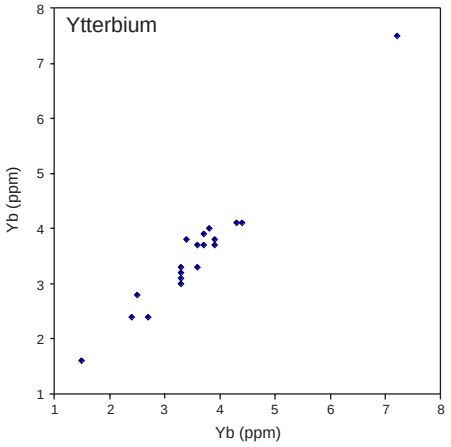

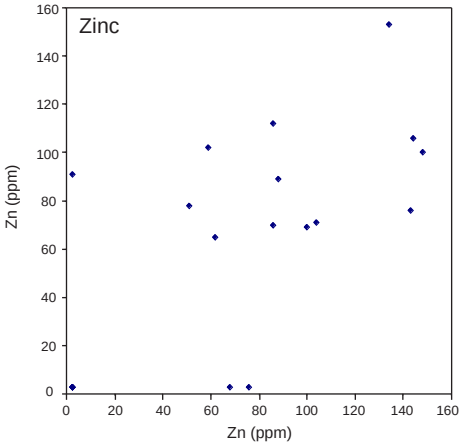

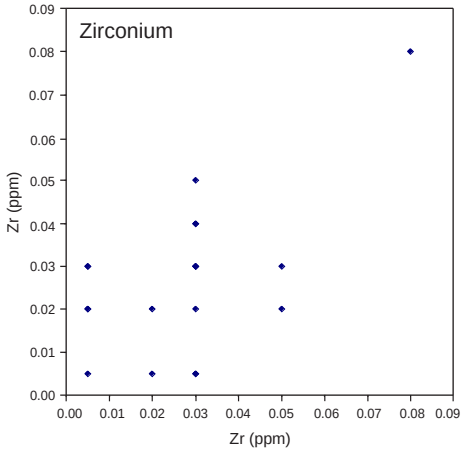

Appendix C: Comparison plots of field duplicates for elements analysed by ICP and AAS (Ag, Rb).

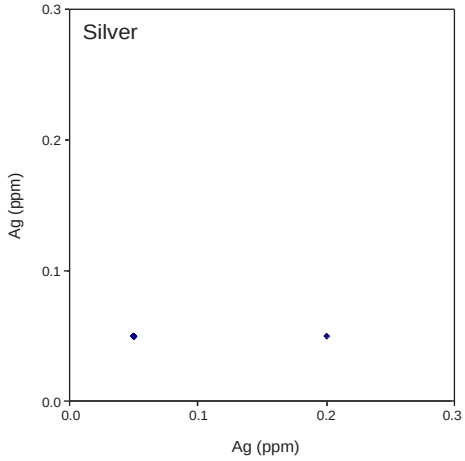

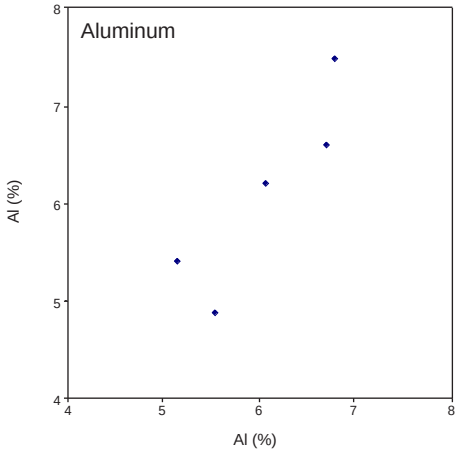

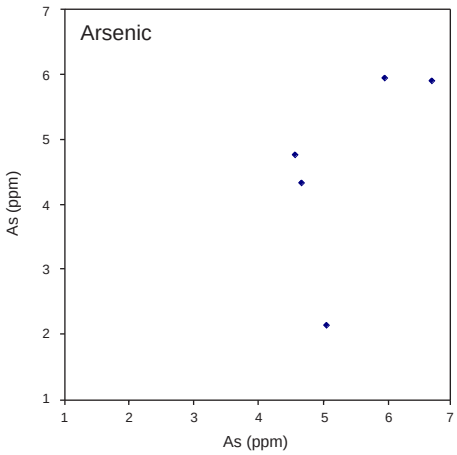

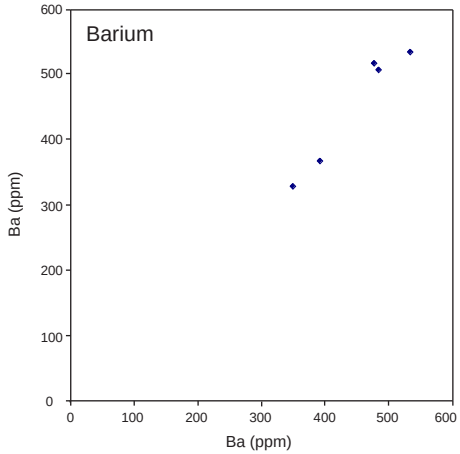

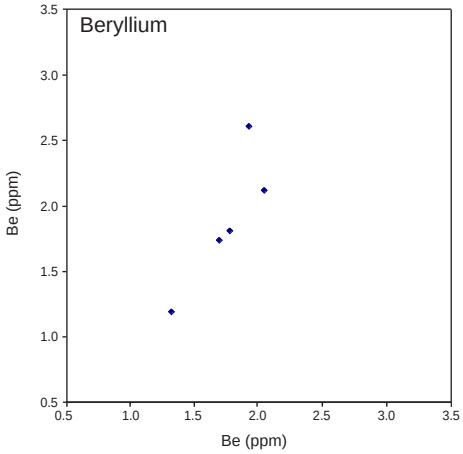

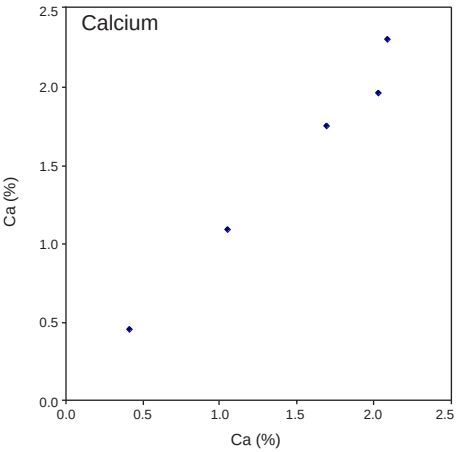

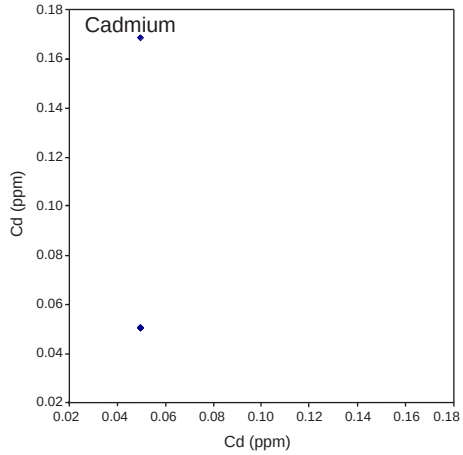

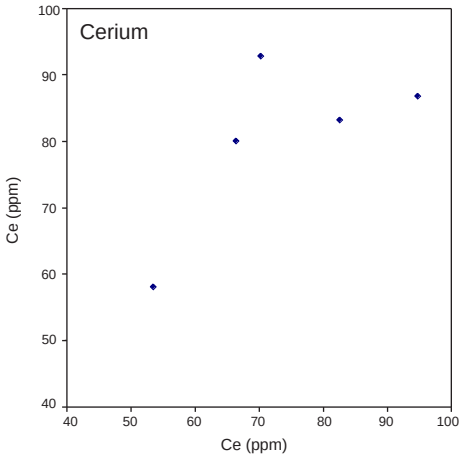

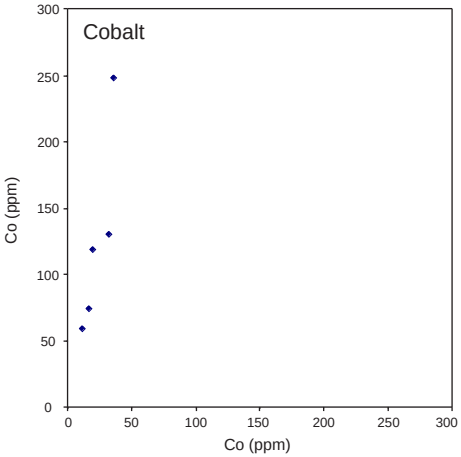

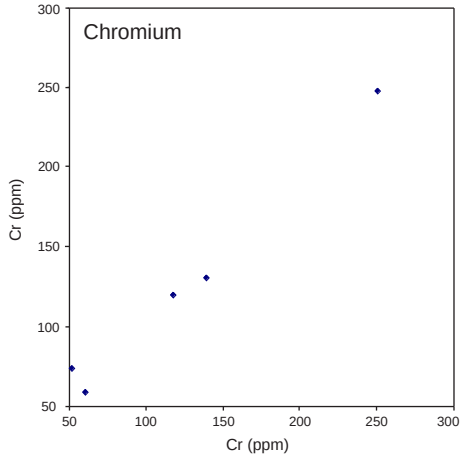

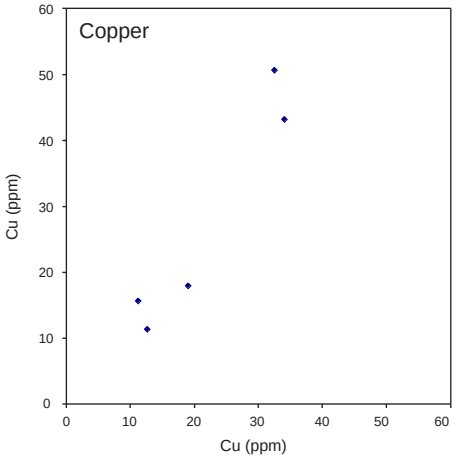

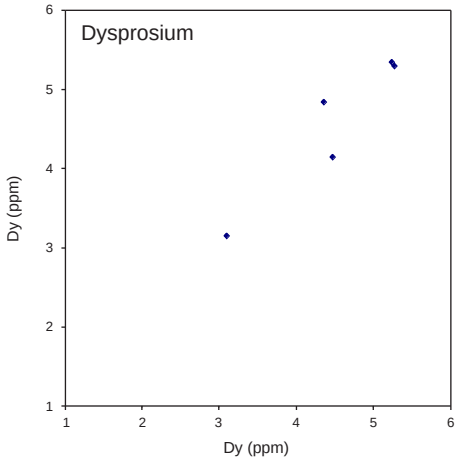

Appendix C: cont.

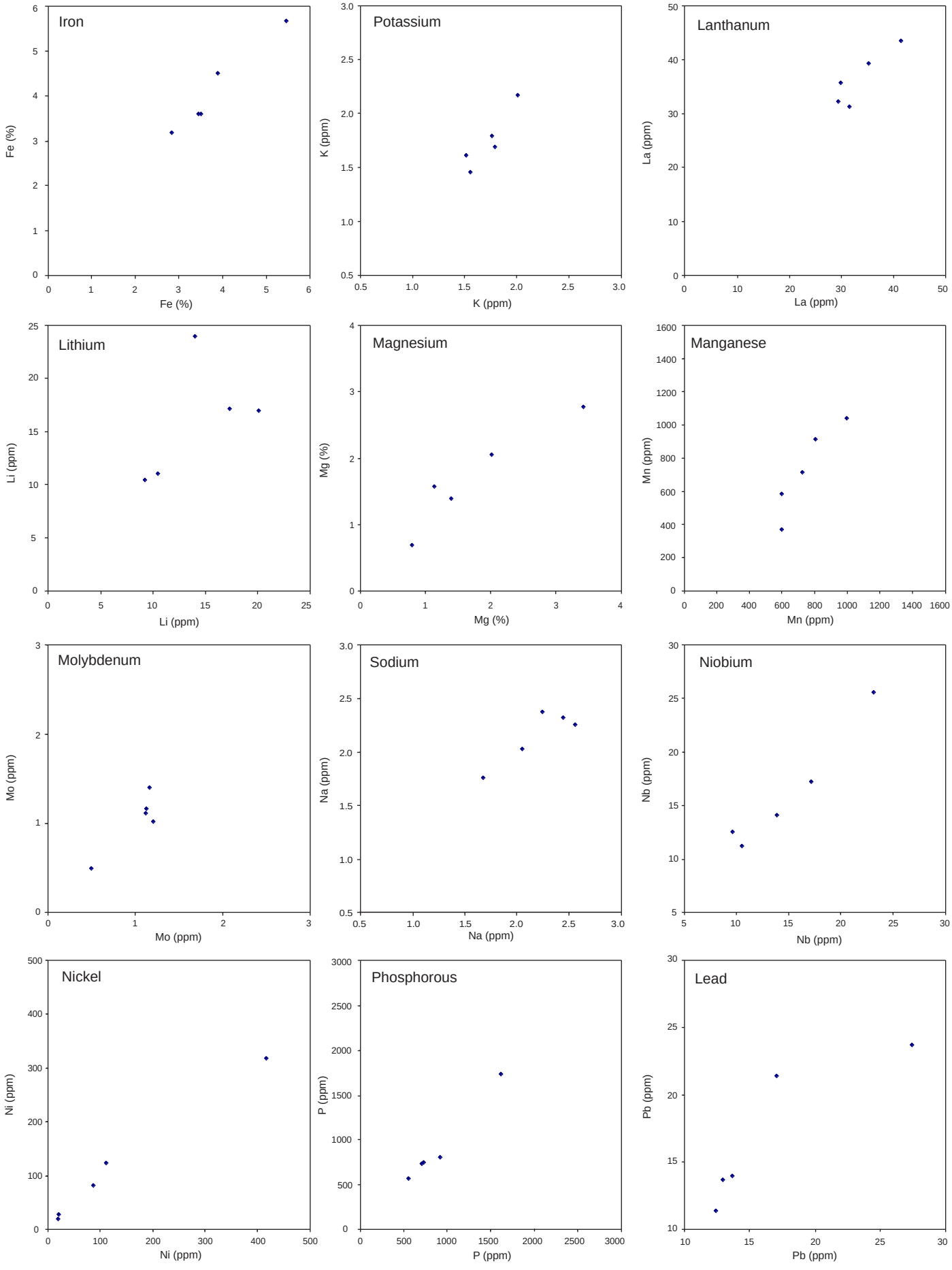

Appendix C: cont.

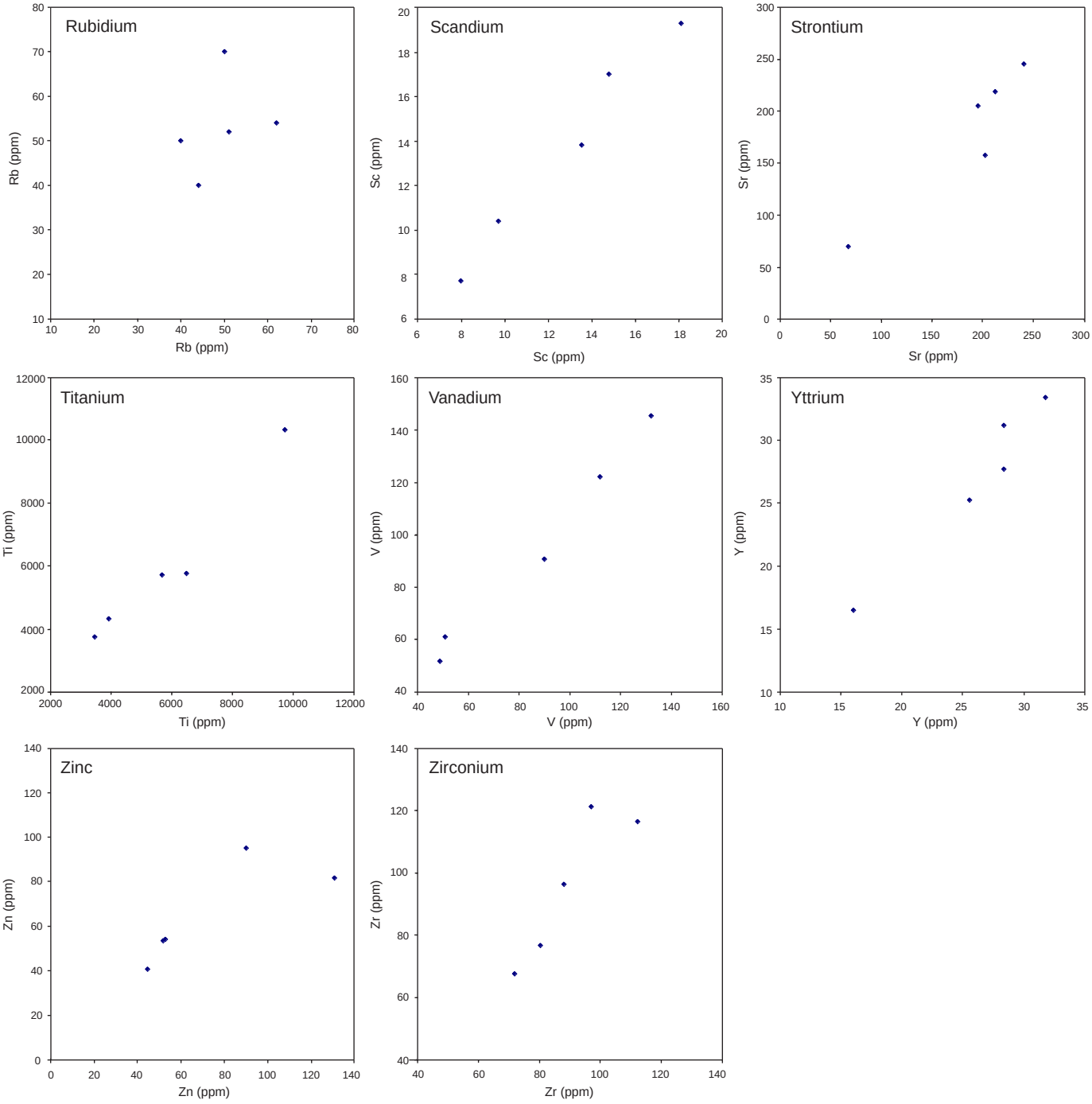

Appendix D: Comparison plots of field duplicates for elements analysed by INAA.

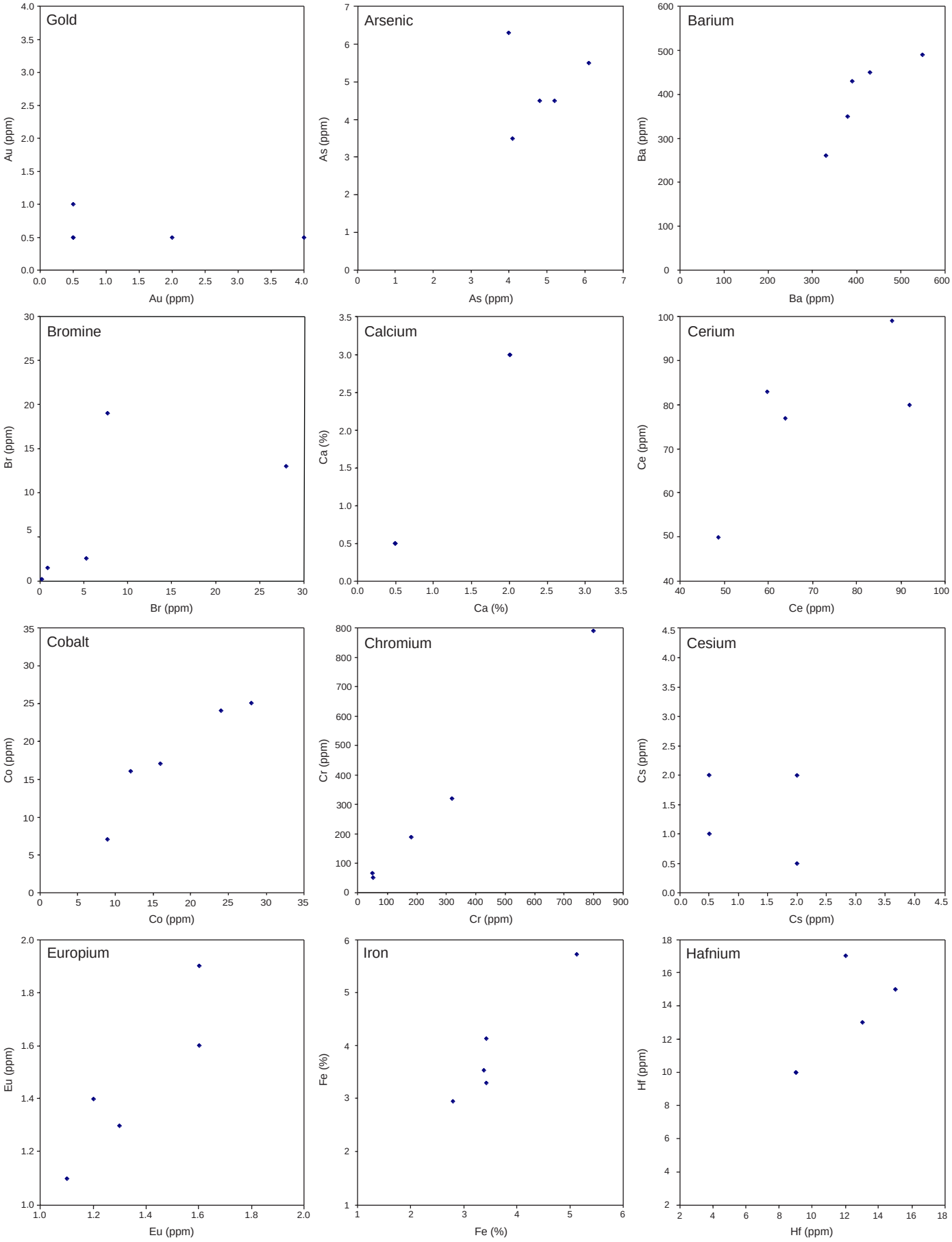

Appendix D: cont.

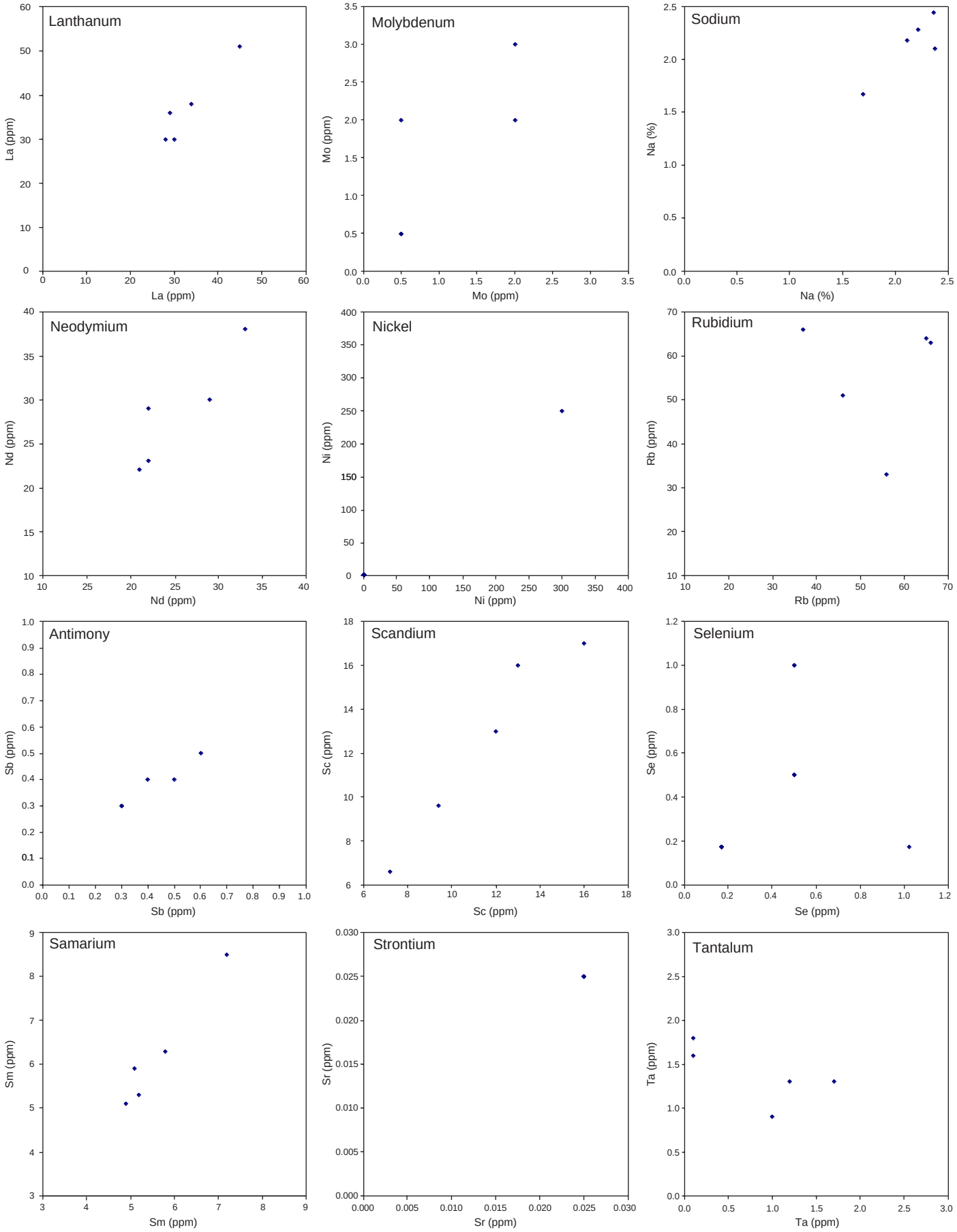

Appendix D: cont.

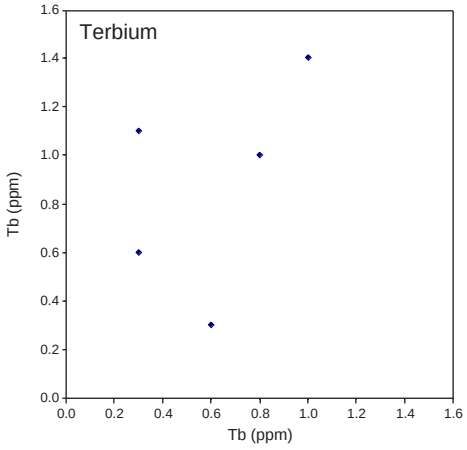

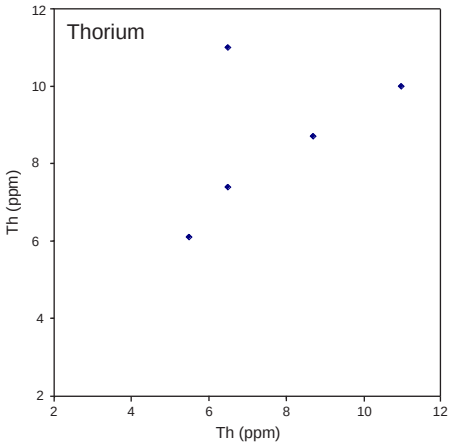

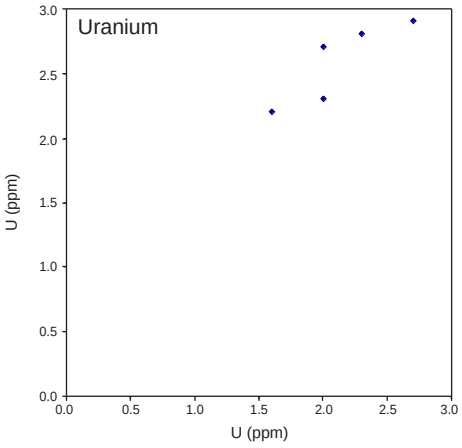

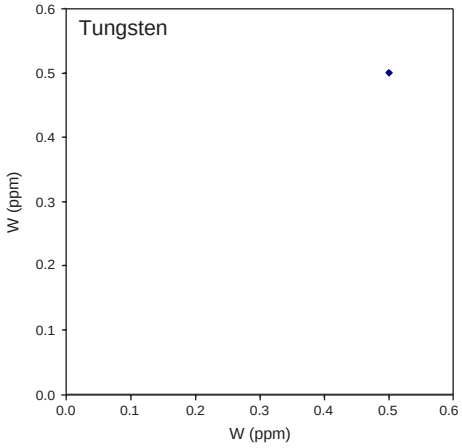

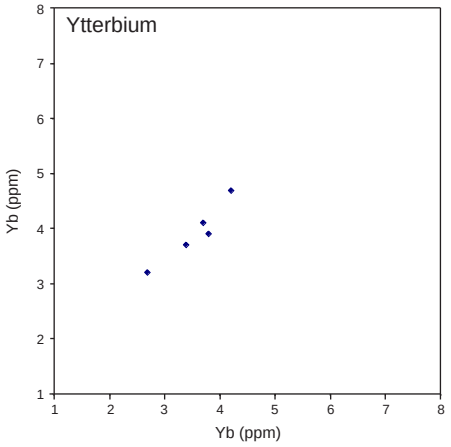

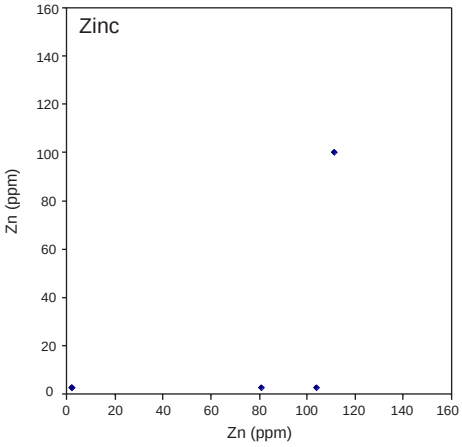

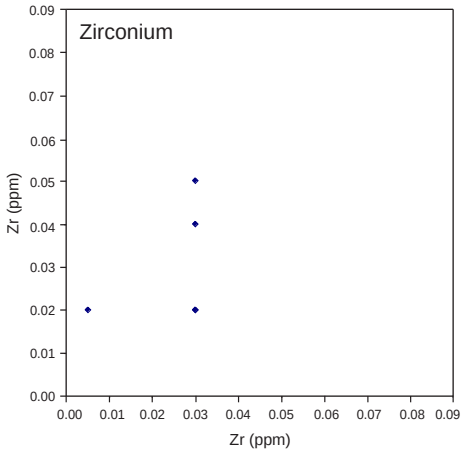

Appendix E

Sample Data Listings

For the data shown in this appendix please see the data files (icp and aas data.csv or icp and aas data.xls and inaa data.csv or inaa data.xls) included on this CD.

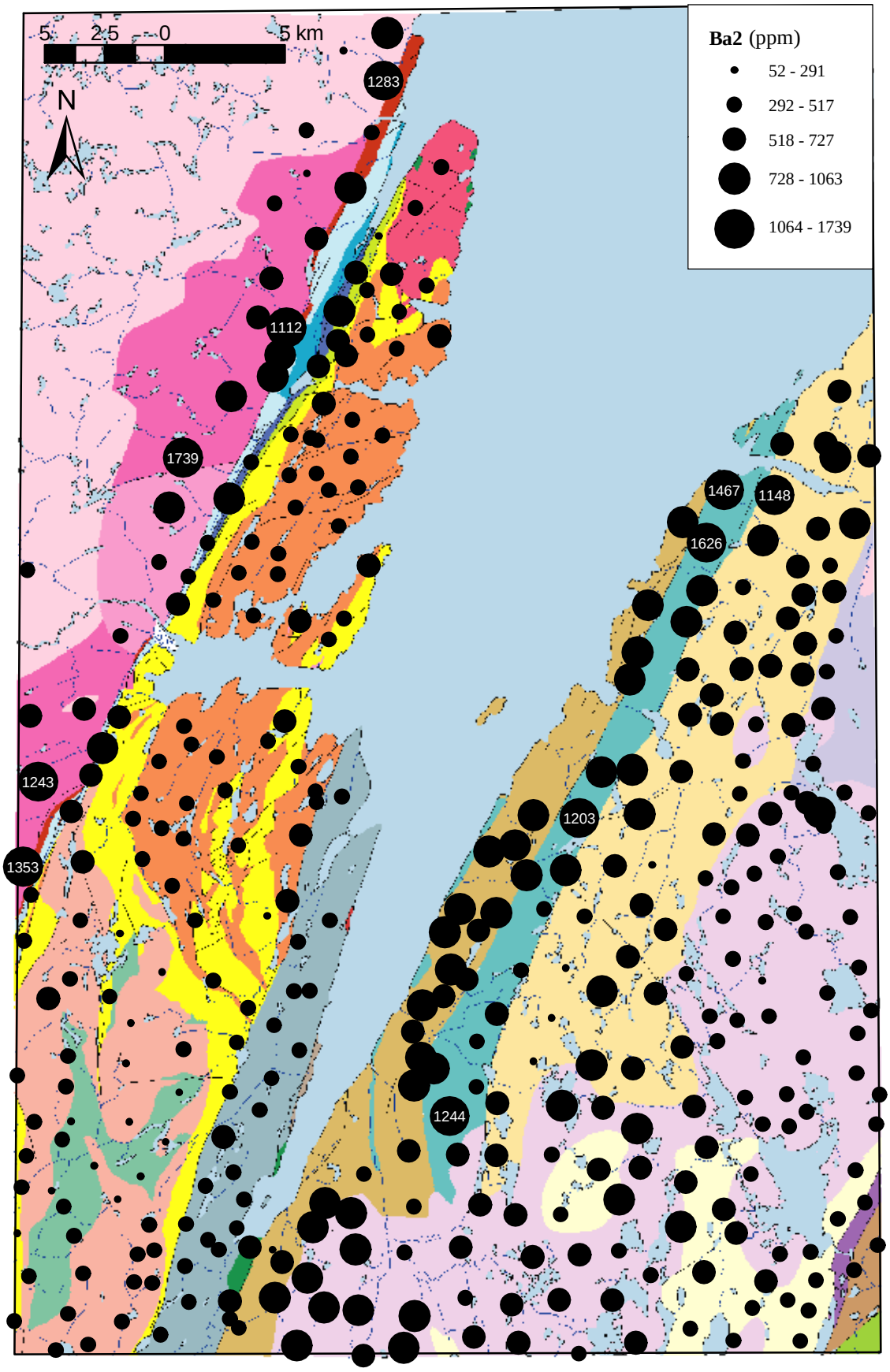

Figure 20. Barium values in till. Open File NFLD/2823.

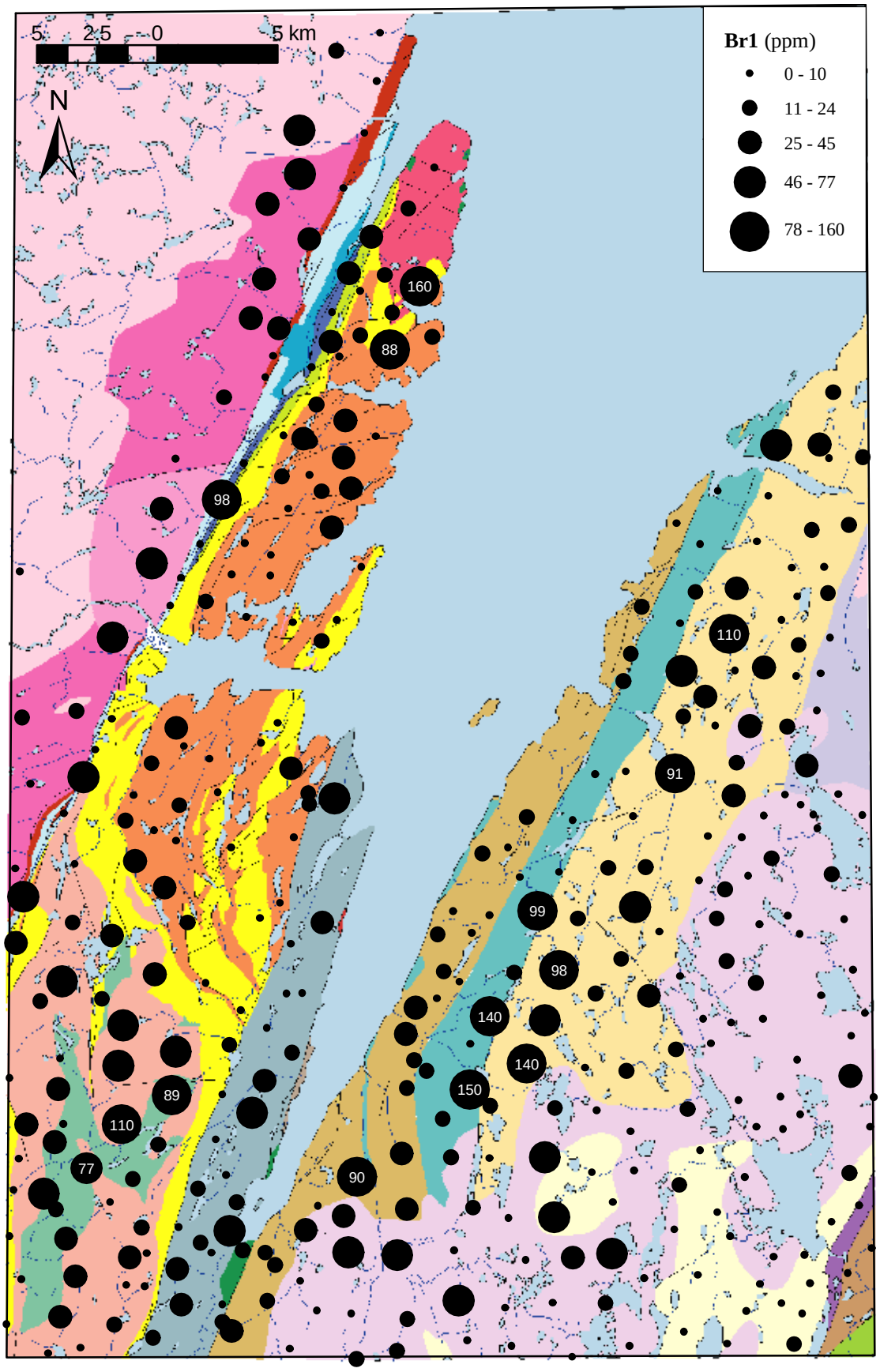

Figure 21. Bromine values in till. Open File NFLD/2823.

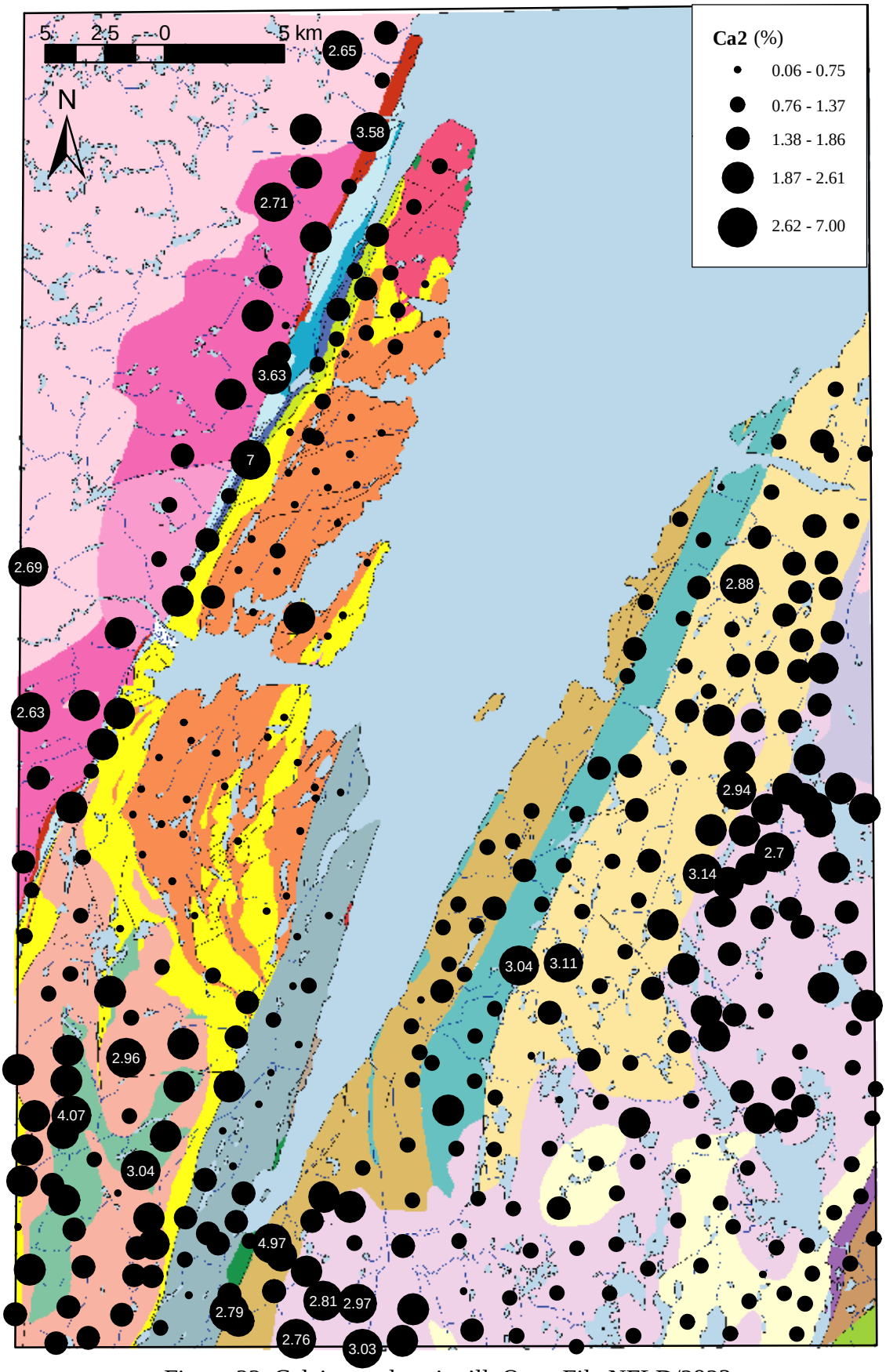

Figure 22. Calcium values in till. Open File NFLD/2823.

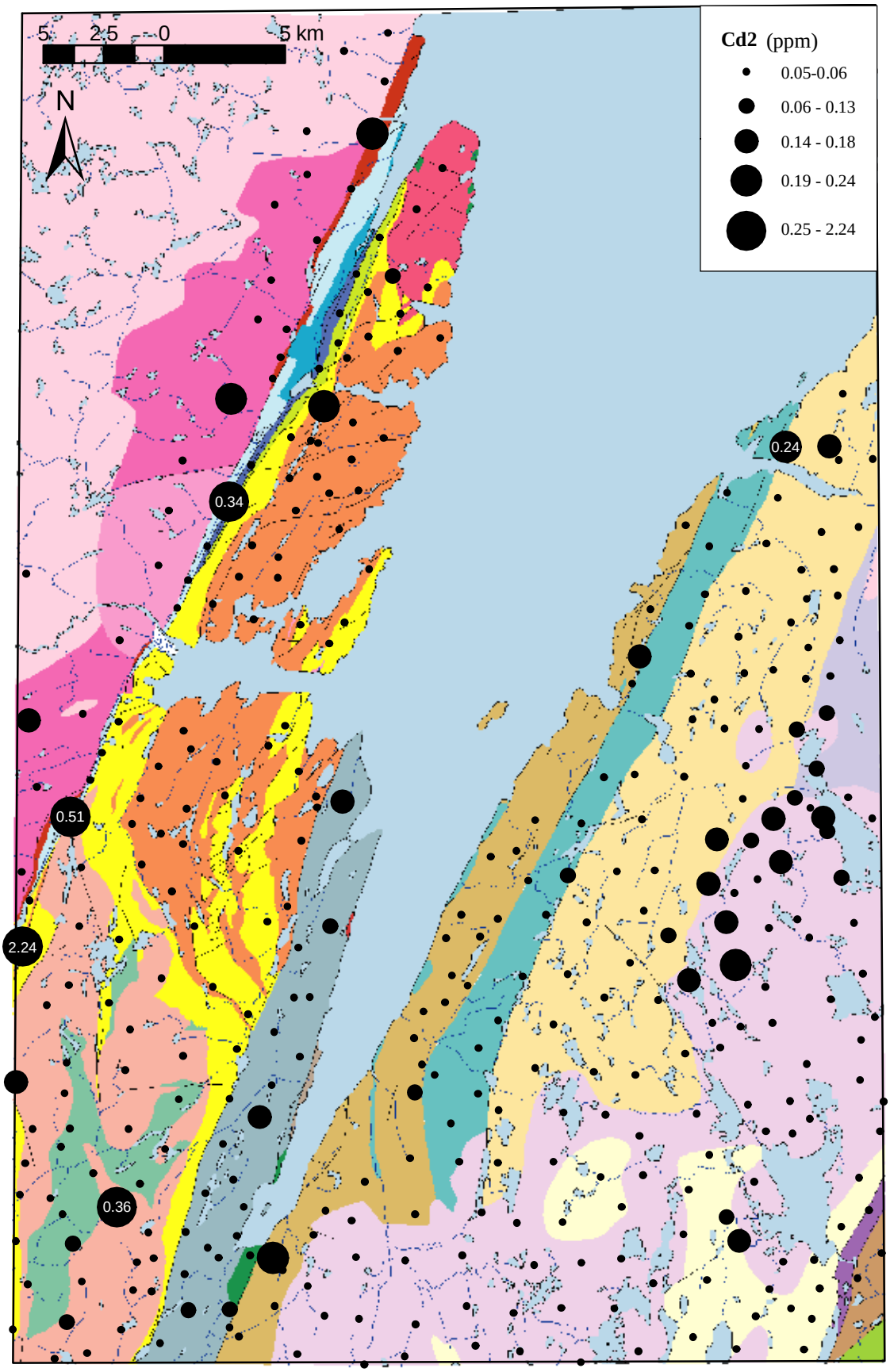

Figure 23. Cadmium values in till. Open File NFLD/2823.

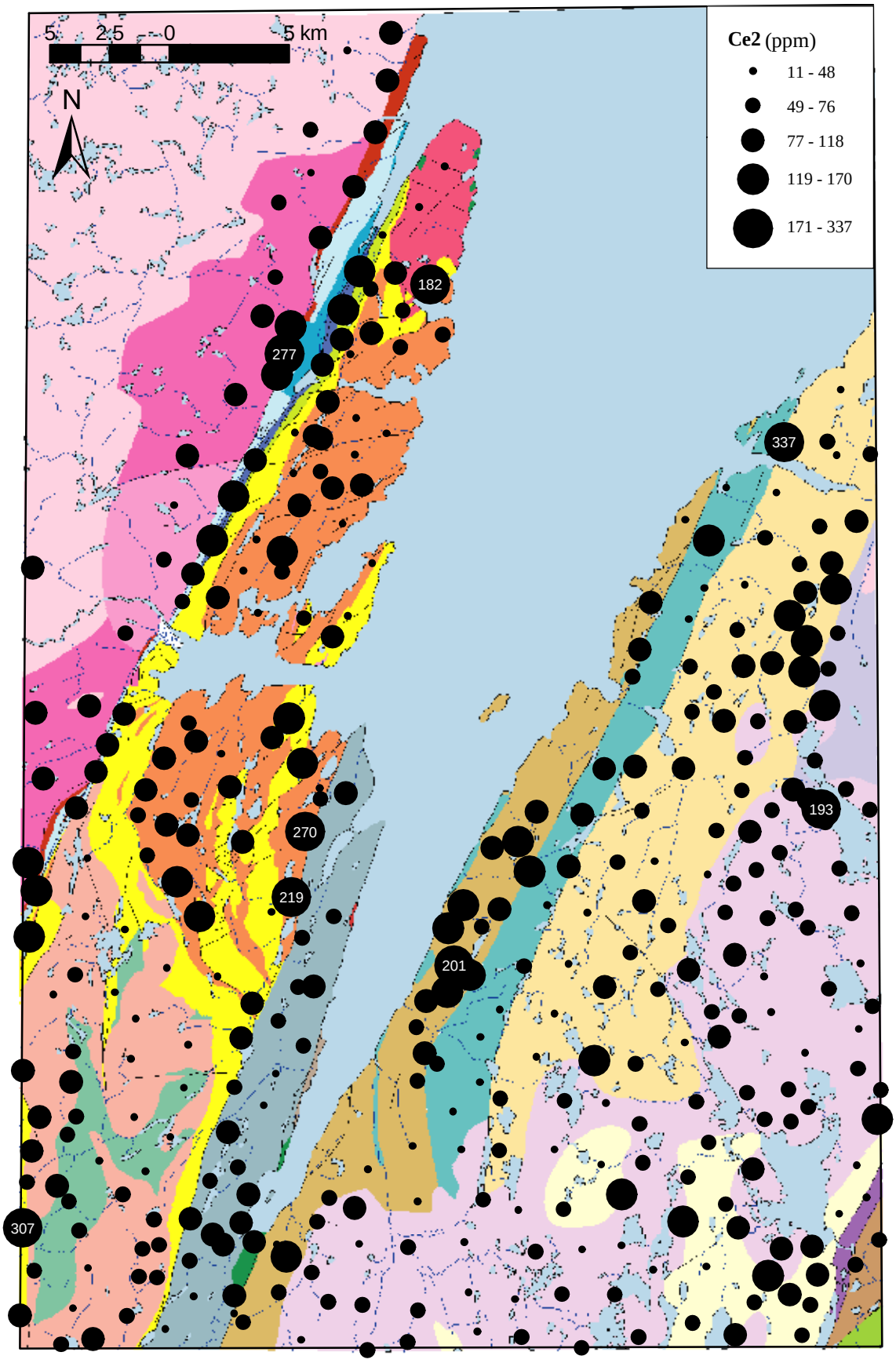

Figure 24. Cerium values in till. Open File NFLD/2823.

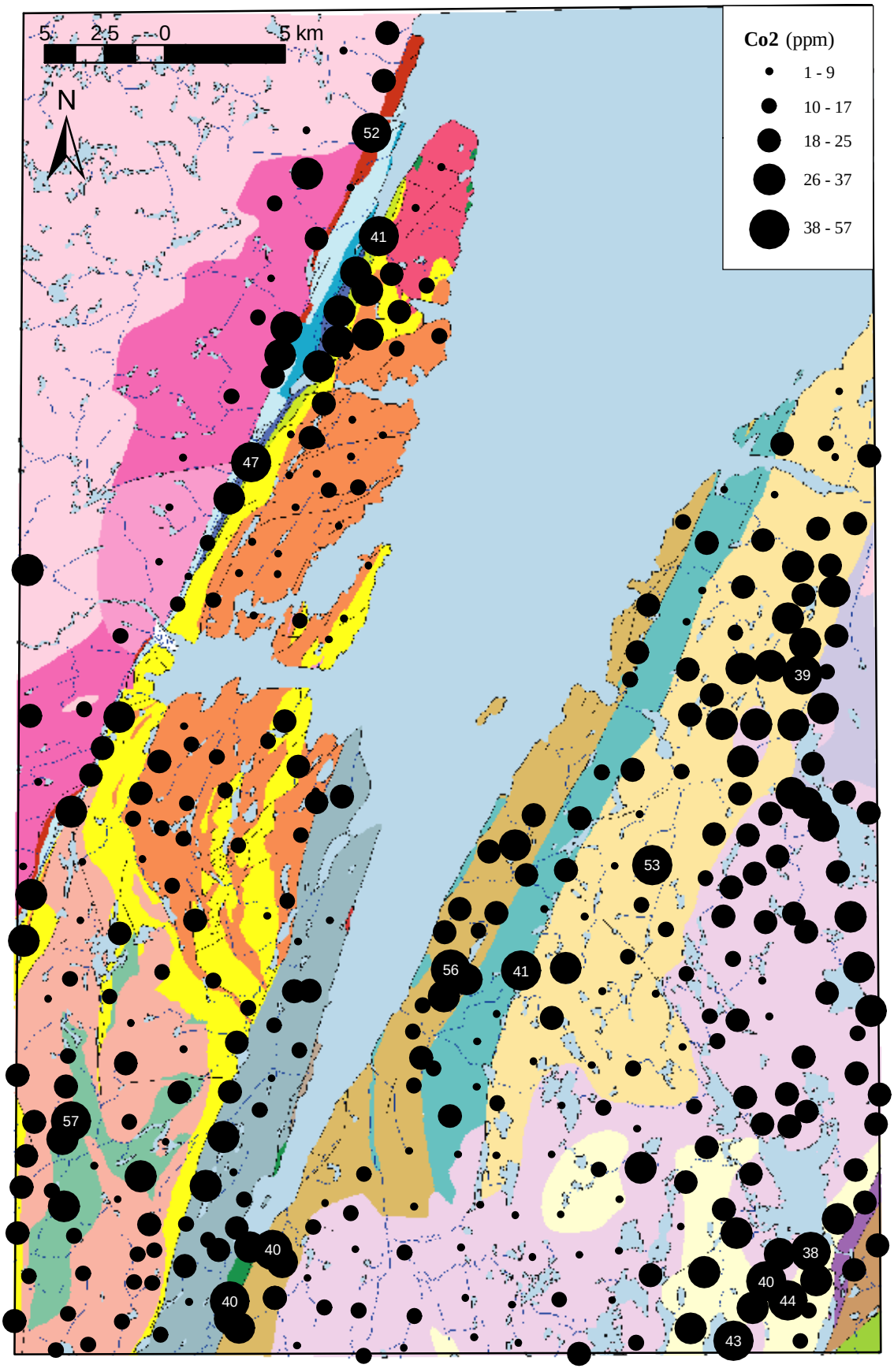

Figure 25. Cobalt values in till. Open File NFLD/2823.

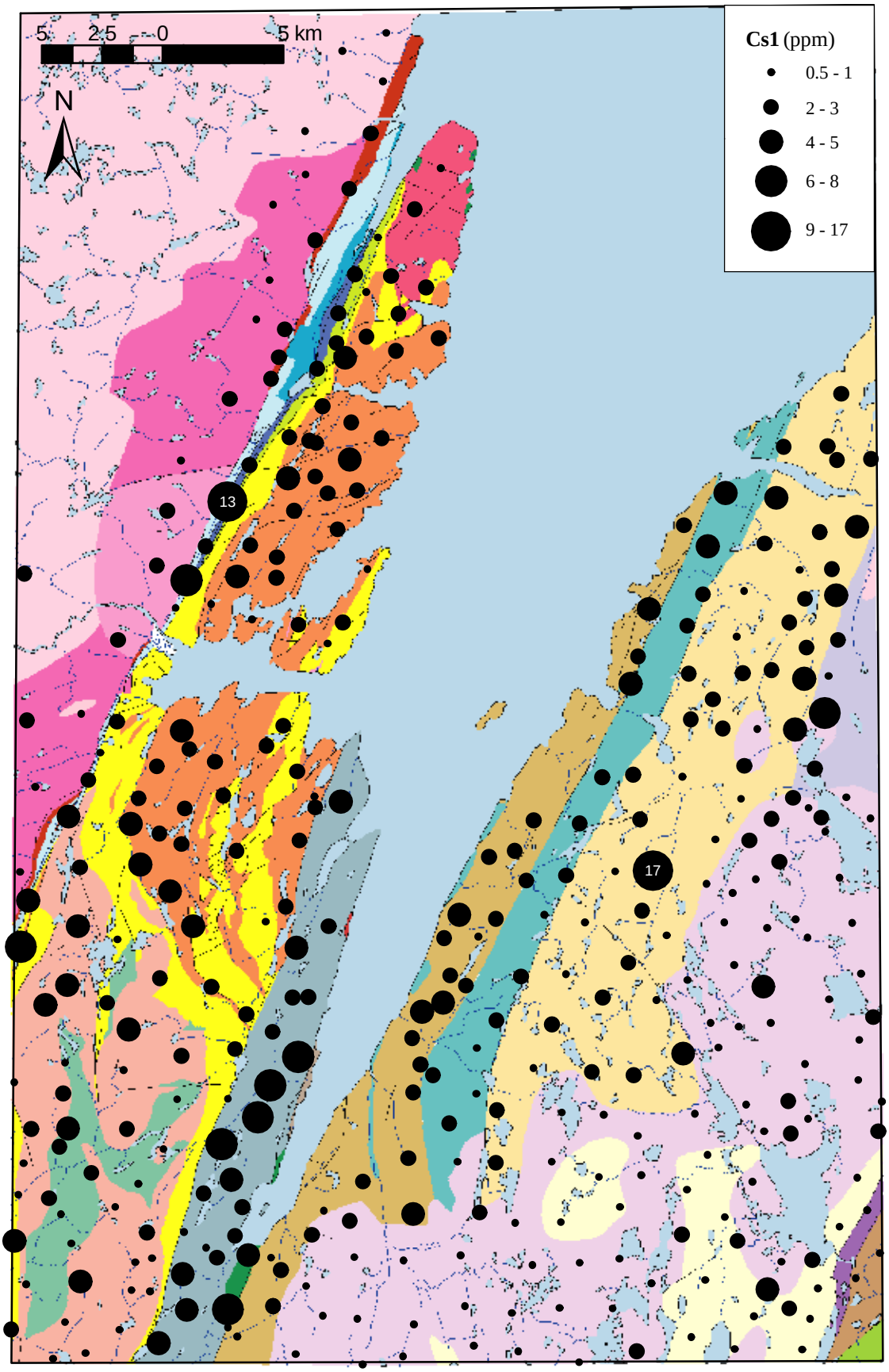

Figure 26. Cesium values in till. Open File NFLD/2823.

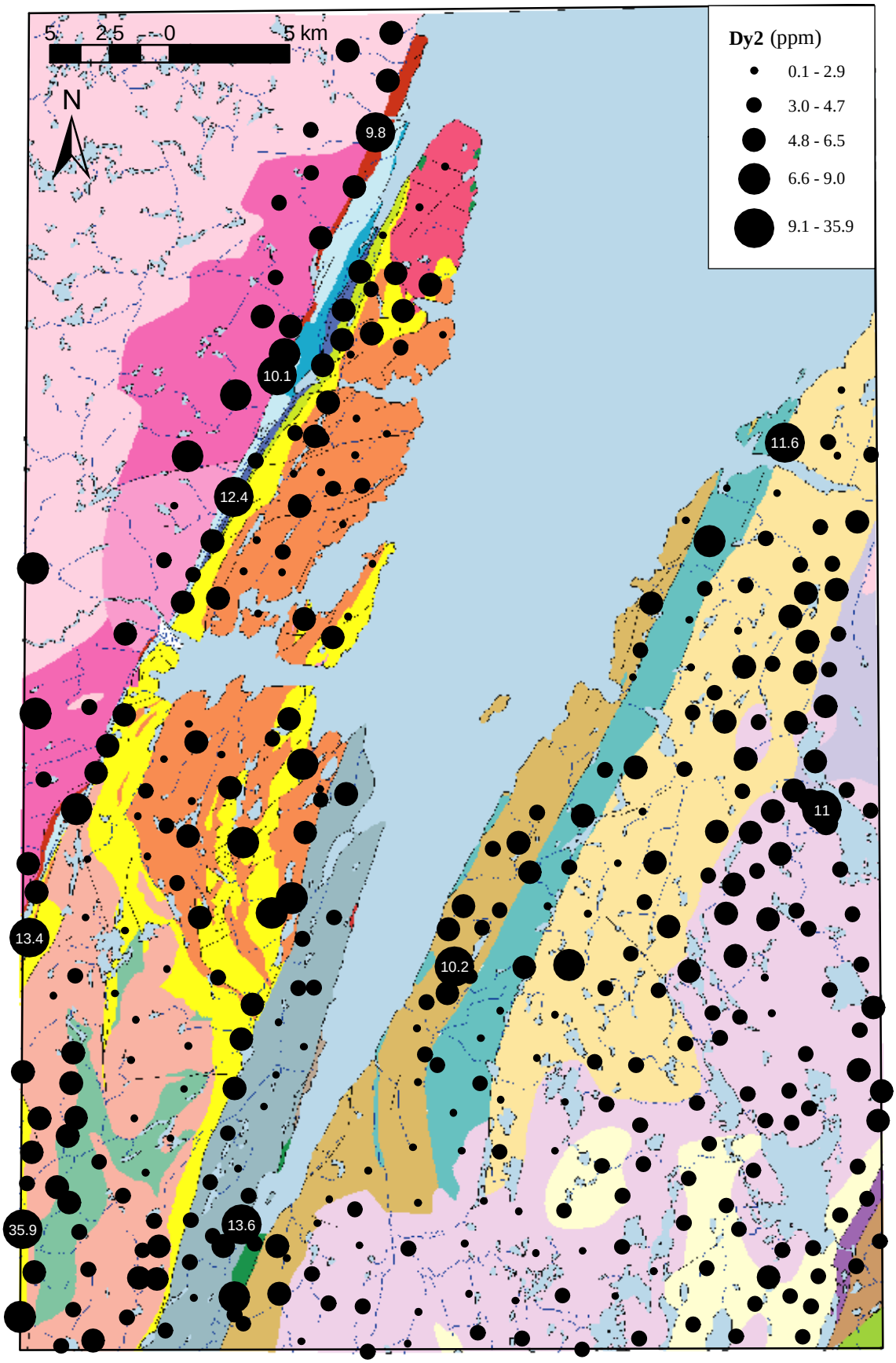

Figure 27. Dysprosium values in till. Open File NFLD/2823.

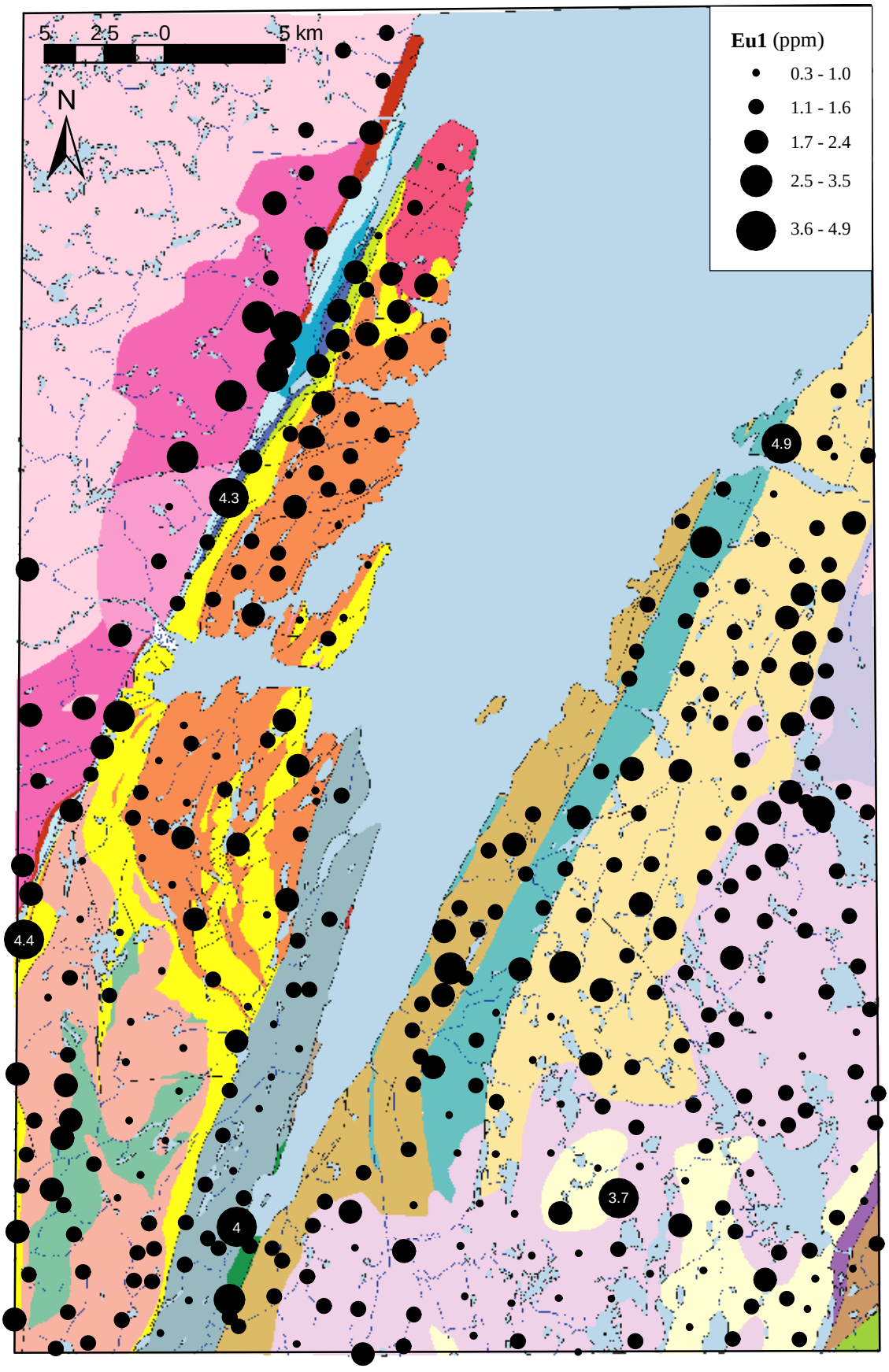

Figure 28. Europium values in till. Open File NFLD/2823.

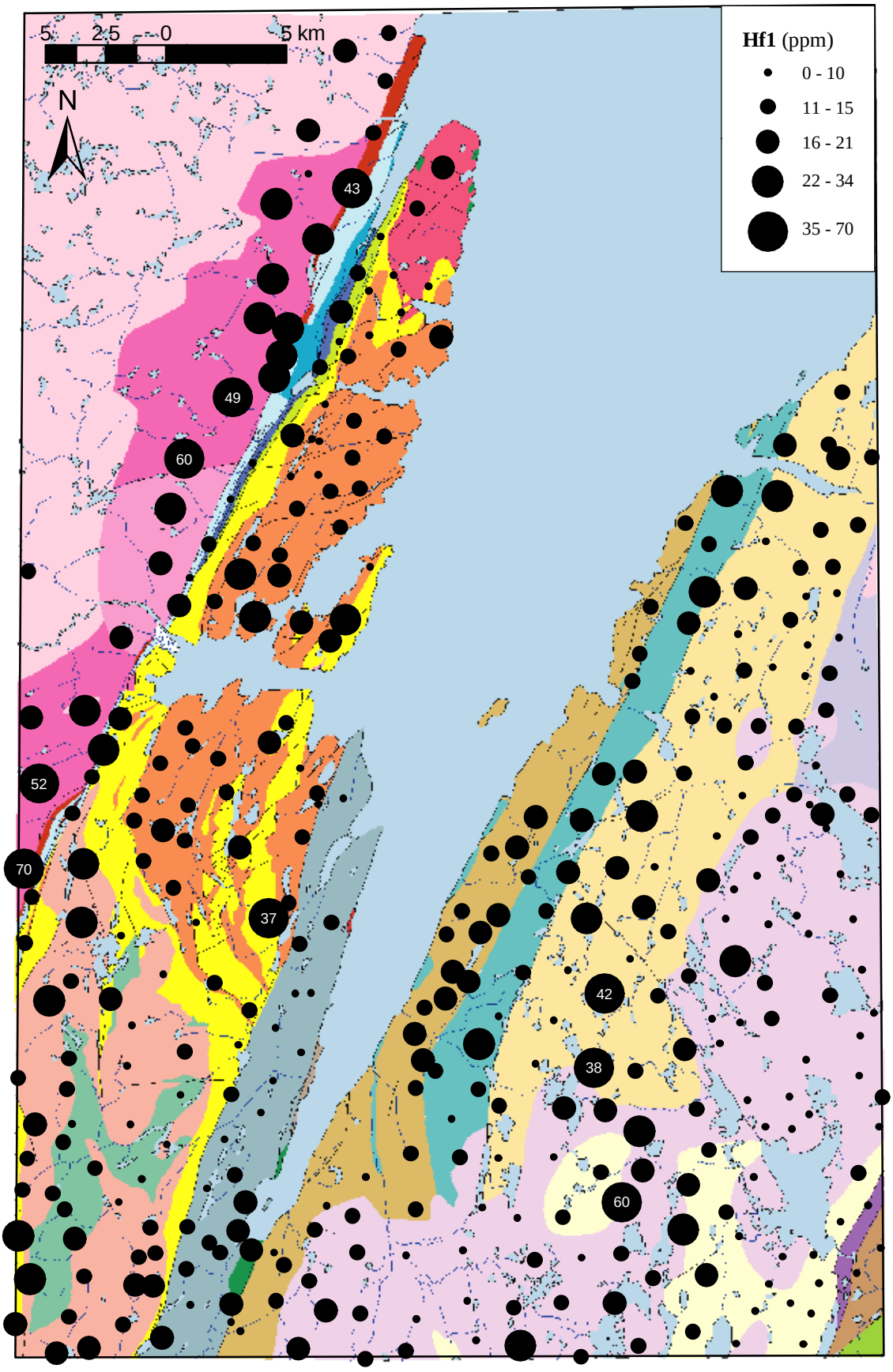

Figure 29. Hafnium values in till. Open File NFLD/2823.

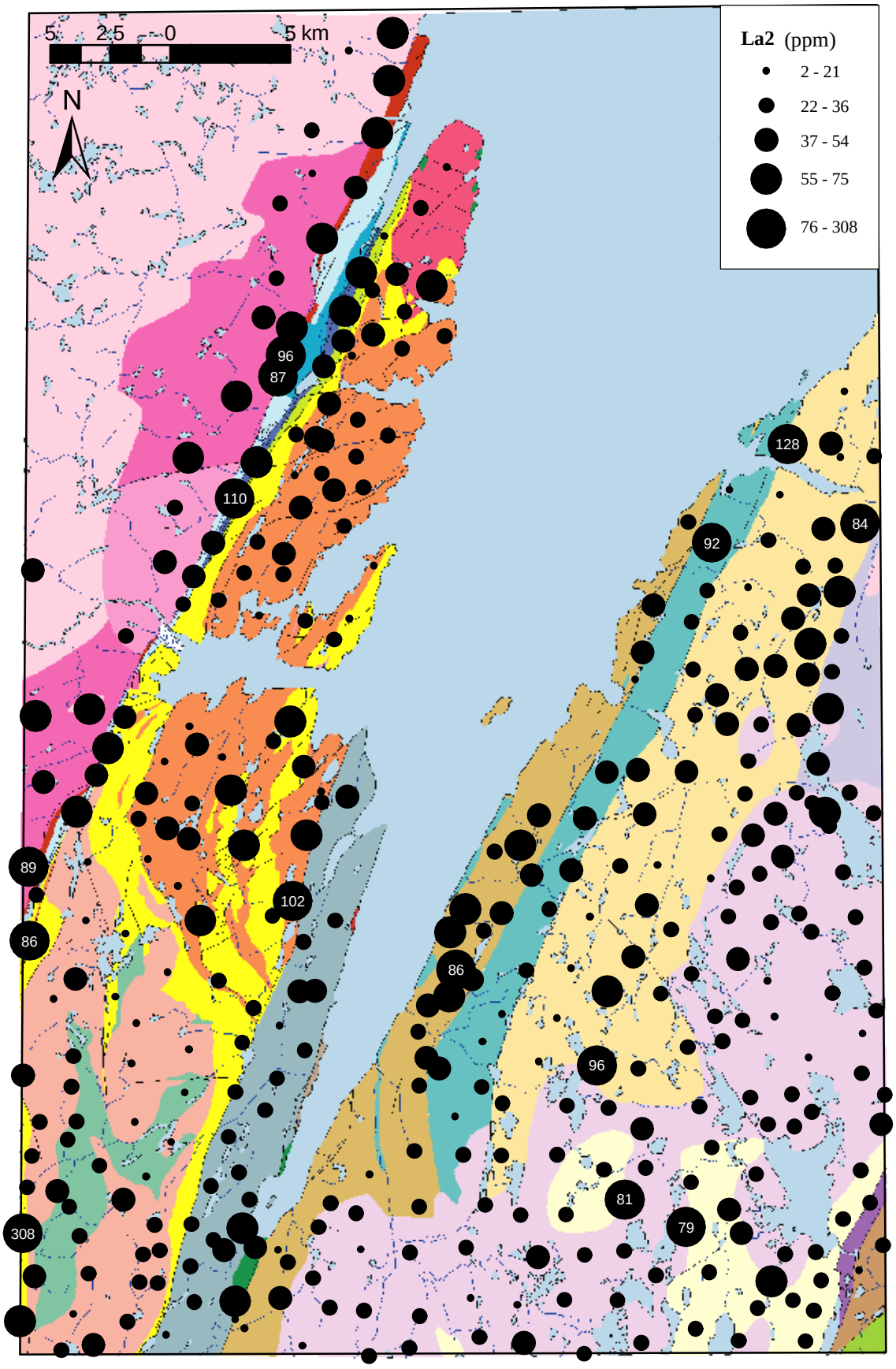

Figure 30. Lanthanum values in till. Open File NFLD/2823.

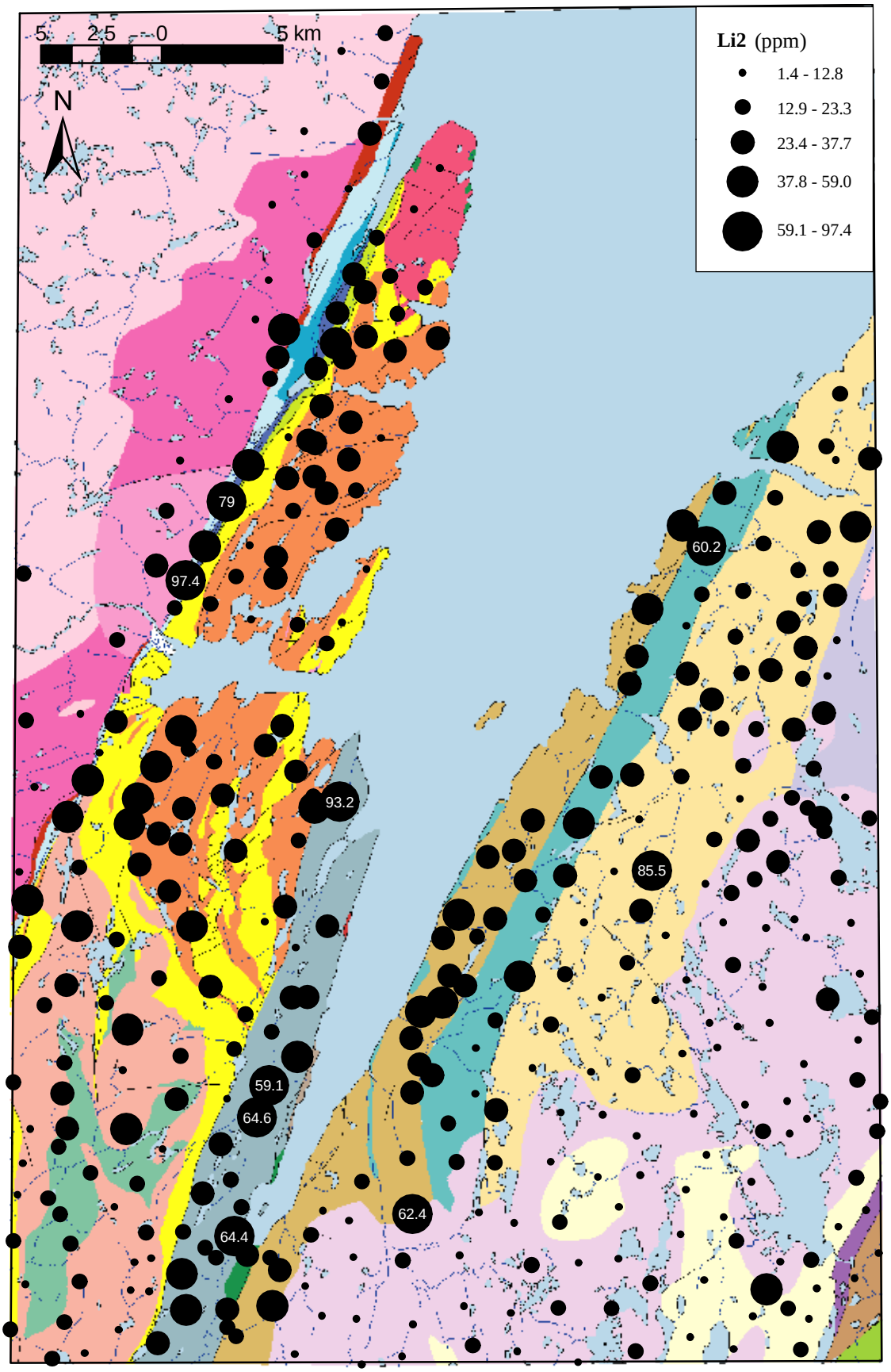

Figure 31. Lithium values in till. Open File NFLD/2823.

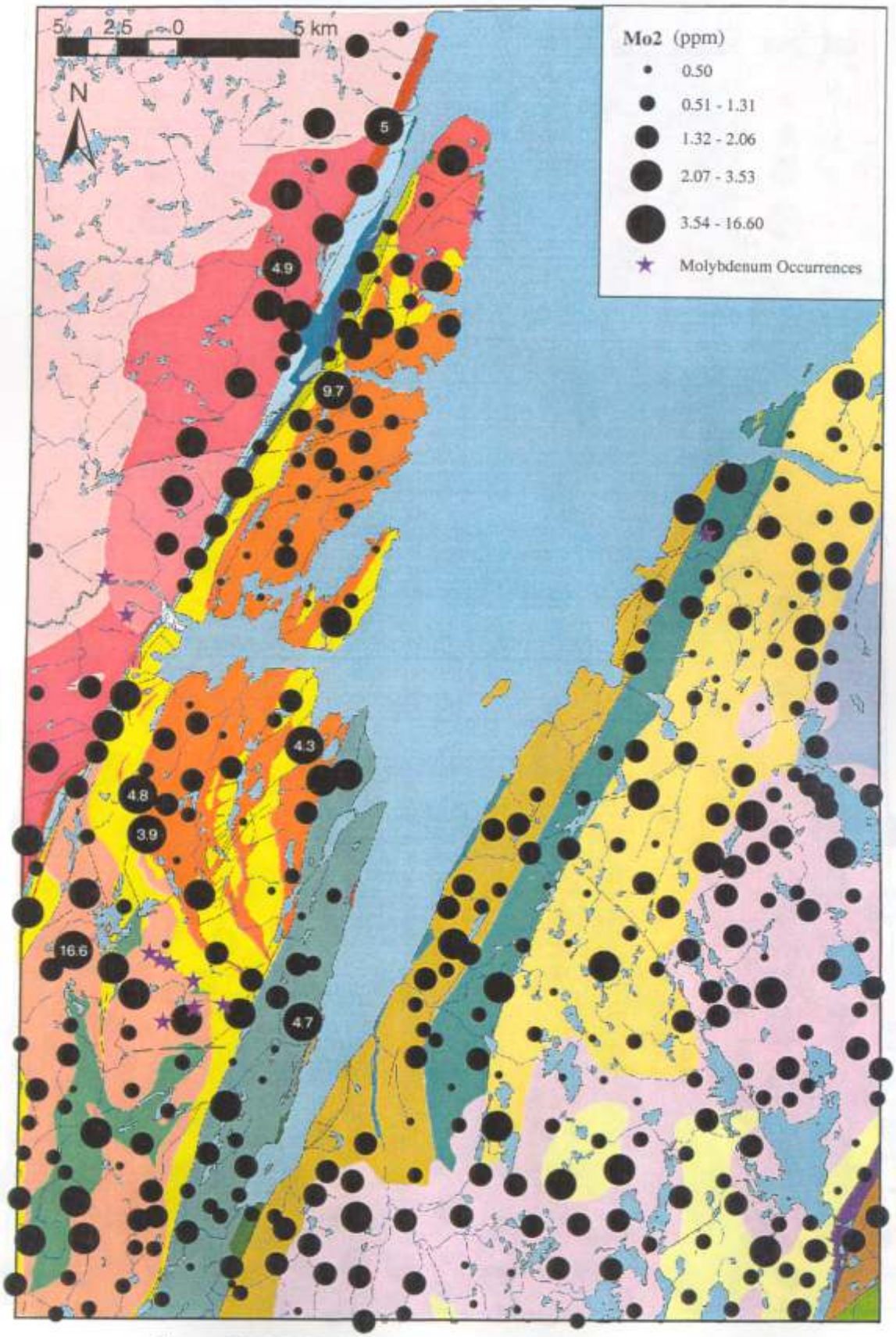

Figure 32. Molybdenum values in till. Open File NFLD/2823.

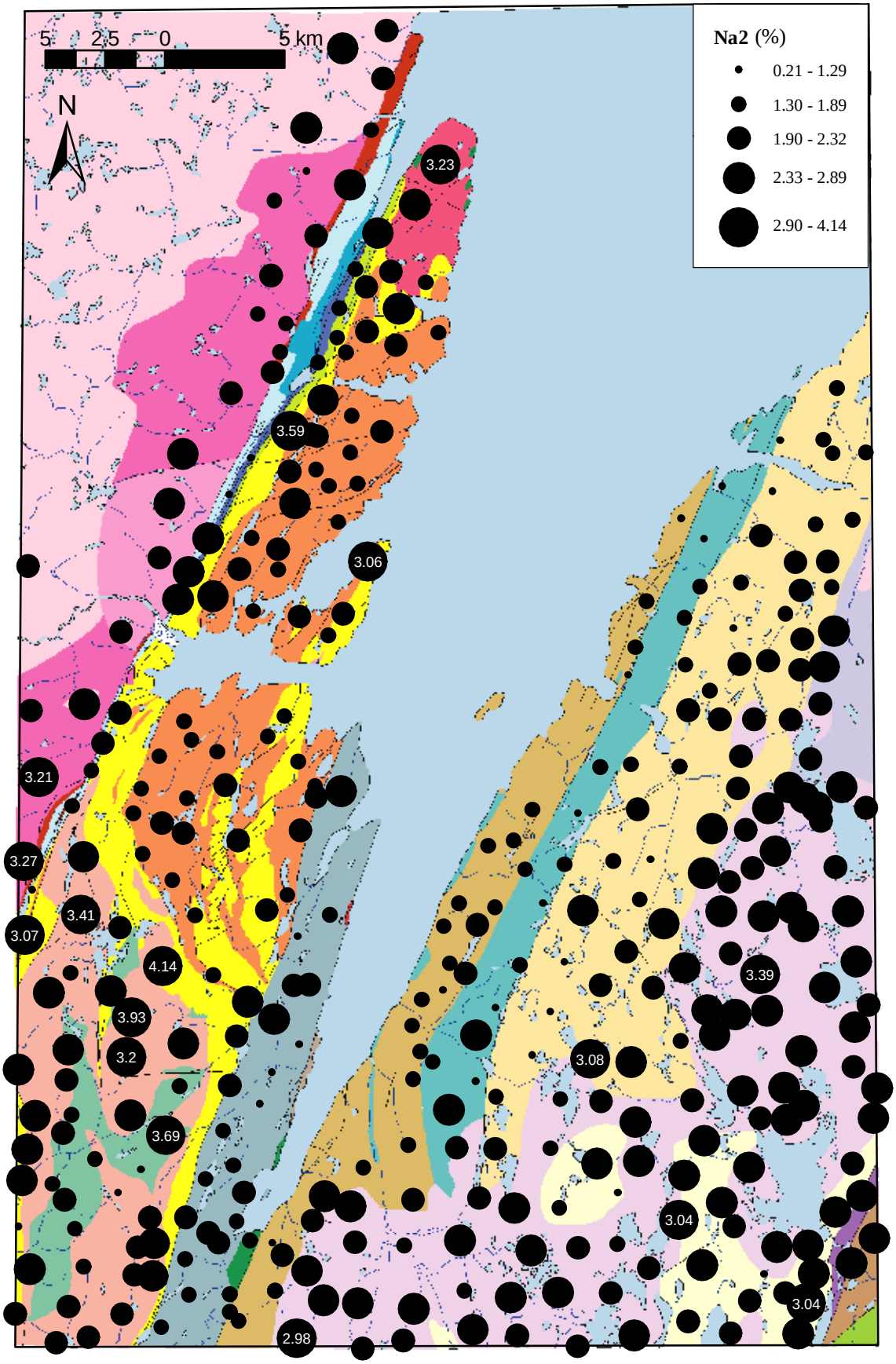

Figure 33. Sodium values in till. Open File NFLD/2823.

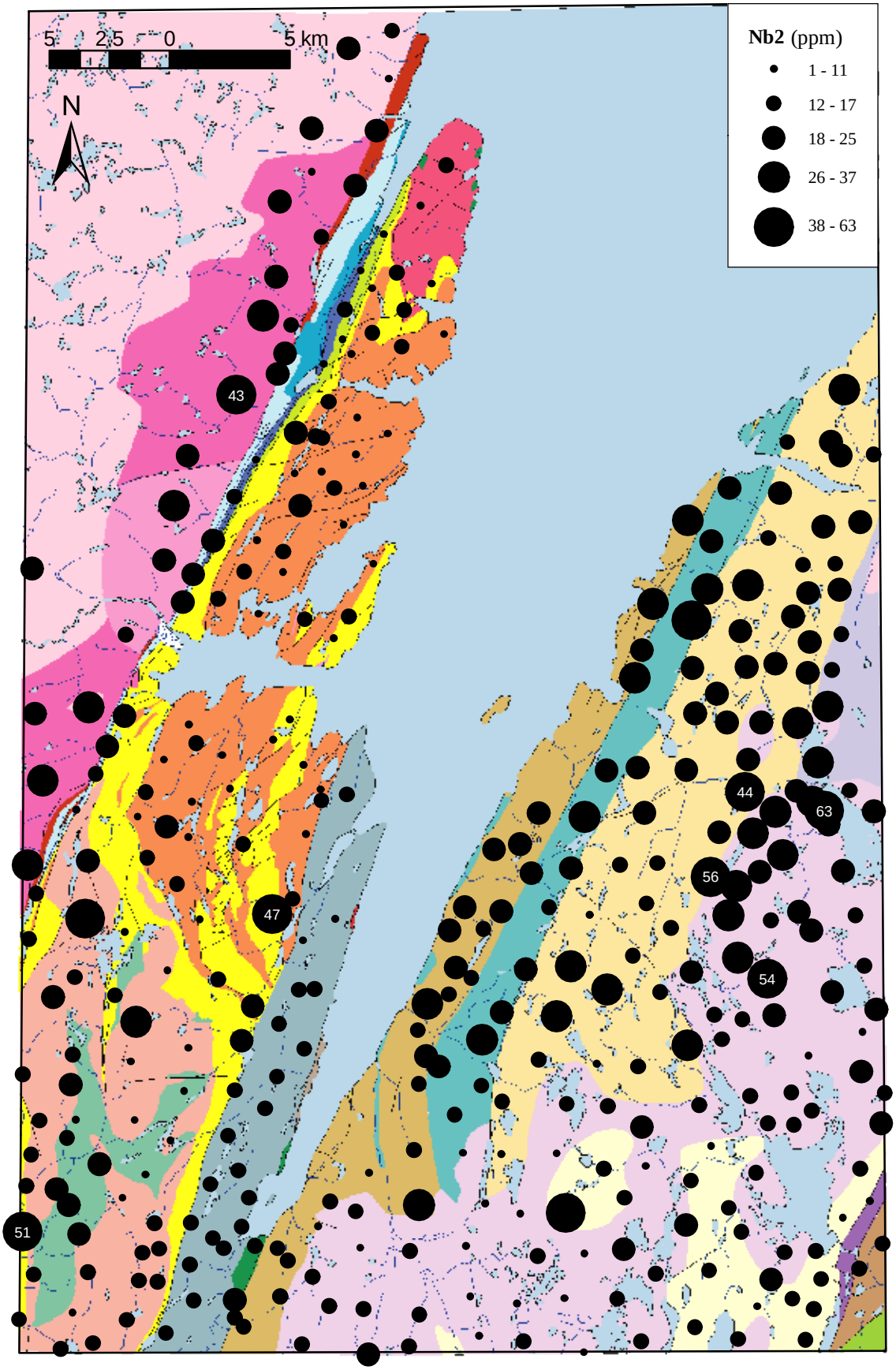

Figure 34. Niobium values in till. Open File NFLD/2823.

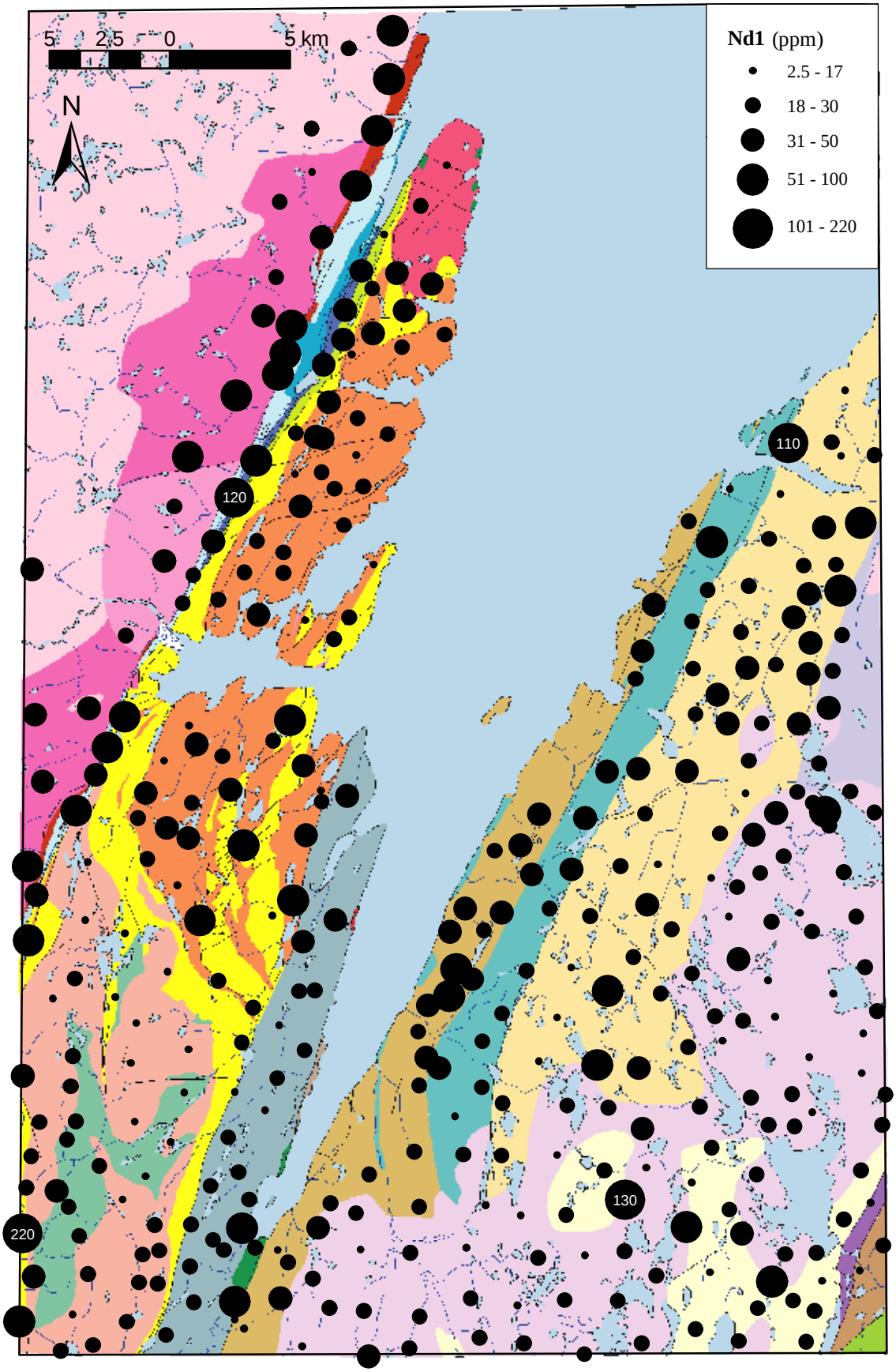

Figure 35. Neodymium values in till. Open File NFLD/2823.

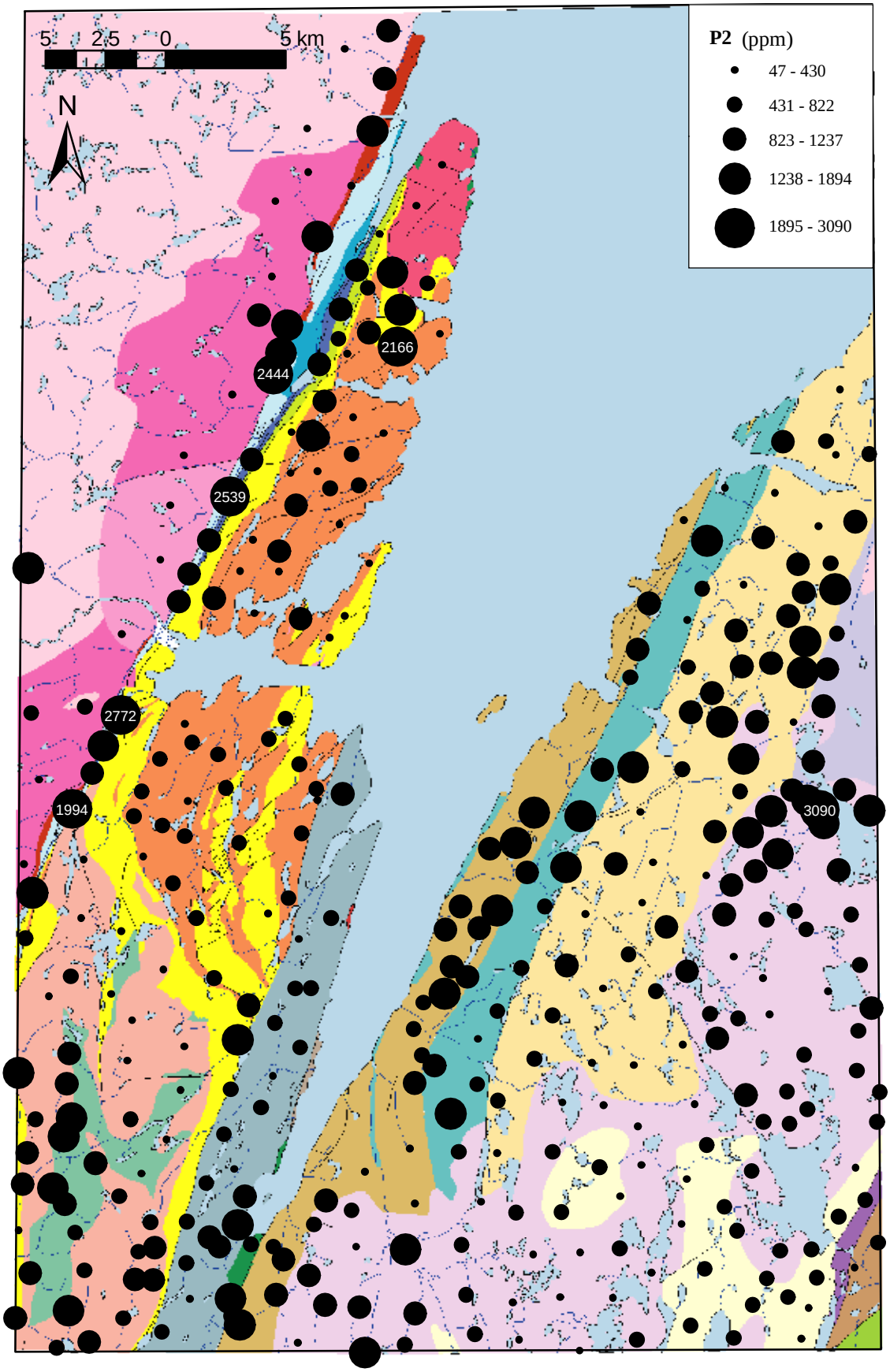

Figure 36. Phosphorous values in till. Open File NFLD/2823.

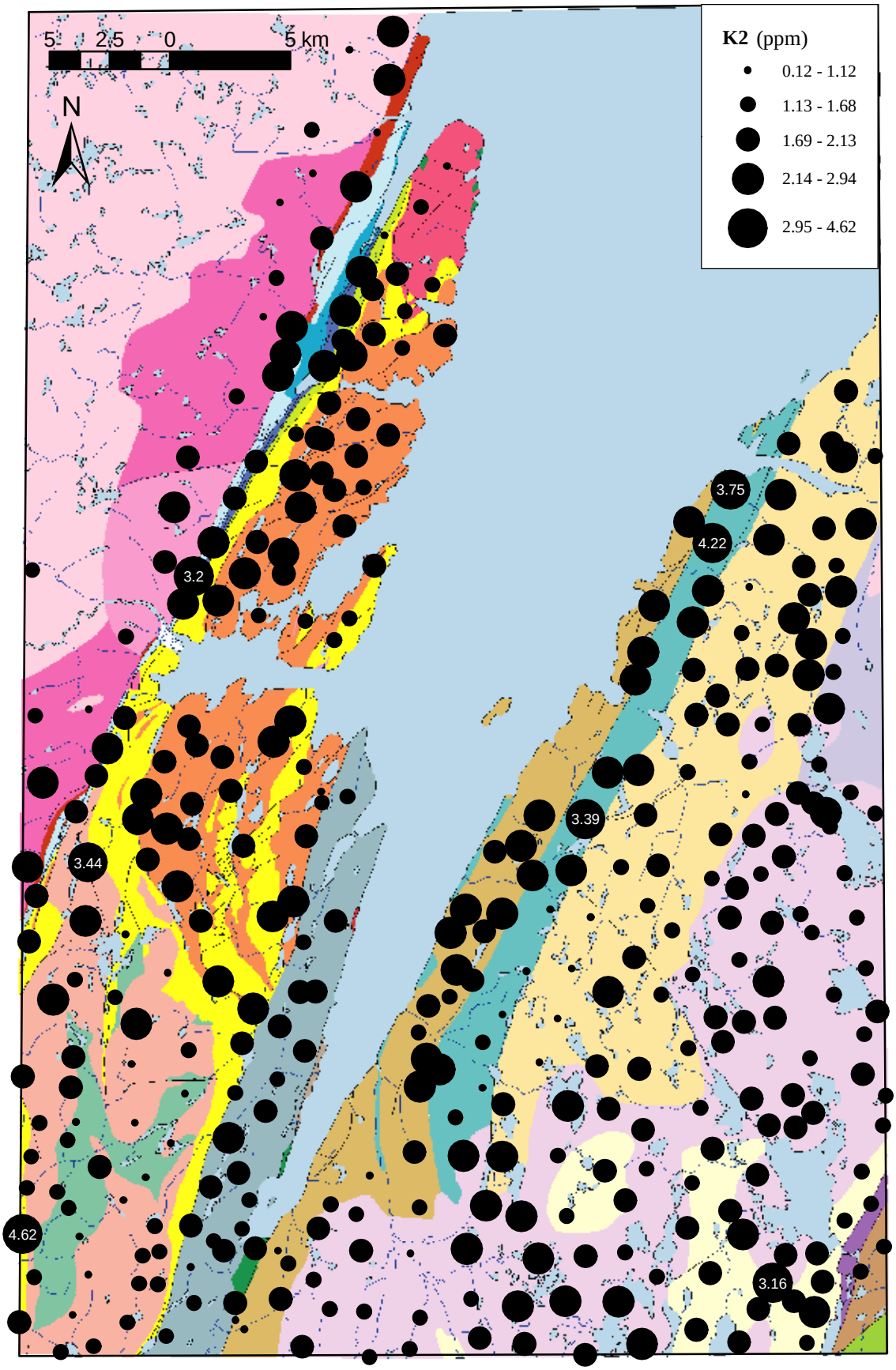

Figure 37. Potassium values in till. Open File NFLD/2823.

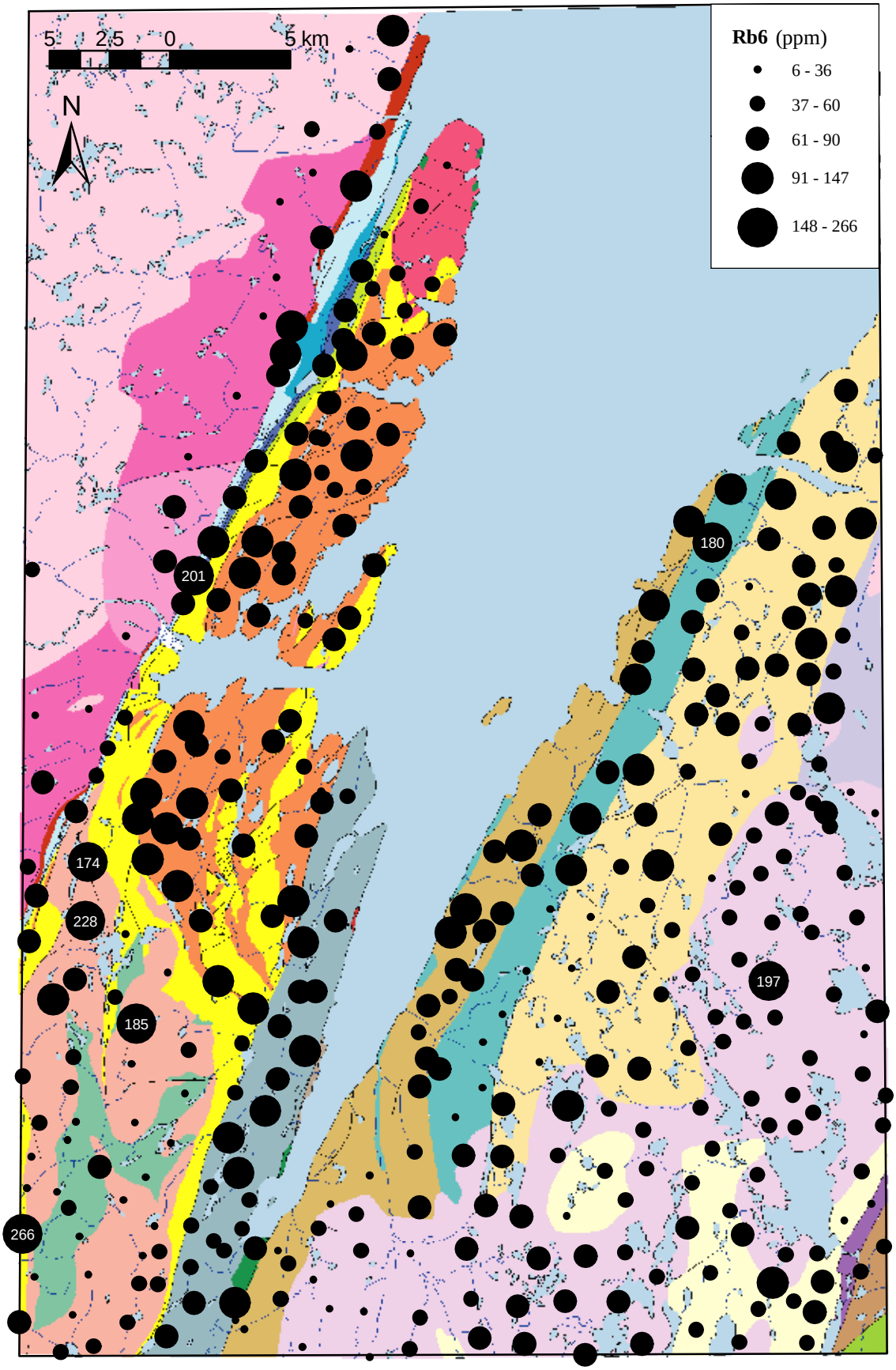

Figure 38. Rubidium values in till. Open File NFLD/2823.

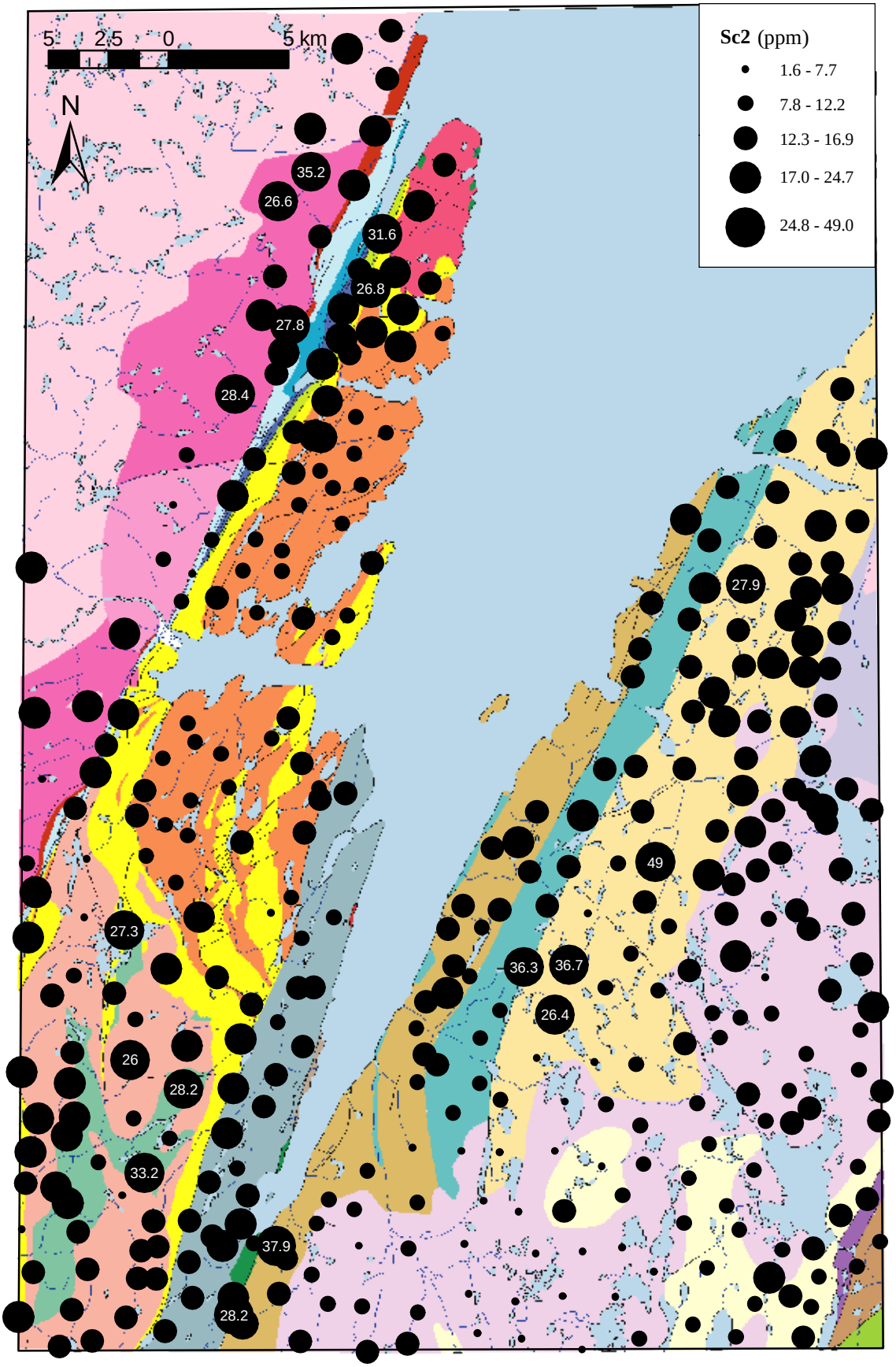

Figure 39. Scandium values in till. Open File NFLD/2823.

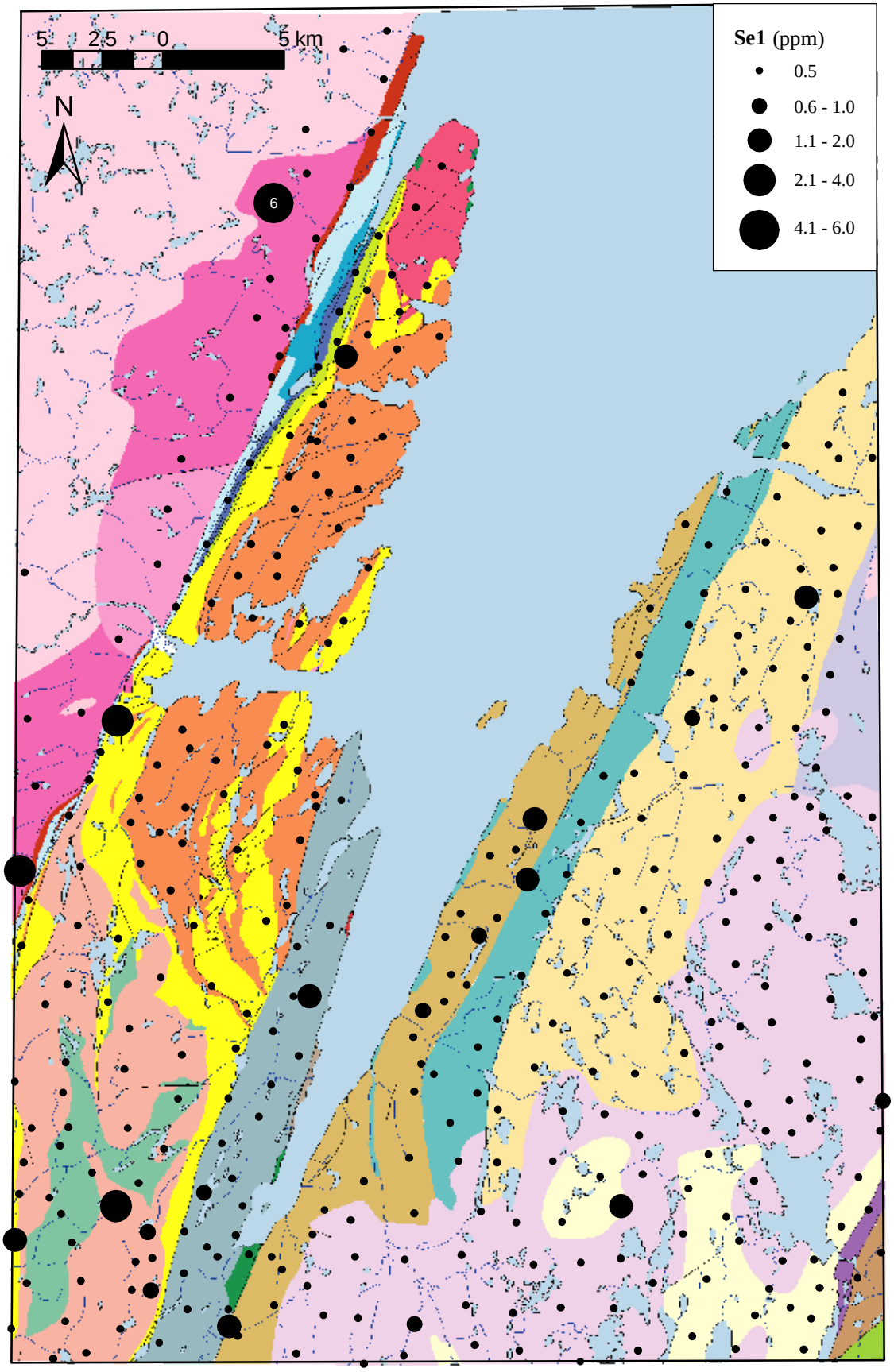

Figure 40. Selenium values in till. Open File NFLD/2823.

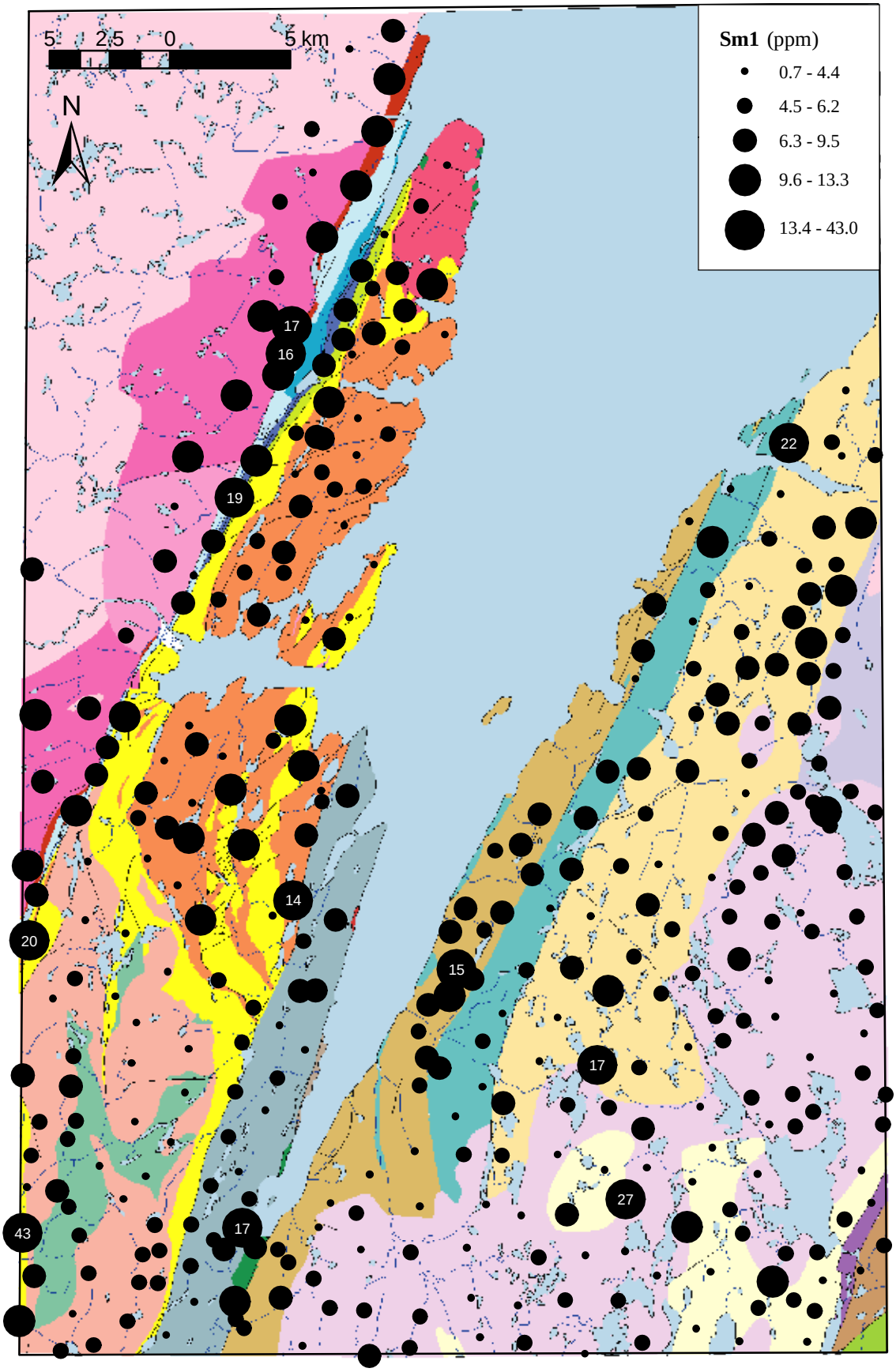

Figure 41. Samarium values in till. Open File NFLD/2823.

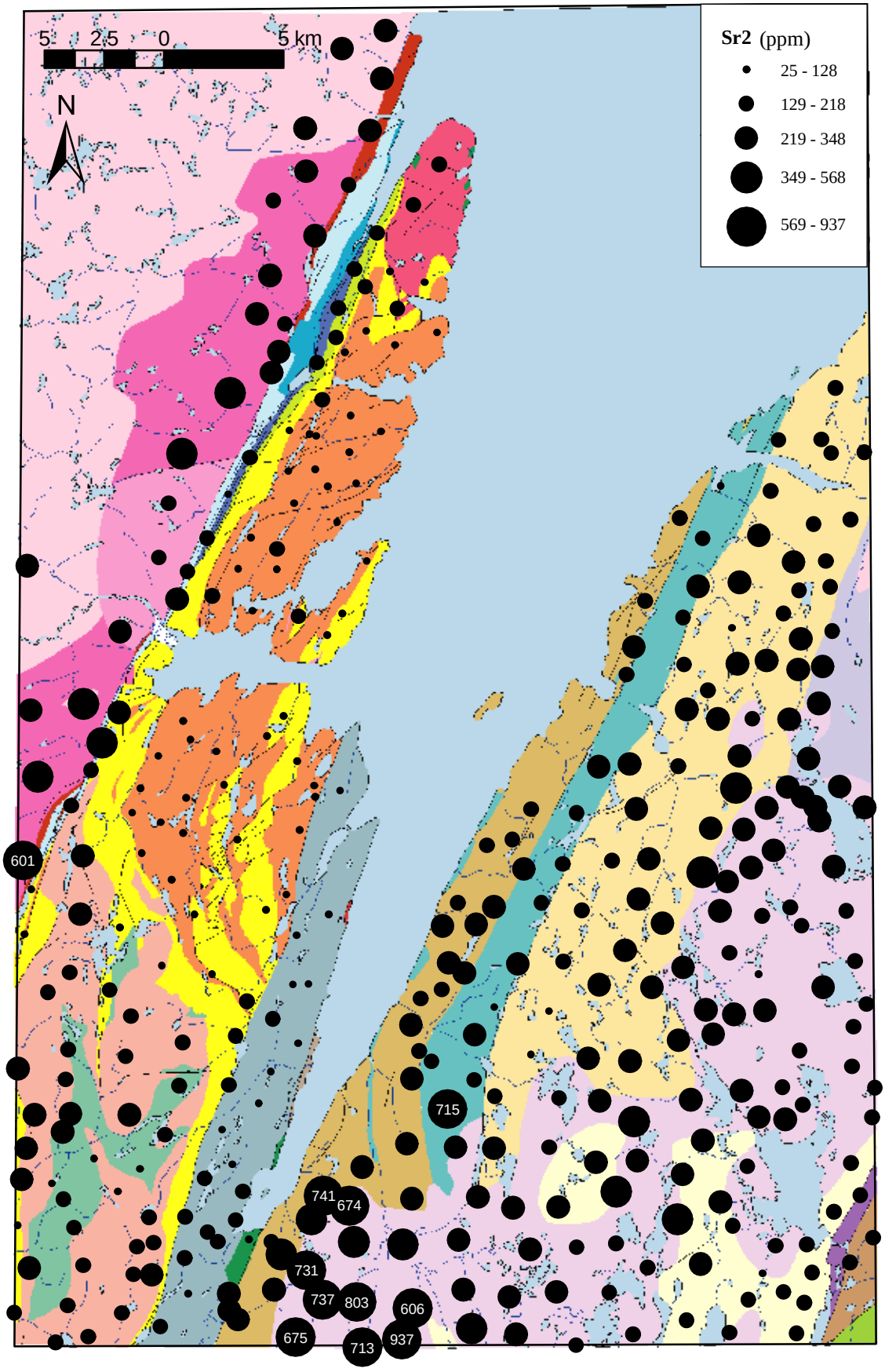

Figure 42. Strontium values in till. Open File NFLD/2823.

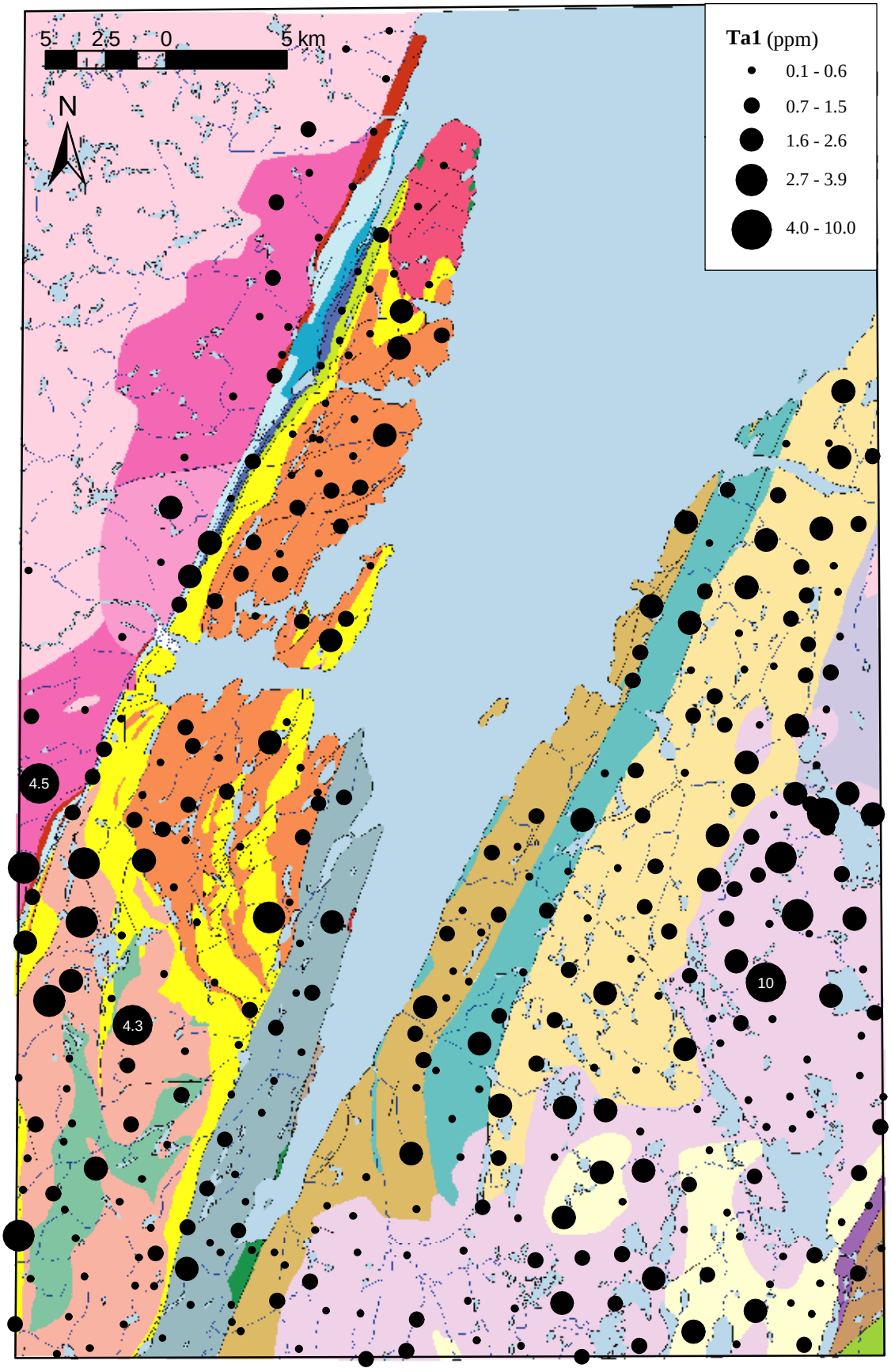

Figure 43. Tantalum values in till. Open File NFLD/2823.

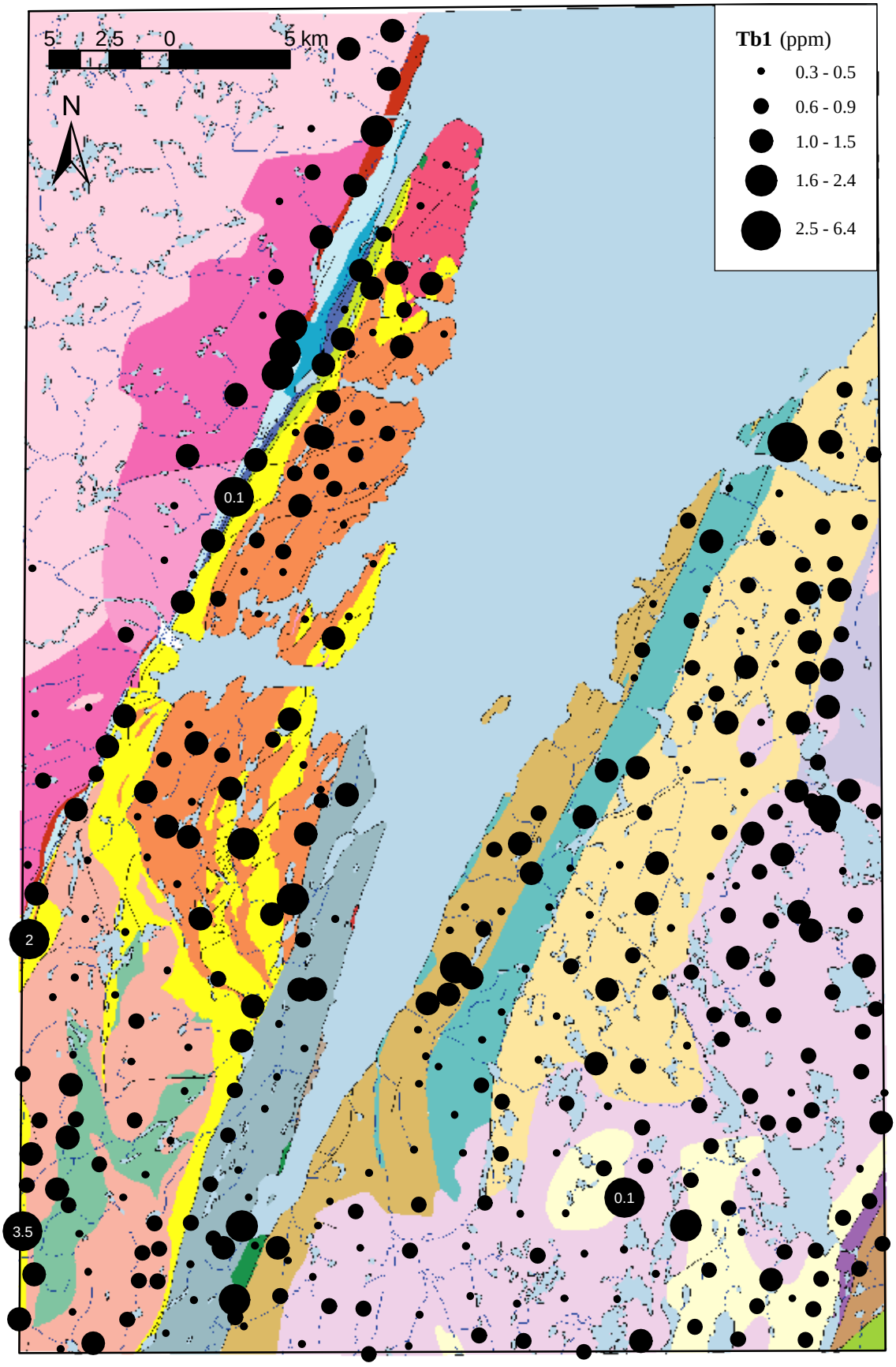

Figure 44. Terbium values in till. Open File NFLD/2823.

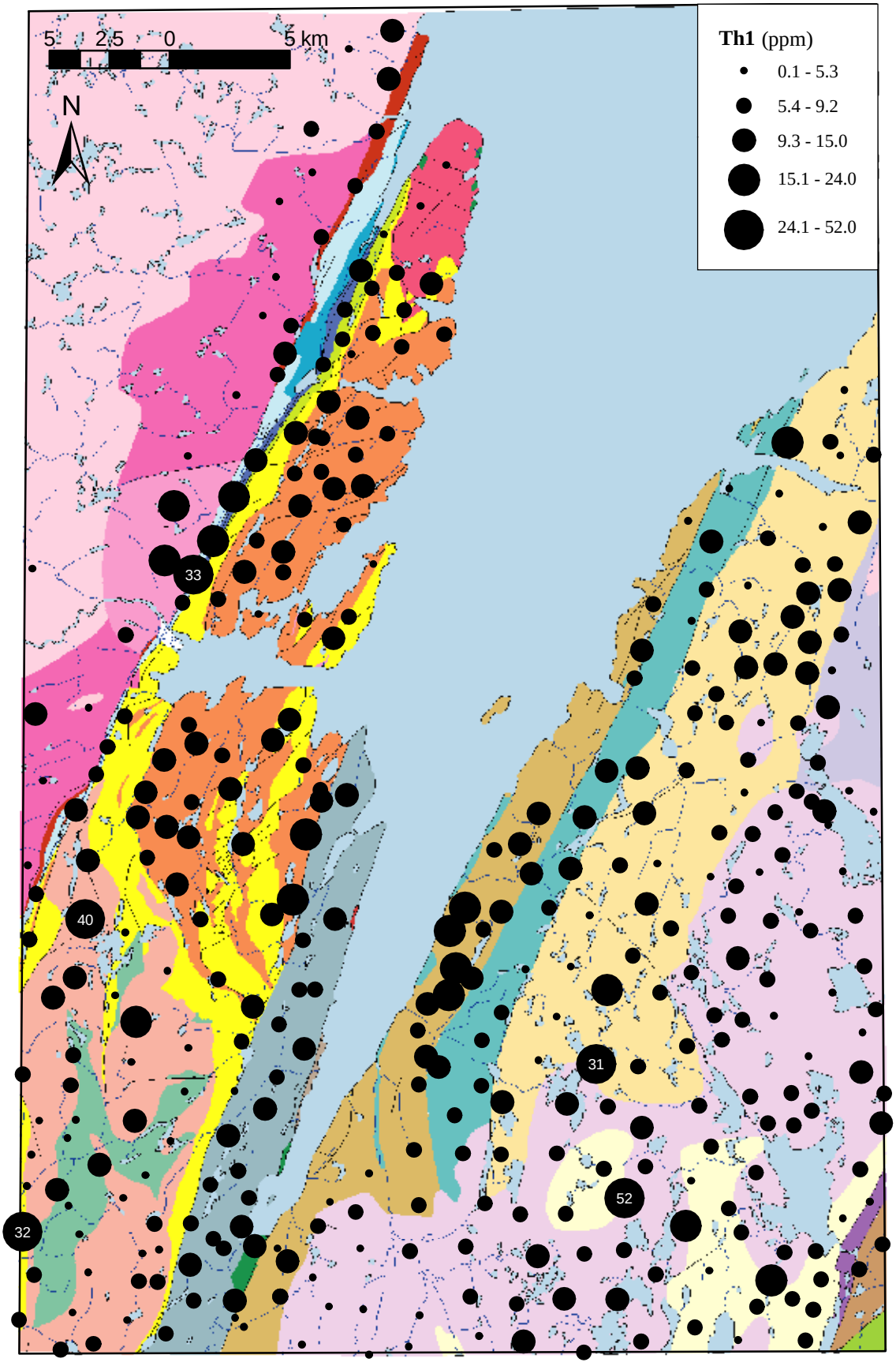

Figure 45. Thorium values in till. Open File NFLD/2823.

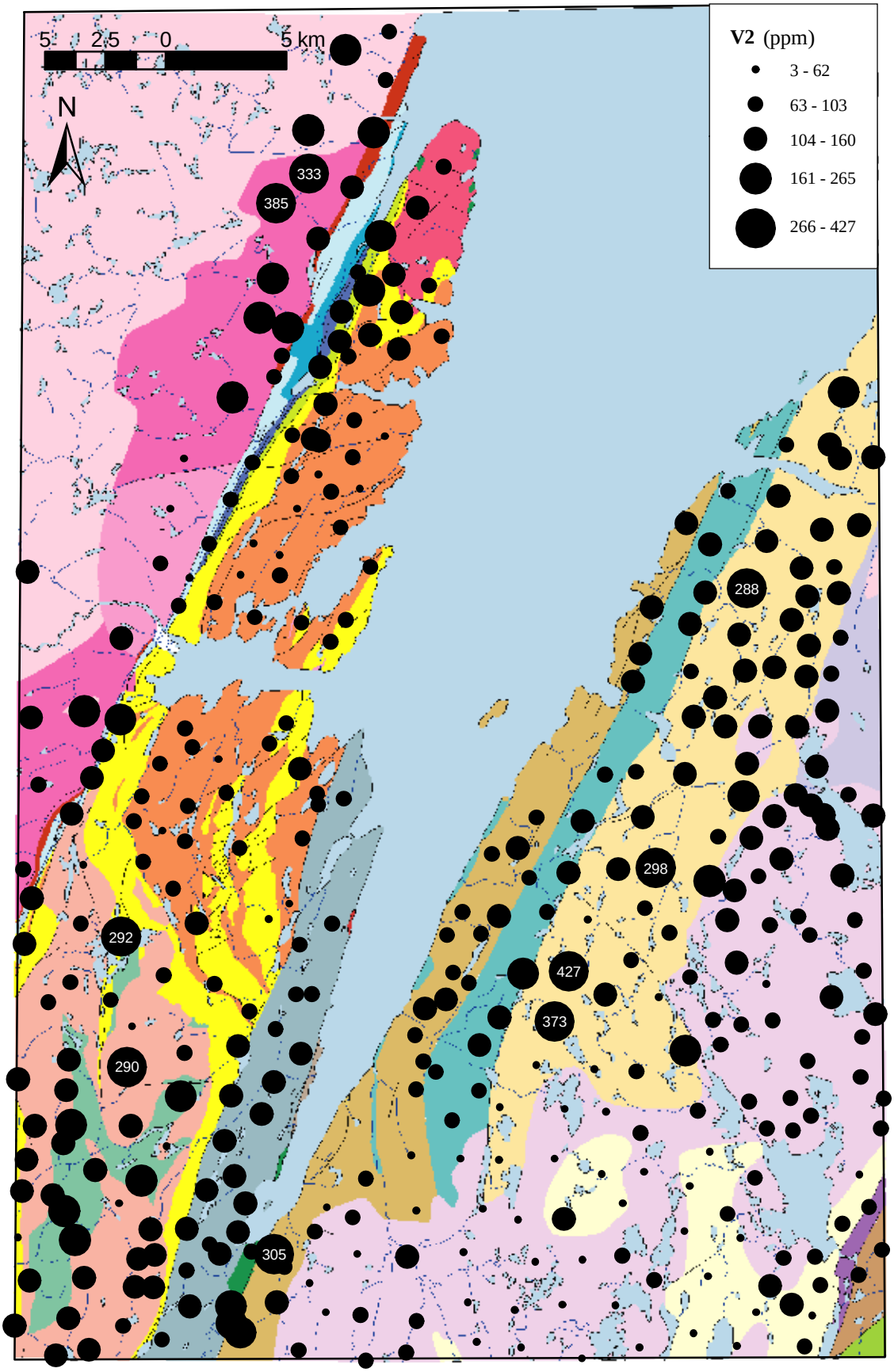

Figure 46. Vanadium values in till. Open File NFLD/2823.

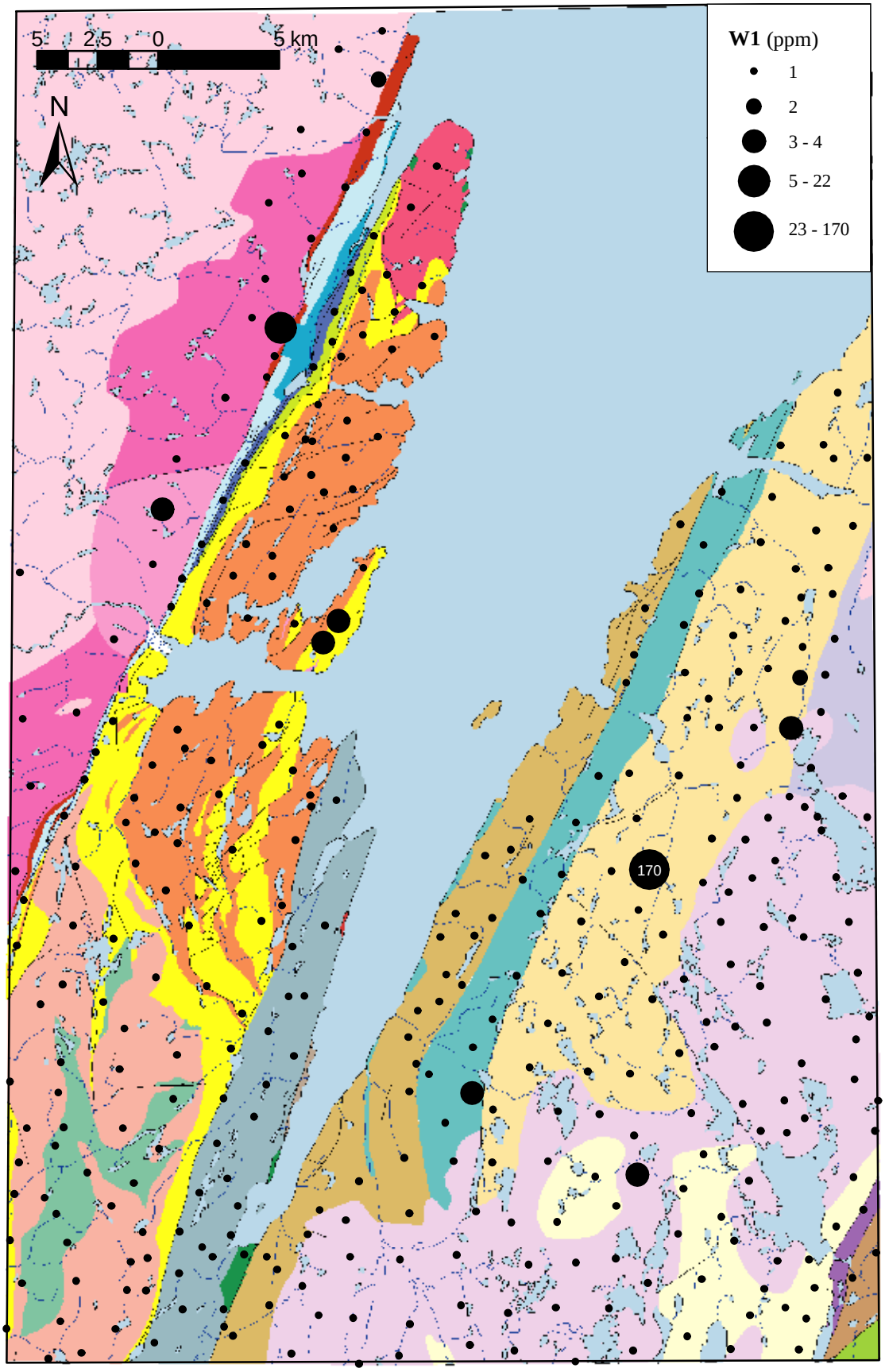

Figure 47. Tungsten values in till. Open File NFLD/2823.

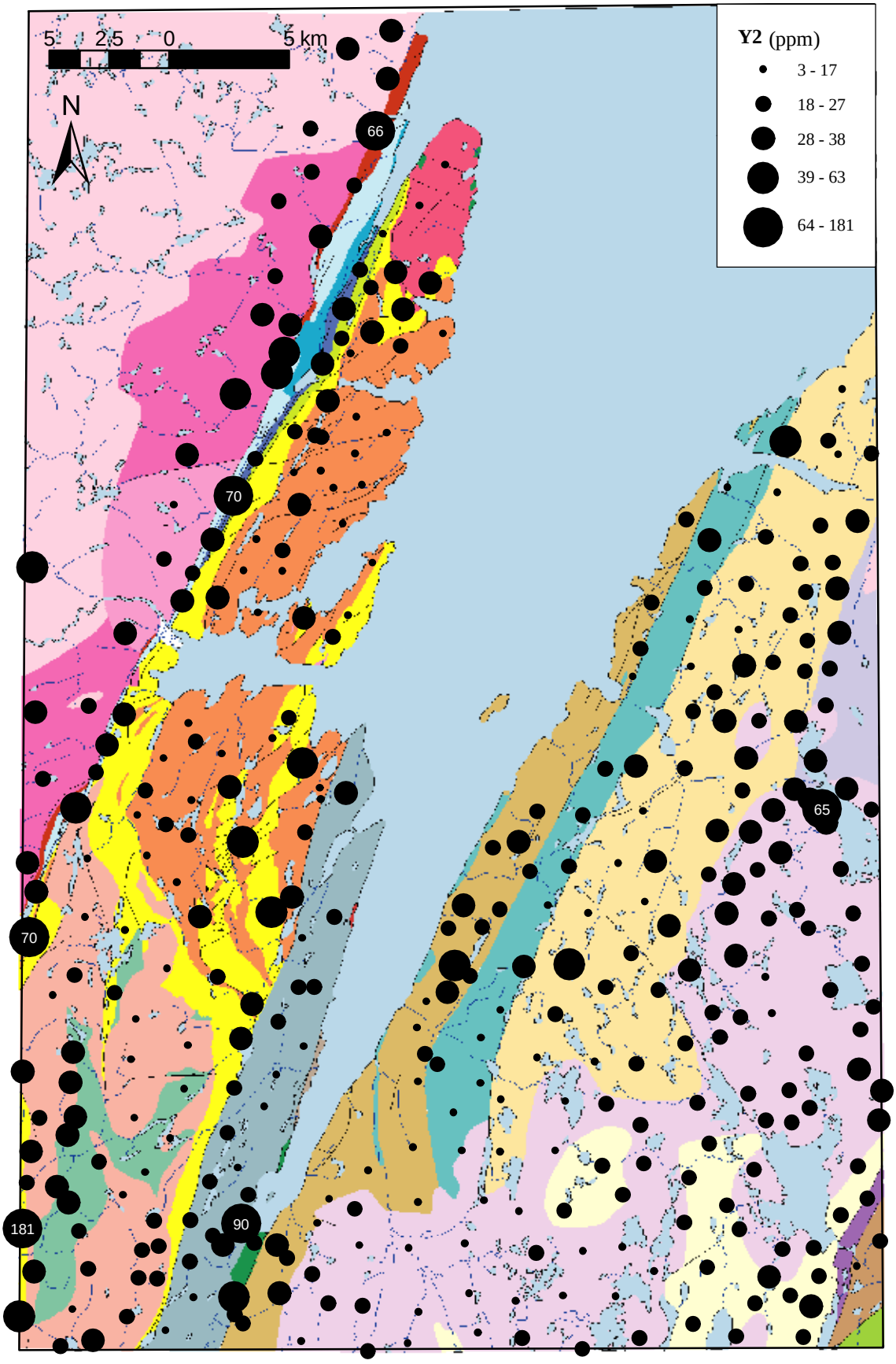

Figure 48. Yttrium values in till. Open File NFLD/2823.

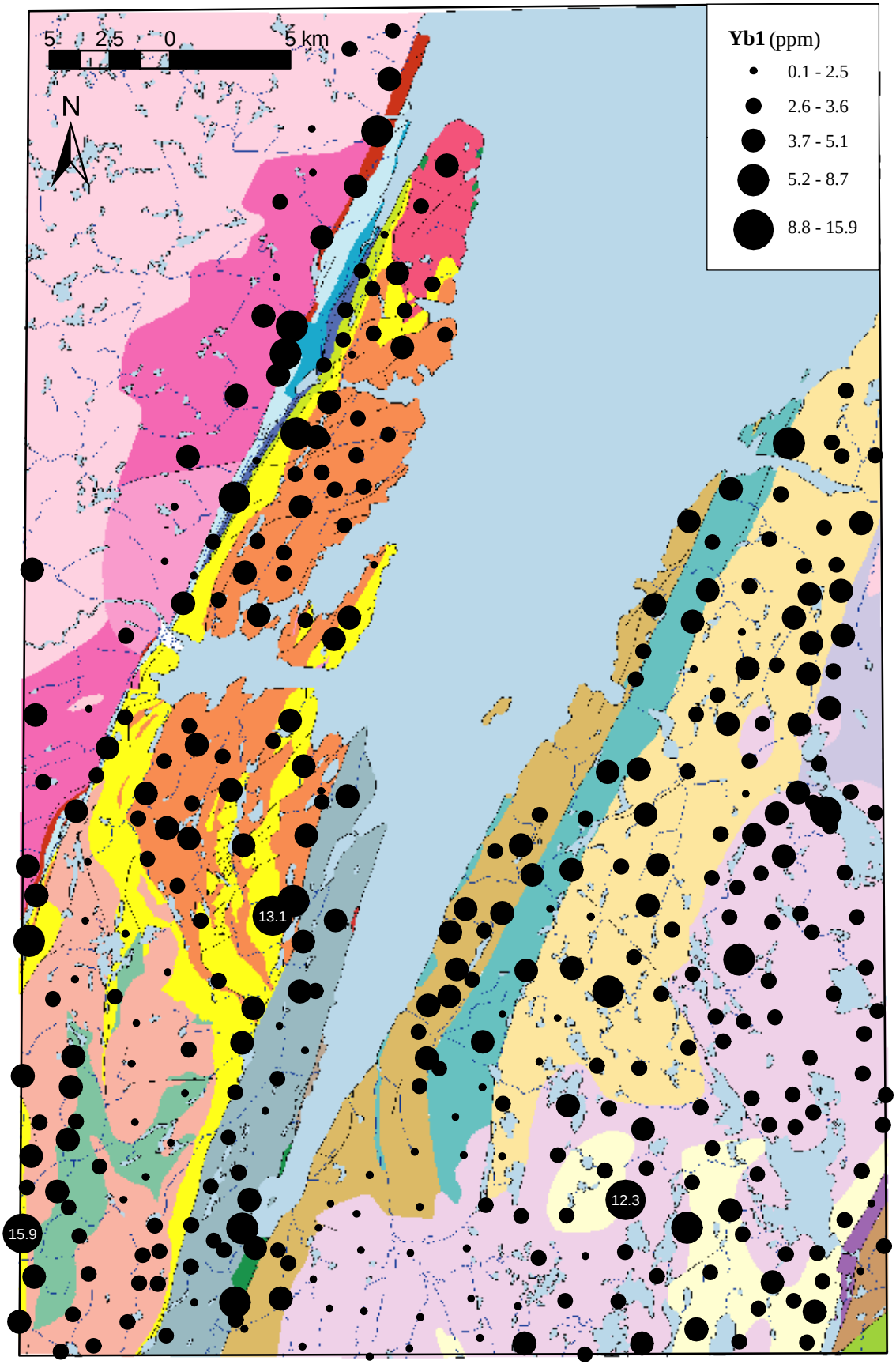

Figure 49. Ytterbium values in till. Open File NFLD/2823.

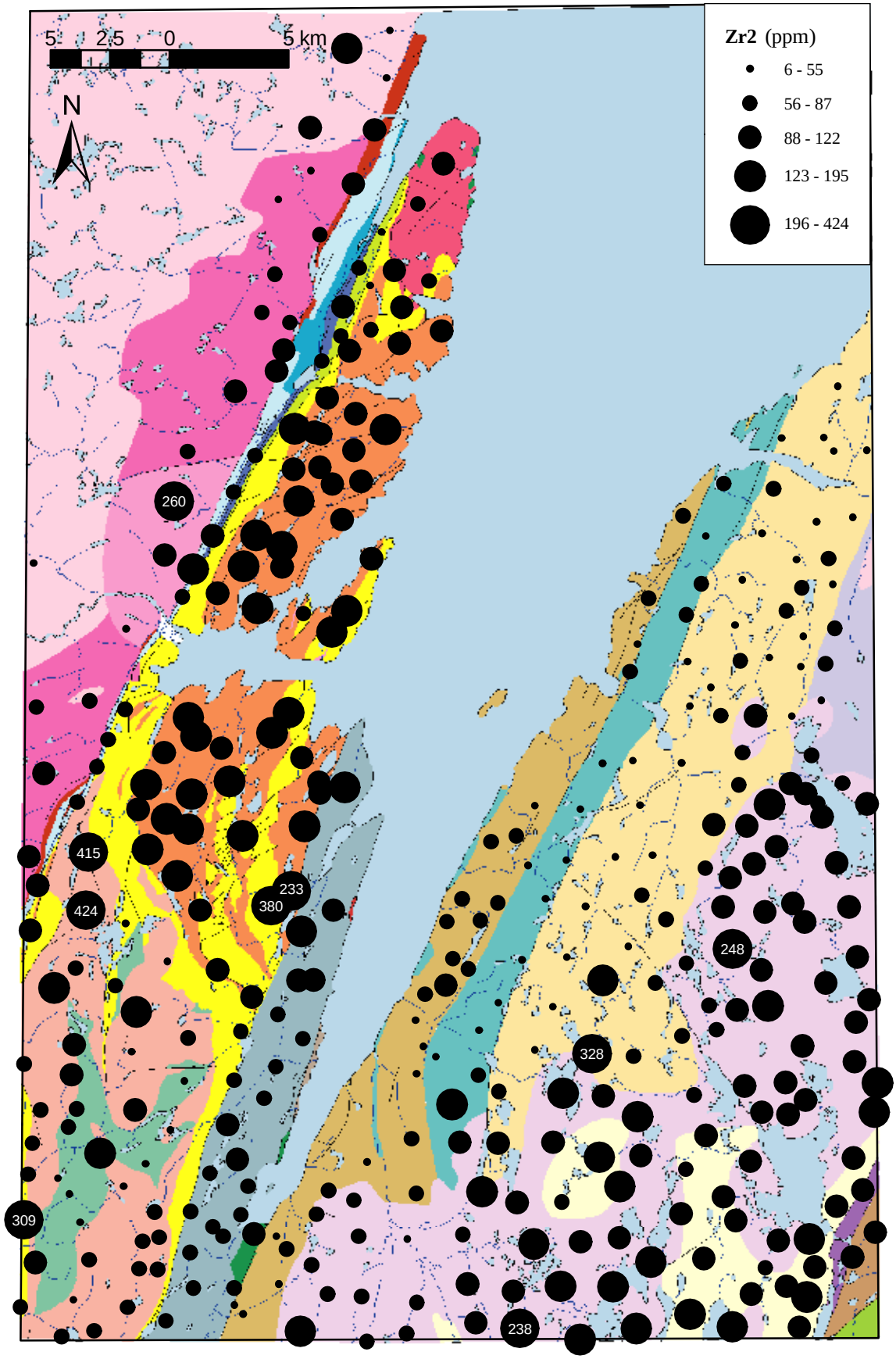

Figure 50. Zirconium values in till. Open File NFLD/2823.